Functional characterization of the interaction between Bex2 and torsinA, a protein involved in early-onset torsion dystonia

der Fakultät für Biologie

der EBERHARD KARLS UNIVERSITÄT TÜBINGEN

zur Erlangung des Grades eines

Doktors der Naturwissenschaften

von

Susann Horn

aus Werdau

vorgelegte

D i s s e r t a t i o n

2007

Tag der mündlichen Prüfung: 25.07.2007

Dekan: Prof. Dr. F. Schöffl

1. Berichterstatter: Prof. Dr. T. Gasser

2. Berichterstatter: Prof. Dr. O. Rieß

Teile dieser Studie wurden bereits veröffentlicht:

Wissenschaftliche Publikationen:

Horn, S., Kullmann, S., Hewett, J. W., Gasser, T., and Kamm, C. (2007) **The early-onset torsion dystonia protein torsinA interacts with Bex2 at the nuclear envelope.** Manuscript submitted.

Grundmann K., Reischmann B., Vanhoutte, G., Huebner, J., Teismann, P., Hauser, T. K., Bonin, M., Wilbertz, J., Horn, S., Nguyen, H. P., Kuhn, M., Chanarat, S., Wolburg, H., Van der Linden, A., and Riess, O. (2007) **Overexpression of human wildtype torsinA and human ΔGAG torsinA in a transgenic mouse model causes phenotypic abnormalities.** *Neurobiol. Dis.* doi:10.1016/j.nbd.2007.04.015

Tagungsbeiträge:

Poster

Horn, S., Kullmann, S., Hewett, J. W., Gasser, T., and Kamm, C. **The early-onset torsion dystonia protein torsinA interacts with Bex2.** Society for Neuroscience 36th Annual Meeting, Atlanta 2006.

Meiner Familie gewidmet

1 SUMMARY

Early-onset torsion dystonia is an autosomal-dominant movement disorder with disease onset in early childhood that manifests in sustained involuntary muscle contractions, often resulting in twisted or distorted postures throughout life. The disorder is caused by a three base-pair deletion encoding a glutamic acid within torsinA, the protein product of the *DYT1* gene. To date, it is not understood how this three base-pair deletion leads to the development of early-onset torsion dystonia and a clear cellular function for torsinA remains to be elucidated.

This study verified Bex2 as a novel torsinA-interacting protein. Bex2, a small 125 amino acid protein, belongs to the Bex family, whose members have been implicated in neurotrophin signalling, cell cycle regulation and neuronal differentiation. Characterization of Bex2 and torsinA revealed co-localization of both proteins around the nucleus, pointing to a common role for Bex2 and torsinA at the nuclear envelope. Moreover, Bex2 and torsinA were shown to associate with cellular membranes and to localize to vesicle-like structures throughout the cytoplasm and along processes of rat neurons, suggesting that Bex2 and torsinA are bound to organelles that are transported along processes of neurons. This assumption is supported by co-localization of Bex2 with kinesin-I in vesicle-like structures throughout the cytoplasm and within processes of rat neurons, as kinesin-I is known to transport organelles and cargo anterogradely along microtubules. Kinesin-I has previously been demonstrated to interact with torsinA at the cytoplasmic face of cellular membranes. As this study shows co-localization of Bex2 with torsinA and kinesin-I, respectively, at vesicle-like structures, all three proteins may form a complex, tightly tethered to organelle membranes via Bex2 and torsinA and which is transported along microtubules via interaction with kinesin-I.

Furthermore, this study demonstrates interaction of Bex2 with the disease-causing, glutamic acid deleted ΔE torsinA variant and co-localization studies showed that this interaction occurs around the nucleus, presumably at the nuclear envelope. Binding affinity of Bex2 to ΔE torsinA tended to be higher than to wildtype torsinA, indicating an altered binding behaviour of mutant ΔE torsinA to Bex2 at the nuclear envelope.

In summary, this study supports the theory that torsinA also interacts with proteins outside the ER and that torsinA plays a crucial role at the nuclear envelope where it binds specific substrates. It furthermore supports the hypothesis that an altered

binding behaviour of ΔE torsinA to those substrates may disturb distinct cellular processes and thus lead to the development of early-onset torsion dystonia.

2   INTRODUCTION

2.1   Definition and classification of dystonia

Dystonia is a heterogeneous group of neurological movement disorders. In the literature, Fahn's (1988) definition has prevailed, which characterizes dystonia by sustained involuntary muscle contractions, causing repetitive movements and abnormal postures (1). The term dystonia goes back to Oppenheim, who in 1911 for the first time described a "dystonia musculorum deformans" in six patients with a generalized abnormal muscle tone, which he could not relate to any other characterized movement disorder at that time (2). Despite subsequent precise descriptions of dystonia (2, 3), it took more than half a century before physicians accepted that these symptoms are due to brain and not muscle disease (4).

The classification of dystonia has evolved over the years and is currently divided in three different ways: (i) By etiology in primary (idiopathic torsion dystonia), dystonia-plus", heredodegenerative dystonia and secondary (symptomatic) dystonia; (ii) Clinically by the age of onset or affected body parts in focal, segmental, generalized, multifocal and hemidystonia, or (iii) using genetic criteria, such as the pattern of inheritance or the disease locus.

To date, fifteen different types of dystonia have been distinguished genetically and were designated dystonia types 1 to 15 (5-7). Six of the fifteen dystonia types are primary forms (DYT1, 2, 4, 6, 7, 13), which, except for DYT2, have an autosomal-dominant mode of inheritance. DYT5, 11, 12, 14 and 15, which are also autosomal-dominantly inherited, belong to the class of "dystonia-plus" syndromes, whereas X-linked inherited DYT3 refers to heredodegenerative dystonia. The paroxysomal dystonia DYT8, 9 and 10 can be categorized as "dystonia-like conditions". Either chromosomal loci or genes have been identified for most of these forms, listed in table 1 (5-7).

Table 1: Genetic classification of primary dystonias

Designation	Locus	Clinical features	Age of onset	Mode of inheritance	Location	Gene/ Product
Dystonia 1 early onset TD, idiopathic TD (ITD), Oppenheim's dystonia	*DYT1*	starts in a limb, may generalize to other body parts as disease progresses	childhood <25 years in most cases	AD, incomplete penetrance	9q34	*DYT1*/ torsinA AAA ATPase
Dystonia 2 autosomal recessive TD	-	early-onset, generalized or segmental TD	-	AR	unknown	unknown
Dystonia 3 X-linked dystonia parkinsonism (XP), 'lubag'	*DYT3*	segmental/generalized TD, parkinsonism unresponsive to L-dopa, progressive neurodegenerative syndrome	adults (Ø 35 years)	XR	Xq13.1	unknown
Dystonia 4 TD 4, whispering dysphonia	-	whispering dysphonia	13-37 years	AD	unknown	unknown
Dystonia 5 dopa-responsive dystonia-parkinsonism, Segawa syndrome	*GCH1*	dystonia with concurrent or subsequent parkinsonism, L-dopa responsive	variable, often childhood	AD, incomplete penetrance	14q22.1-q22.2	*GCH1*/ GTP cyclohydrolase I
Dystonia 6 adult-onset ITD of mixed type	*DYT6*	focal or generalized, cranial, cervical or limb dystonia	Ø 19 years	AD	8p21-8p22	unknown
Dystonia 7 adult-onset ITD, idiopathic focal dystonia (IFD)	*DYT7*	focal dystonia and postural tremor, torticollis, writer's cramp, dysphonia/blepharospasm	28-70 years	AD, incomplete penetrance	18p	unknown
Dystonia 8 paroxysomal non-kinesigenic dyskenisia (PNKD), paroxysomal dystonic choreoathetosis	*PNKD*	attacks of dystonia or choreoathetosis, precipitated by alcohol, hunger, nicotine, caffeine, stress and fatigue	variable, early childhood, adolescence, adulthood	AD, incomplete penetrance	2q33-q35	unknown
Dystonia 9 paroxysomal choreoathetosis, spasticity and episodic ataxia	*CSE*	involuntary movements and dystonia, precipitated by alcohol, fatigue and stress, spastic paraplegia between attacks	2-15 years	AD	1p21-p13.3	unknown
Dystonia 10 paroxysomal kinesigenic choreoathetosis	*PKC*	Choreoathetosis precipitated by sudden unexpected movements	6-16 years	AD, incomplete penetrance	16p11.2-q12.1	unknown
Dystonia 11 myoclonus dystonia	*SGCE*	myoclonus and/or dystonia, responsive to alcohol	variable, often early childhood	AD, incomplete penetrance	7q21	*SGCE*/ ε-sarcoglycan
Dystonia 12 rapid-onset dystonia-parkinsonism (RDP)	-	dystonia or parkinsonism developing over hours or weeks	childhood, adolescence or adulthood	AD, incomplete penetrance	19q13	unknown
Dystonia 13 focal dystonia with cranio-cervical features, multi-focal/segmental dystonia	*DYT13*	segmental dystonia with cranial-cervical and upper limb involvement	5 years to adulthood	AD, incomplete penetrance	1p36.13-36.32	unknown
Dystonia 14 dopa-responsive dystonia (DRD)	*DYT14*	dystonia with concurrent or subsequent parkinsonism, L-dopa responsive	variable, often childhood	AD, incomplete penetrance	14q13	unknown
Dystonia 15 myoclonus dystonia	*DYT15*	myoclonus and/or dystonia, alcohol-responsive	variable, often early childhood	AD incomplete penetrance	18p11	unknown

TD, torsion dystonia; AD, autosomal-dominant; AR, autosomal-recessive; XR, X-linked recessive

Different types of dystonia are listed in table 2, using the classification of affected body parts. Whereas focal dystonia affects a single body part, segmental dystonia affects adjacent body parts or a segment of the body and generalized dystonia is related to two or more body segments of the entire body.

Etiologically, primary dystonia refers to syndromes, in which dystonia is the only phenotypic manifestation, usually without signs of structural abnormality in the brain. In "dystonia-plus", dystonic symptoms are combined with other neurological changes, usually myoclonus or parkinsonism, without indications of neurodegeneration. In heredodegenerative dystonia, the dystonia is part of a more widespread neurodegenerative syndrome, whereas secondary dystonia encompasses dystonic symptoms caused by environmental insults, such as strokes, tumors, infections, drug administration and toxins (8).

As this study deals with early-onset torsion dystonia (EOTD), which belongs to the heterogeneous group of primary dystonia, both primary dystonia and EOTD are more comprehensively discussed in chapter 2.2 and 2.3, respectively.

Table 2: Classification of dystonia by affected body parts.

Focal dystonia: single body part is affected
Eyelids (blepharospasm)   Mouth (oromandibular dystonia, musician's cramp)   Larynx (dystonic adductor dysphonia or whispering dysphonia)   Neck (cervical dystonia, previously known as spasmodic torticollis)   Hand and arm (writer's cramp)
Segmental dystonia (adjacent body parts are affected)
Cranial (two or more parts of cranial and neck musculature affected)   Axial (neck and trunk affected)   Brachial (one arm and axial; both arms with or without neck, with or without trunk)   Crural (one leg and trunk; both legs with or without trunk)
Generalized dystonia (two or more body segments are affected)
Combination of segmental crural and any other segment
Multifocal dystonia
Two or more non-contiguous body parts affected
Hemidystonia
Ipsilateral arm and leg affected

*Modified from Nemeth et al. (2002) (9)

Primary dystonia

Primary dystonia is one of the most common forms of dystonia, in which dystonia is the only phenotypic manifestation and no other neurological abnormalities are present. In patients with primary dystonia there is no history of a brain injury and no consistent associated brain pathology. However, a remarkable number of physiological changes have been described in patients with primary dystonia, ranging from alterations in the excitability of spinal and brainstem reflex pathways to changes in cerebral cortical activity during movement. This led to the assumption that a reduced inhibition at different levels of the motor system may cause the excessive muscle activity in dystonia patients (10).

Four systems make essential and distinct contributions to motor control: the local spinal cord and brainstem circuits, descending modulatory pathways, the basal ganglia and the cerebellum. The primate basal ganglia include the striatum (putamen, caudate nucleus and nucleus accumbens), the external and internal segment of the globus pallidus, the subthalamic nucleus and the substantia nigra (pars compacta, pars reticulate and pars lateralis). The circuitry of the basal ganglia can be divided into the direct pathway, which provides positive feedback to precentral motor fields, and the indirect pathway, which contributes negative feedback (11-14). In the direct pathway, transient inhibitory projections from the caudate and putamen project to tonically active inhibitory neurons in the internal segment of the globus pallidus. These in turn project to the thalamus, which results in cortical input. The motor circuits of the basal ganglia are thought to play a key role in the preparation and execution of normal movement generated in the cerebral cortex (4, 10, 14). It has been proposed that in EOTD patients a hyper-activity of the putamenopallidal direct pathway leads to an increase of thalamic input to the motor cortex, which subsequently may result in excessive muscle activity (Fig. 1).
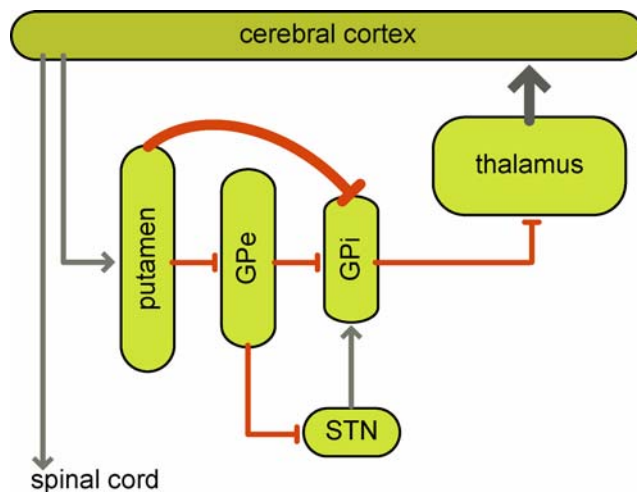
Fig. 1: Highly simplified scheme of basal ganglia circuitry in dystonia.

The hyper-activity of the putameno-pallidal direct pathway leads to reduced inhibitory output of the internal globus pallidus and increased thalamic input to the cortex. GPi, internal globus pallidus; GPe, external globus pallidus; STN, subthalamic nucleus

Modified from Berardelli et al. (1998) (10)

2.2   Predominantly generalized dystonia – EOTD

Familial primary dystonia can further be subdivided into predominantly focal and predominantly generalized dystonia, although there is no absolute distinction between these subtypes. The latter will be discussed in this chapter.

Predominantly generalized dystonia, also known as idiopathic torsion dystonia (ITD), generalized primary torsion dystonia (PTD), Oppenheim's dystonia or EOTD is the most common and severe form of primary dystonia. Typically, symptoms of EOTD develop in a limb with onset in the middle to late childhood (age 5 to 20), and progression of the disease leads to generalized dystonia within approximately five years in about 30% of patients. While these patients are severely physically handicapped, they are intellectually normal (15-17).

It was found that the prevalence of EOTD is five to ten times higher in Ashkenazi Jews than in non-Jewish populations: 1 per 2000 to 1 per 6000 in the Ashkenazi Jewish population compared to 1 per 300,000 to 1 per 200,000 in the general European population (5, 18, 19). Thus, it is assumed that a founder mutation occurred ~350 years ago in Lithuania or Byelorussia. This mutation has been mapped to the *DYT1* locus on chromosome 9q32-q34 in both Ashkenazi Jews and non-Jewish families, in which a GAG trinucleotide is deleted in-frame in exon five of the *DYT1* gene (Fig. 2). This results in loss of one of a pair of glutamic acid residues (ΔE) at position 302/303 in the C-terminus of the corresponding protein, torsinA (20-23). To date, only one single patient has been described with a different mutation in the *DYT1* gene, a heterozygous 18 bp in-frame deletion (966-983del, Phe323-Tyr328del) in exon 5 (Fig. 2) (24). This patient suffered from early-onset dystonia with myoclonic

features and was later found to additionally carry a missense mutation in the *SGCE* gene, causing myoclonus-dystonia (25).

Approximately 90% of Jewish and 50-70% of non-Jewish EOTD patients are hetero-zygous for the *DYT1* GAG deletion and no homozygous case has been reported. The disease is autosomal-dominantly inherited with an incomplete penetrance of about 30-40% (15, 21, 26-30). The reason for incomplete penetrance is not known, but environmental and/or additional genetic factors are suggested to contribute to the development of the disease. Thus, alteration in the torsinA amino acid sequence is necessary but not sufficient for the development of clinical symptoms in DYT1 patients. Interestingly, most carriers who do not develop EOTD before the age of 28 remain unaffected for the duration of their lives (31). However, phenotypic variability including late age of onset has been reported in some EOTD patients (32-34).

The age of disease onset (typically 5 to 28 years) is a developmental period, charac-teristic for motor learning and synaptic plasticity in the basal ganglia (15). Several lines of evidence suggest that the disease is caused by a malfunction of the basal ganglia: (i) The striatal [^{18}F]DOPA uptake is mildly reduced in affected *DYT1* GAG deletion carriers (35). (ii) Measurements using [^{18}F]fluorodeoxyglucose and PET scanning showed an increased metabolic activity in the lentiform nucleus and premotor cortices (36, 37). (iii) Expression levels of torsinA within the human brain are highest in dopaminergic neurons of the substantia nigra (38). (iv) An increase in the ratio of dopamine metabolites to dopamine was found in the postmortem striatum of EOTD patients compared to controls (39). (v) A phenotypically similar form of inherited dystonia, dopa-responsive dystonia, is caused by insufficient synthesis of dopamine (40). (vi) Symptomatic dystonia frequently affects patients with acquired lesions of the basal ganglia (41, 42). Remarkably, although several features of neuronal dysfunction are evident in brains of EOTD patients, there are no obvious signs of neurodegeneration. However, dopaminergic neurons of EOTD patients appear to be enlarged (43) and perinuclear inclusion bodies in specific brainstem areas of EOTD patients have been described (44).

2.3   TorsinA – structure and expression

TorsinA is the translated gene product of the *DYT1* gene, in which the deletion of a single GAG trinucleotide causes the development of EOTD. The *DYT1* gene is composed of 5 exons, in which the GAG deletion is located in the last exon covering

either nucleotides 946-948 or 949-951 (Fig. 2A). Human torsinA consists of 332 amino acids (aa) with a predicted molecular weight of 37 kD (Fig. 2B, C). The protein contains an N-terminal signal sequence (aa 1-20), which is removed from the mature protein and is proposed to target the protein to the endoplasmic reticulum (ER) (45, 46). Furthermore, it contains a stretch of hydrophobic amino acid residues (aa 21-40), representing a putative transmembrane domain or mediating the peripheral association of torsinA to membranes (21, 47). Moreover, *in silico* analyses of its amino acid sequence revealed the existence of domains with similarity to proteins of the AAA$^+$ superfamily of ATPases (<u>A</u>TPases <u>a</u>ssociated with a variety of cellular <u>a</u>ctivities) (21, 48). These include a conserved ATPase domain, which is made up of two domains: a core region that contains the nucleotide binding site (aa 102-109) within a Walker A motif, a Walker B motif (aa 95-119 and aa 164-175, respectively), and a C-terminal α-helical domain, termed sensor 1 (aa 198-211, Fig. 2C) (48-52). Sensor 1 domains have been proposed to mediate substrate interactions and are critical for ATP hydrolysis (53, 54). TorsinA contains another canonical AAA$^+$ motif, the sensor 2 (aa 272-238), which is a helical bundle with four α-helical segments, located C-terminal of the core ATPase domain. This helical module has been suggested to mediate the transmission of the free energy of ATP hydrolysis by AAA$^+$ proteins to their respective substrates (55). Interestingly, the EOTD-causing ΔE mutation is located within this sensor 2 region (Fig. 2C). Furthermore, human torsinA contains two potential *N*-linked glycosylation sites at Asn-143 and Asn-158, matching the consensus sequence NxT/S, which have been shown to be glycosylated *in vivo* (56, 57). Additionally, some authors also suggest the presence of a bipartite nuclear localization sequence **KK**IILNAVFGFINNP**K**P**KK** (aa 76-94, basic amino acids in bold) (58). However, a possible presence and function of torsinA within the nucleus remains controversial.

TorsinA is one of four members of the torsin protein family in mammals. A closely homologous gene encodes for another member of this family, torsinB, which shares 70% sequence homology with torsinA. In the human genome at least two more related genes are known, *torp2* (*torp2a*) and *torp3* (*torp3a*), both sharing 50% homology with torsinA. In contrast to mammals, *C. elegans* expresses three (OOC-5, TOR2 and Tor3) and *D. melanogaster* only one single torsinA-related protein, torp4A (21, 47, 59).

In humans, both *DYT1* mRNA and torsinA protein are ubiquitously distributed throughout various tissues, such as brain, liver and kidney (21, 58). *DYT1* mRNA expression was shown to be highest in the cerebellum, hippocampus, frontal cortex, Purkinje cells, thalamus and dopaminergic neurons of the substantia nigra (38, 60). At the protein level torsinA is enriched within the same brain structures and expression is primarily found within axons, dendrites and cytoplasm of neurons (38, 43, 61). The expression of torsinA is temporally and spatially regulated during brain development, beginning 4 to 8 weeks after birth within the cerebellum (Purkinje cells), dopaminergic neurons of the substantia nigra, hippocampus and basal ganglia, and by 2 months is abundant in almost all brain regions and remains so into adulthood (62).

In the putamen, cerebellar cortex, hippocampus (pyramidal neurons), cerebellum (Purkinje cells) and substantia nigra of EOTD patients, no major differences from control brains or any overt pathology have been observed. Only subtle changes in form of enlarged dopaminergic neurons and occasional ubiquitin-containing inclusions in the midbrain were noted (43, 44, 63). So far, only one study showed the presence of perinuclear inclusion bodies in brains of genetically confirmed *DYT1* patients (44). Inclusions were found within neurons of the pedunculopontine nucleus, cuneiform nucleus and griseum centrale mesencephali and stained positively for torsinA, ubiquitin and lamin A/C. Consistent with previous studies McNaught and colleagues (2004) found no evidence of torsinA-positive inclusions in the substantia nigra, striatum, hippocampus and selected regions of the cerebellar cortex.

However, cell culture studies revealed that overexpression of mutant ΔE torsinA leads to the formation of large spheroid intracellular inclusions, in which ΔE torsinA co-localized with the protein disulfide isomerase (PDI) ER marker protein (56). In addition, electron microscopy studies revealed that these inclusions consist of multilayered membrane whorls, apparently derived from the ER (56, 57, 64). Moreover, it has recently been shown that overexpression of high levels of human wildtype torsinA is also detrimental to neurons, as disruption of the nuclear envelope (NE) and formation of inclusions around the nucleus have been observed in neurons of both ΔE torsinA and wildtype transgenic mouse lines (65). Hence, there is a discrepancy between histological, cell culture and mouse model studies and as only one histological study on DYT1 brains has shown neuropathology, these results should be considered critically.
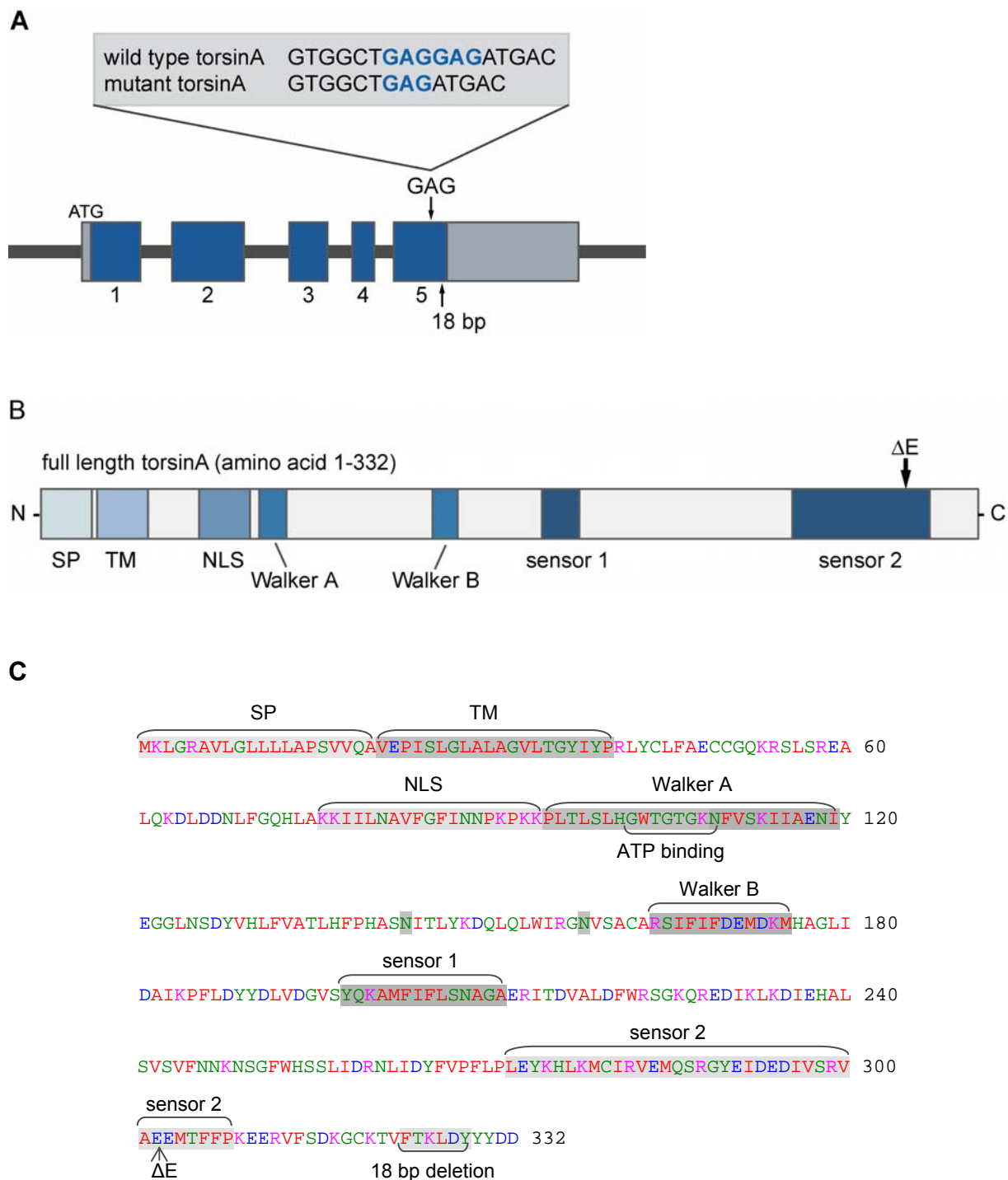
Fig. 2: Structure of the *DYT1* gene and its translated product torsinA.

A) The *DYT1* gene is composed of 5 exons with an open reading frame of 998 bp (translated regions are depicted in blue). The EOTD causing GAG deletion and an 18 bp deletion are located in exon 5 (arrows). **B)** The predicted domain structure of torsinA contains a signal peptide sequence (SP), a hydrophobic, putative transmembrane domain (TM), a putative bipartite nuclear localization signal (NLS), an ATPase domain that includes the nucleotide binding domain (Walker A and Walker B) and the ATP hydrolysis domain (sensor 1). The AAA$^+$ sensor 2 motif mediates energy transmission from the AAA$^+$ protein to the respective substrate. The arrow indicates the glutamic acid deletion ΔE. **C)** Sequence motifs in human torsinA are highlighted, corresponding to: SP aa 1-20; putative TM aa 21-40; putative NLS aa 76-94; ATP binding site (aa 102-109) within the Walker A (aa 95-119) motif, *N*-linked glycosylation sites (N143 and N158), Walker B motif (aa 164-175), sensor 1 (aa 198-211) and sensor 2 (aa 272-238). The glutamic acid deletion ΔE in sensor2 is indicated with an arrow and the 18 bp deletion is highlighted.

2.4　TorsinA - putative functions

Although the precise cellular function of torsinA is not known, some ideas about torsinA and related proteins have emerged. (i) TorsinA is thought to be involved in the transport of ER-derived membranes, as it resides in the lumen of the ER, within axons, growth cones and interacts with kinesin light chain (KLC), a subunit of the plus-end molecular motor protein kinesin-I, which transports membranous organelles along microtubules (46, 56, 57, 61, 66). (ii) TorsinA is considered to act as a molecular chaperone - one hint are sequence homologies to AAA^+-ATPases and the heat shock protein (HSP)/Clp ATPase (21, 48, 67, 68). (iii) TorsinA has been observed to protect cells from toxicity of H_2O_2 and to be sensitive to oxidative stress (46, 69). (iv) TorsinA is suggested to be involved in maintaining the spacing and structure of the inner and outer membranes of the NE (70-73). (v) TorsinA may participate in intracellular trafficking of the dopamine transporter and other polytopic membrane proteins (74). (vi) TorsinA has been described to interact with the cytoskeleton (75, 76).

The proposed various functions of torsinA and related proteins are described in detail in the following chapters.

2.4.1　TorsinA in the endoplasmic reticulum

The ER is a central eukaryotic cell compartment, involved in protein and lipid synthesis, protein folding, sorting, and membrane trafficking. A major fraction of torsinA is associated with ER membranes, most probably in a type II transmembrane orientation – with a single membrane spanning domain and its C-terminus located to the ER lumen (Fig. 3A). Localization of torsinA in the ER was demonstrated by double-label immunocytochemical studies in cell culture. Using antibodies against torsinA and the ER marker proteins PDI and BiP, a great extent of co-localization between torsinA and these markers was observed in a punctuate pattern throughout the cytoplasm and processes (56, 57). In contrast, ΔE torsinA was found in large spheroid inclusions, lacking BiP signal (57, 64). However, another study observed PDI positive signal within ΔE torsinA inclusions (56). The orientation of wildtype and ΔE torsinA in the ER membrane has been assessed by their sensitivity against proteases in the absence and presence of nonionic detergents (57). Both torsinA and ΔE torsinA were sensitive to either trypsin or chymotrypsin after membrane

permeabilization with Triton X-100 or digitonin but not in the absence of detergents, suggesting a lumenal orientation for both proteins. Furthermore, fractionation of cell homogenates by sucrose density gradient centrifugation revealed torsinA in the microsomal fraction along with the ER resident protein calnexin. Subsequent proteinase K digestion of the microsomal fraction revealed torsinA protease resistance in the absence of detergent, and torsinA digestion in the presence of detergent, confirming a lumenal orientation (46).

Moreover, localization of torsinA in the ER is supported by the presence of a N-terminal signal sequence, allowing entry into the ER (21). Cleavage of the signal peptide at amino acid 20 during translation was demonstrated by overexpression of torsinA in *D. melanogaster* S2 cells, following immunoprecipitation, gel purification and N-terminal sequencing (46). Moreover, it has been suggested that the signal peptide cleavage occurs through the signal peptidase complex (SPC). In fact, altering the putative SPC cleavage site of torsinA by amino acid substitution (V18F and A20F, respectively) reduced the amount of signal sequence cleavage (77).

Callan and colleagues (2007) showed that the hydrophobic residues that remain after signal peptide cleavage are fully translocated into the lumen of the ER. The researchers mutated residue valine 33 to asparagine, thereby introducing a putative glycosylation site in torsinA. This site was efficiently modified, as endoglycosidase H treatment increased the protein size, indicating a complete translocation of the N-terminus into the ER (77). Previous findings suggest torsinA to be an integral membrane protein, as sodium carbonate extraction assays showed association of torsinA with the ER membrane (45). Contrary to these findings, Callan and colleagues (2007) found that lumenal torsinA associates peripherally with the ER membrane, as alkaline extractions at pH 11.3 revealed torsinA in the soluble protein containing supernatant (77).

Although the above discussed studies indicate that torsinA is a lumenal ER membrane associated protein, functional interactions of torsinA may also occur at the cytoplasmic face of the ER membrane, as determined by cross-linking and biotinylation assays (66). In rat brain torsinA co-fractionated with kinesin heavy chain (KHC), which is located at the cytoplasmic surface of vesicles and the ER, within the vesicle-enriched P3 fraction. Fraction P3 was subsequently used to cross-link cytoplasmically oriented proteins. Subsequent immunoprecipitation yielded both torsinA and KHC immunopositive signals.

A
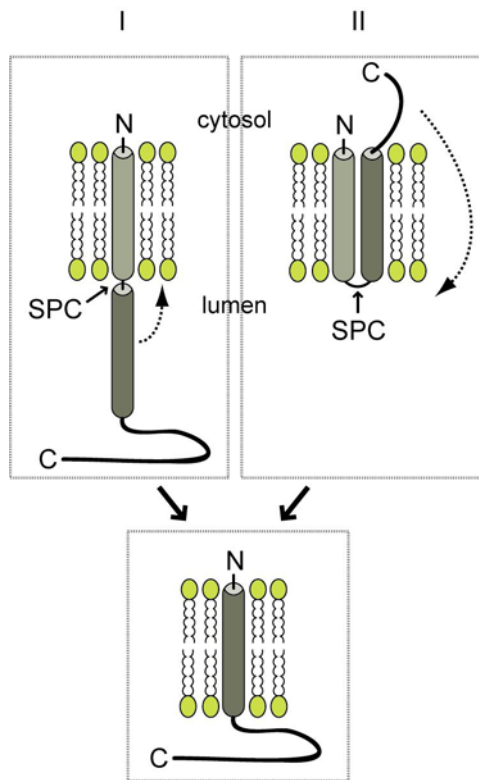
Fig. 3: Models for torsinA localization in the ER.

A) Putative mechanisms of torsinA insertion into the ER membrane to a type II orientation. Model I suggests that the putative transmembrane domain (dark grey) is fully translocated into the ER lumen and after SPC cleavage inserts into the ER membrane. Alternatively, as depicted in model II, the N-terminus is initially inserted towards the ER lumen and the C-terminus re-orientates after signal peptide cleavage (SPC). **B)** Model for possible orientations of torsinA in the ER: (I) The C-terminus is located lumenally and the N-terminal hydrophobic sequence anchors the protein in the membrane; (II) The C-terminus is located lumenally and the hydrophobic N-terminus associates peripherally to the membrane; (III) The C-terminus locates to the cytoplasm and the hydrophobic N-terminus associates peripherally to the membrane; (IV) The C-terminus is oriented cytoplasmically and the hydrophobic N-terminus integrates into the membrane.

Modified from Callan et al. (2007) (77).

B
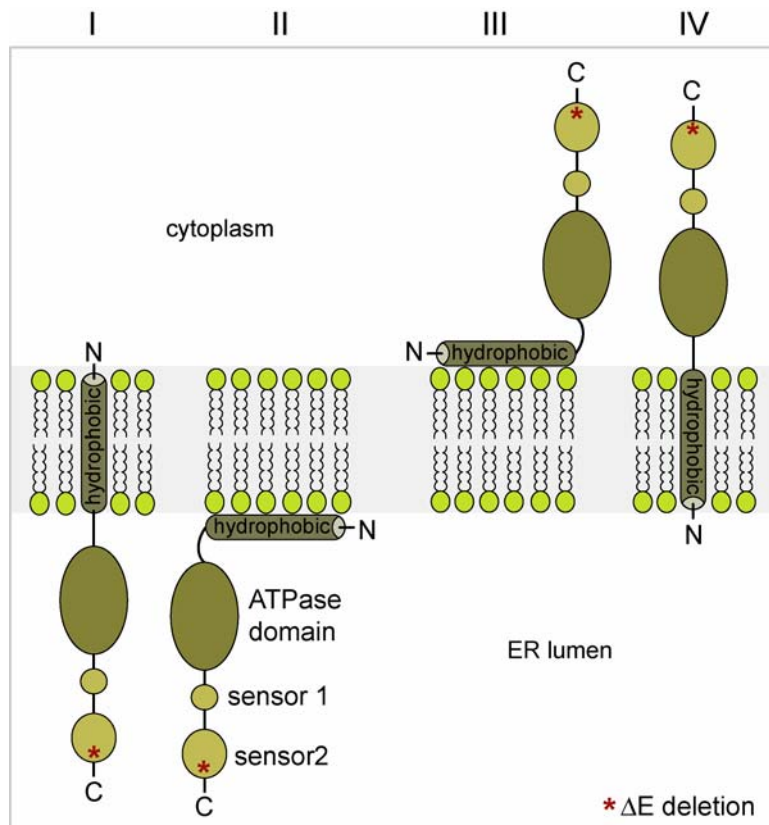
Furthermore, biotinylation of membrane surface proteins immunoprecipitated torsinA and KHC, indicating that a significant fraction of membrane-associated torsinA is exposed to the cytoplasm (66). Additionally, torsinA has been shown to bind proteins that are located outside the ER: kinesin-I, which is the molecular motor that anterogradely transports organelles and molecules along microtubules (66, 78, 79), and vimentin, a type III intermediate filament protein (75, 76).

Taken together, these results indicate that torsinA exists in lumenal and cytoplasmic orientations, thereby either integrated into or peripherally associated with the ER membrane (Fig. 3B).

2.4.2   TorsinA – an AAA$^+$ protein with chaperone function

Several features indicate that torsinA is a member of the large AAA$^+$ superfamily, including AAA$^+$ ATPases and the heat shock protein (HSP)/Clp ATPases. Sequence similarities to this family comprise a Walker ATP/Mg^{2+}-binding domain, 11 conserved motifs, including AAA$^+$ sensor 1 and sensor 2 motifs, and similar predicted secondary structures (21, 48, 67, 68, 80). ATPases are present in all organisms and use energy from ATP hydrolysis to participate in numerous cellular functions, among others vesicle fusion, organelle biogenesis, intracellular trafficking, protein folding and degradation (48, 55, 81). AAA$^+$ ATPases typically form homohexameric ring structures, which are essential for their ATPase activity and function (55, 81). It has been speculated that torsinA also forms homohexamers and that loss of the glutamic acid in torsinA might lead to a conformational change in the normal ring structure. Thus, deletion of the glutamic acid may inhibit activity and function of torsinA in a dominant negative manner, as depicted in Fig. 4 (47).
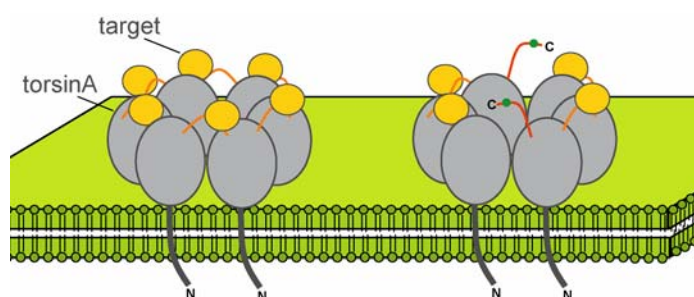
Modified from Breakefield et al. (2001) (47)

Fig. 4: Hypothetical model for a dominant-negative effect of ∆E torsinA.

TorsinA monomers (gray) form a hexameric ring that are presumebly tethered to the ER membrane via its N-terminal hydrophobic domain. The ∆E mutation in torsinA might lead to disruption of this ring structure and/or interfere with binding target protein (yellow).

Yeast Hsp 104, a chaperone that is capable of disaggregating misfolded proteins, also exhibits sequence similarities to torsinA (21). HSPs are critical factors of the cellular unfolded protein response, as they are involved in proper folding of proteins, prevention of aggregation, ubiquitination and degradation of misfolded proteins. Studies in brains of patients affected by dementia with Lewy bodies showed torsinA and several HSPs to co-localize with α-synuclein in neuropathological protein inclusions. TorsinA has also been found to accumulate within Lewy bodies in brains of Parkinson's disease patients (82, 83). Given the sequence similarity of torsinA to the Hsp 104 chaperone and the aggregation in Lewy bodies, torsinA may be involved in protein refolding and/or degradation. Moreover it has been demonstrated that overexpressed torsinA has the ability to prevent the formation of α-synuclein aggregates in cell culture models, as well as polyglutamine aggregates in *C. elegans* (82, 83). In contrast, no aggregation preventing effect has been observed in these studies when overexpressing ΔE torsinA.

However, torsinA does not seem to be a classical "heat shock" type of chaperone, as it is not up-regulated in response to a variety of stresses, including ER stress, induced by geldanamycin (inhibits the cytoplasmic chaperone hsp 90), tunicamycin (blocks glycosylation) and excytotoxicity mediated by the Ca^{2+} ionophore A23187 (increases Ca^{2+} influx). No response to oxidative stress, such as antimycin A (inhibits mitochondrial electron transport through complex III), sodium azide and deoxyglucose to deplete ATP, was observed. Furthermore neither ethanol, toxins, heat nor kainic acid produced any changes in torsinA expression (46). Nevertheless, torsinA is sensitive to some type of oxidative stress, as changes in its normal distribution and an increase in the apparent size from 37 kDa to 37.2 kDa were observed after treatment with H_2O_2 (46, 69). Additionally, overexpression of torsinA in cell culture models has unveiled a protective role against oxidative stress induced cell death (69).

In summary, these results suggest that torsinA acts within the ER to help cells survive environmental stresses, but the mechanism is yet not understood.

2.4.3 TorsinA at the nuclear envelope (NE)

The subcellular localization of torsinA extends from the ER (see 2.4.2) to the NE, which is a specialized subdomain of the ER, consisting of an inner and outer nuclear membrane, connected by nuclear pore complexes (NPC, Fig. 5) (84). Thus, the

localization of torsinA suggests that it plays a role at the NE. Likewise, the disease-causing mutant ΔE torsinA revealed an abnormally high concentration at the NE in patient-derived fibroblasts, cultured neurons and cells (70, 71, 85). The NE, also known as perinuclear envelope or nuclear membrane, separates the nuclear contents from the cytosol. Furthermore, the NE provides an anchoring site for chromatin and via its NPCs facilitates the exchange of proteins and RNA between nucleus and cytoplasm (84, 86, 87). The outer membrane is continuous with the ER, whereas the inner membrane associates to the nuclear lamina, a filamentous protein network mainly consisting of lamins (Fig. 5) (88). The nuclear membrane and lamina are connected by peripheral and integral proteins of the inner nuclear membrane that are anchored at the lamina (89, 90). One of those lamin-binding proteins, LAP1 (lamina-associated polypeptide 1), has been demonstrated to interact with torsinA and ΔE torsinA and moreover recruited torsinA to the NE (91). Likewise, a re-localization of torsinA from the ER to the NE through ΔE torsinA has been observed in patient tissue and neurons of ΔE torsinA transgenic mice (70). However, enrichment of torsinA at the NE could not be confirmed by Hewett and colleagues (2006), who also examined the expression of torsinA in fibroblasts derived from EOTD patients (76).

A translocation of torsinA has also been observed by introducing mutations into the conserved ATP-binding/hydrolysis motifs of the ATPase domain, which generated torsinA protein variants with alterations, predicted to change binding behavior to nucleotides and substrates (71). Mutating lysine 108 to alanine created an ATP-binding mutant of torsinA, K108A-torsinA, which was predicted to only poorly bind substrates. On the other hand, mutating glutamic acid 171 to glutamine generated a nucleotide-bound ATP-hydrolysis mutant, E171Q-torsinA, functioning as a substrate trap. Overexpression of wildtype or ATP-binding mutant K108A-torsinA resulted in an even distribution of both protein variants throughout the ER. In contrast, the ATP-hydrolysis mutant E171Q-torsinA was found to concentrate around the nucleus. An independent study revealed similar findings in neuroblastoma cells, in which overexpression of ΔE torsinA, but not wildtype torsinA, enriched vimentin, a type III intermediate filament protein, at the NE and within inclusions (76). Another striking finding was that overexpression of the mutant E171Q-torsinA led to alterations of the NE structure. Stretches of the inner and outer membrane were excessively separated from each other, forming large blebs and at some sites the nuclear membrane was

detached from the nuclear lamina. Thus, an involvement of torsinA in maintaining the spacing and structure of the inner and outer membranes of the NE is supposable (70-73). This in turn is accompanied by the suggestion that the main part of torsinA binds to substrates that reside within the NE and that ΔE torsinA, like the ATP-hydrolysis mutant E171Q-torsinA, does exhibit an altered substrate interaction by binding tighter to them (71, 91). Hence, it has been hypothesized that EOTD may be caused by an altered substrate binding behavior of ΔE torsinA in the NE.
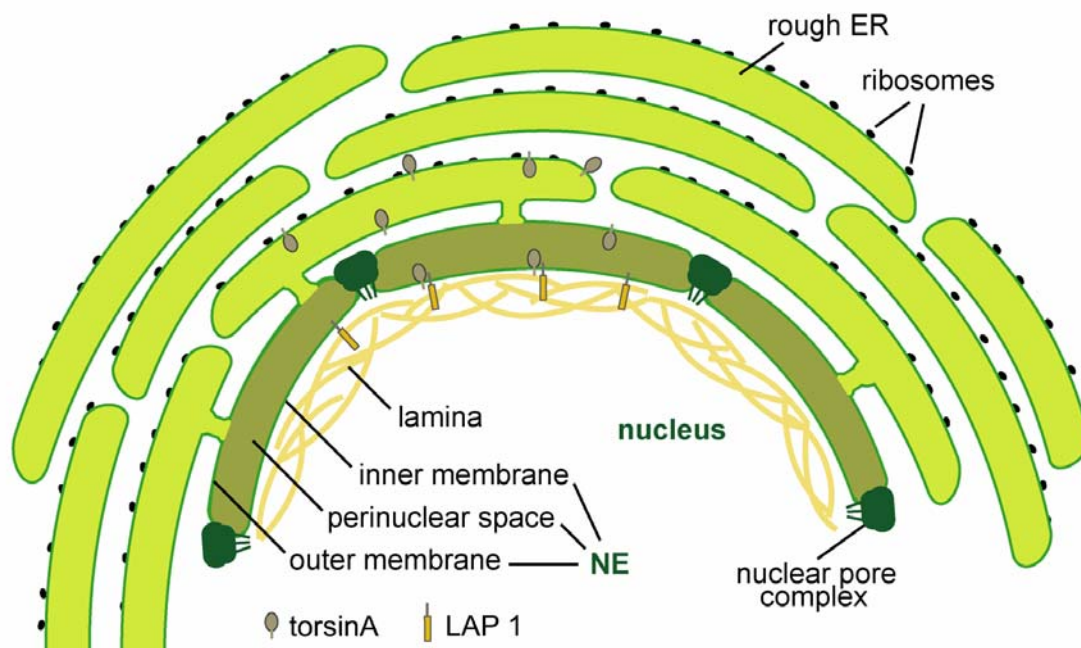
Fig. 5: Structure of the NE and ER.
The outer NE membrane is continuous with the ER membranes. The NE anchors chromatin and shuttles proteins and RNA through its nuclear pore complexes between nucleus and cytoplasm and is associated with the lamina, a network composed of lamin proteins. TorsinA is thought to be associated to membranes of the NE and ER, thereby interacting with LAP1.

2.4.4   TorsinA in dopaminergic neurons

Given that torsinA is expressed in many human tissues (21), it is astonishing that the only described phenotype in EOTD patients are neurological symptoms. However, it emerged that in most neurological diseases mutations in ubiquitously expressed proteins appear to generally effect selective neuronal subpopulations (92). Expression levels of torsinA in the human brain were found to be highest within dopaminergic neurons of the substantia nigra and neurons in the locus ceruleus, cortex, hippocampus, and basal ganglia (38). Moreover, torsinA protein was found to be present in Lewy bodies of dopaminergic neurons, which are especially sensitive to

cellular stress. Therefore, it was hypothesized that torsinA may function as a chaperone to resolve protein aggregates and prevent cellular stress (46, 69, 82, 83, 93). The effect of torsinA specifically on neurotransmission and survival of neuronal subpopulations, which are affected in EOTD, was studied in a *C. elegans* model. Dopaminergic neurons in *C. elegans* undergo a reproducible pattern of neurodegeneration, when treated with the neurotoxin 6-hydroxydopamine (6-OHDA). It was found that overexpression of wildtype torsinA in *C. elegans* dopaminergic neurons was able to suppress OHDA-induced neurodegeneration. This protective ability of torsinA seems to be due to a down regulation of DAT-1 (dopamine transporter 1), which mediates uptake of 6-OHDA (94). In contrast, overexpression of either ΔE torsinA or combined wildtype and ΔE torsinA greatly abated this protective effect. These results are supported by an independent study in mammalian cell lines, which has shown that overexpression of torsinA reduced the cell surface expression of DAT, as well as other polytopic membrane-bound proteins. Furthermore, in *C. elegans* mutants that are lacking DAT-1 function, overexpression of torsinA prevented against α-synuclein-induced neurodegeneration (74).

It has long been speculated that dysfunction of the dopamine system in nigrostriatal dopaminergic neurons is one potential causative factor for the clinical symptoms of EOTD (95, 96). This hypothesis is supported by the torsinA-mediated neuroprotection against 6-OHDA-induced toxicity through altered DAT cell surface levels, which may result in a disturbed dopamine reuptake and signaling. This in turn may contribute to the development of clinical symptoms of EOTD (94).

2.4.5   TorsinA, cell polarity and the cytoskeleton

An implication for torsinA in the establishment of cellular polarity has been discussed in numerous studies. A crucial hint came from a torsin family member, the nematode homolog OOC-5. This protein is required for controlling spindle orientation and nuclear-centrosome complex rotation during asymmetric cell divisions in early embryogenesis of nematodes (97, 98). Mutations in *ooc-5* result in defect spindle orientation and polarity in *C. elegans* embryos by affecting the PAR (partitioning defective) proteins. PAR proteins are critical for generating asymmetry during cell divisions at the two-cell stage. Thus, OOC-5 is suggested to play a role in spindle orientation through correct PAR protein localization (47, 97, 98).

Furthermore, torsinA has been discussed to be involved in cytoskeletal dynamics, demonstrated by the association with the cytoskeletal protein vimentin (75, 76). Vimentin is a type III intermediate filament protein and is known to be involved in motility, chemotaxis, adhesion, and intracellular signaling (99, 100). This protein binds to a variety of other cytoskeletal components, including kinesin, actin, tubulin and myosin. It is thought to influence neuronal shape and nuclear movement during neurite outgrowth (75, 101-103). Interestingly, immunoprecipitation of vimentin from fibroblasts co-precipitated torsinA, as well as α-tubulin, kinesin, actin and LAP1, the NE protein which was previously shown to interact with torsinA (76). Morphological and functional differences were observed for vimentin in EOTD patient derived fibroblasts, expressing ΔE torsinA compared to control cells, including enrichment of vimentin at the NE and a delay in the rate of cell adhesion to substratum. In addition, overexpression of ΔE torsinA inhibited neurite outgrowth in neuroblastoma cells, whereas vimentin and torsinA were found to be enriched perinuclear and within inclusions. These results led to the conclusion that the mutant form of torsinA may inhibit vimentin function, as well as the interaction between wildtype torsinA and vimentin. Consequently, torsinA may be involved in cytoskeleton dynamics, controlling neurite outgrowth and may play a role in cell polarity.

2.5   Mouse models of early onset torsion dystonia

Several approaches have been undertaken to date to shed light on the mechanisms leading to the development of EOTD by establishing mouse models. First, a transgenic mouse model was generated in which mice are overexpressing human ΔE torsinA under control of a rat neuron-specific enolase promoter (104). These transgenic mice showed an abnormal motor phenotype, with self-clasping of limbs, hyperkinesias and rapid bi-directional circling, as well as pathological and neurochemical changes similar to those found in EOTD patients. Perinuclear aggregates and/or inclusions positively staining for torsinA and ubiquitin were found in cholinergic neurons of the pontine and mesencephalic brainstem. Furthermore, those mice showed altered dopamine levels compared to wildtype mice.

Another transgenic EOTD mouse model was generated by Sharma and colleagues (2005), with mice overexpressing either the human ΔE mutant or wildtype torsinA protein under control of the human cytomegalovirus immediate early promoter (105). Whereas wildtype torsinA transgenic mice did not exhibit any overt behavioral deficit,

the ΔE torsinA overexpressing mice showed an age-dependent abnormality in motor learning. No evidence for torsinA-positive inclusions or enrichment at the NE was detected within the CNS of transgenic lines.

However, the relevance of the findings in both transgenic mouse models is questionable for two major reasons. First, driving expression of the ΔE torsinA transgene by an enolase or cytomegalovirus promotor, but not a native DYT1 promotor, may lead to ectopic expression of the protein (106). Secondly, overexpression of the mutant protein at non-physiological levels may produce artefacts, which could obscure the true phenotype.

These obstacles were circumvented by generating torsinA null and knock-in mice (106, 107). Dang and colleagues (2005) observed that only male transgenic mice heterozygous for the human ΔGAG *DYT1* allele displayed an impairment of fine motor coordination and balance. Likewise, changes in dopamine metabolism, such as a reduction in homovanillic acid, could be observed in male knock-in mice. Furthermore, an altered response of striatal cholinergic interneurons to D2 receptor activation, resulting in an excitatory effect, was discovered in this ΔGAG *DYT1* knock-ins (108). This observation is consistent with other findings, pointing to impairment of striatal signaling in EOTD (96, 109). A recent study reports that *DYT1* knock-down mice with reduced levels of torsinA protein also displayed motor deficits and exhibited reduced levels of 3, 4-dihydroxyphenylacetic acid (DOPAC), as it has been similarly observed in *DYT1* knock-in mice (106, 110).

Goodchild and colleagues (2005) went one step further and created knock-in mice containing the ΔGAG mutation within the endogenous mouse Tor1a gene (Tor1a$^{\Delta GAG/\Delta GAG}$), as well as knock-out mice lacking the Tor1a gene (Tor1a$^{-/-}$) (107). They observed that neurons from both homozygous Tor1a$^{\Delta GAG/\Delta GAG}$ knock-in and Tor1a$^{-/-}$ null mice exhibited severely damaged nuclear membranes, whereas heterozygous animals Tor1a$^{+/\Delta GAG}$, Tor1a$^{+/-}$ were indistinguishable from littermate controls. Tor1a$^{\Delta GAG/\Delta GAG}$ and Tor1a$^{-/-}$ mice died within 48 hours postnatal because of their inability to feed and vocalize. The striking similarity between Tor1a$^{\Delta GAG/\Delta GAG}$ and Tor1a$^{-/-}$ mice suggests that Tor1a$^{\Delta GAG}$ may be a loss-of function allele. This is further supported by the finding that animals, carrying the ΔGAG *DYT1* allele over a null allele (Tor1a$^{\Delta GAG/-}$) also died within 48 hours after birth. Interestingly, the NE abnormalities observed in homozygous mutant torsinA mice could not be found in any other cell type than neurons. Moreover, the torsinA protein levels were

decreased in knock-in mice, as compared to wildtype mice, assuming that the ΔE mutation contributes to a reduced stability of ΔE torsinA protein.

Taken together, these results led to the hypothesis that loss of torsinA function within the NE may contribute to the development of EOTD. The similar phenotypes of Tor1a$^{ΔGAG/ΔGAG}$, Tor1a$^{-/-}$ and Tor1a$^{ΔGAG/-}$ mice suggest that Tor1a^{ΔGAG} is a loss-of function allele and may lead to an instable form of mutant torsinA protein.

Recently, Grundmann and colleagues (2007) generated human wildtype and mutant ΔE torsinA transgenic mouse models under control of the murine prion protein (prp) promotor (65). They showed for the first time that not only overexpression of ΔE torsinA leads to cellular dysfunction of neurons but that overexpression of high levels of wildtype torsinA also causes disruption of the NE and formation of intracellular inclusions. Furthermore, these researchers argue that the pathology of mutant torsinA is not restricted to a dopaminergic dysfunction of striatal neurons, as ΔE torsinA transgenic animals displayed increased levels of serotonin and its metabolite 5-HIAA in the brainstem. Thus, their studies point to alterations in the serotonergic system, suggesting that the alterations of brain networks underlying DYT1 dystonia are more complex and comprise more brain regions and neurotransmitter systems than previously assumed. However, the observed behavioral abnormalities of transgenic mice did not resemble DYT1 dystonia - ΔE torsinA transgenic mice showed reduced performance on the rotarod and hyperactivity, whereas wildtype torsinA transgenic mice had abnormalities in fine motor control and balance and were hypoactive.

2.6   TorsinA interactors

2.6.1   TorsinB

TorsinB belongs to the family of torsins and is highly homologous to torsinA (70% homology at the amino acid level). The torsinB gene, *TOR1B*, is located on chromosome 9q34 adjacent to *DYT1*, the torsinA encoding gene (111). Both proteins share several important features, such as an N-terminal signal sequence, hydrophobic amino acid residues, an ATP binding site and a similar molecular weight (torsinB ~38 kD, torsinA ~37 kD) (21). Additionally, torsinB and torsinA are N-glycosylated and reside primarily within the ER and NE in cultured cells. Co-immuno-precipitation and immunocytochemical studies showed that torsinB associates with

both wildtype and ΔE mutant torsinA (111). Moreover, overexpression of torsinB led to an enrichment of immunopositive signal in the perinuclear region and the formation of spheroid inclusions, as it has already been described for ΔE torsinA (56, 57, 111, 112). Immunohistochemical studies in the developing human brain revealed that torsinB protein expression is temporarily and spatially expressed in a similar fashion as torsinA, beginning at 4 to 8 weeks in the cerebellum (Purkinje cells), dopaminergic neurons of substantia nigra, hippocampus and basal ganglia (113). One major difference to torsinA was a higher immunoreactivity of torsinB at the NE. The functional role of torsinB has yet not been elucidated. However, based on the high sequence similarity between torsinB and torsinA, their cellular localization and association, torsinB is suggested to have similar functions like torsinA (111, 113, 114).

2.6.2   Kinesin-I

As eukaryotic cells are organized in different compartments, such as the nucleus, ER and Golgi complex, it is essential to have a set of molecular motors that facilitate intracellular transport of macromolecules and organelles between those. Three types of cytoplasmic motors are known: myosins, which move along actin filaments and kinesins and dyneins that are using microtubules to transport cargo (78, 115, 116). All three motor proteins use energy through ATP hydrolysis to undergo small conformational changes in a globular motor domain, subsequently translated into motion. Additional domains outside the motor are responsible for dimerization, regulation and interaction with cargo.

Kinesin-I, a plus-end directed molecular motor protein was found to associate with torsinA, as a yeast two-hybrid screen revealed KLC1 to specifically interact with torsinA (66). KLC1 is part of the heterotetrameric protein kinesin-I and is thought to be involved in cargo binding and/or regulation of the activity of kinesin-I (79, 117, 118). Binding occurred between the tetratricopeptide repeat domain of KLC1 and the C-terminal region of torsinA. Co-immunoprecipitation confirmed the association of torsinA and kinesin-I and immunocytochemical studies showed co-localization and enrichment of both proteins at growth cones. Furthermore, biotinylation and cross-linking assays revealed that both proteins are cytoplasmatically oriented. As kinesin-I transports organelles anterogradely along microtubules, the above mentioned findings led to the hypothesis that torsinA is transported by kinesin-I, thereby

regulating kinesin-I activity and binding to cargo and thus may be involved in intracellular transport of ER-derived membranes (66).

2.6.3 Vimentin

An involvement of the cytoskeleton in neurologic diseases, such as Parkinson's disease, Alzheimer's disease, amyotrophic lateral sclerosis (ALS) and hereditary spastic paraplegia, has been described (75, 119, 120). A hallmark of these diseases are inclusion bodies, which frequently contain intermediate filament proteins, such as vimentin (121), and microtubule-associated proteins, such as tau (122). Alzheimer's disease is characterized by neurofibrillary tangles consisting of tau and plaques containing the amyloid ß-peptide and also torsinA immunoreactivity has been observed in those inclusions (123, 124). In Parkinson's disease, Lewy bodies contain α-synuclein, γ-tubulin, as well as torsinA and vimentin (93, 125, 126).

Vimentin is a type III intermediate filament that influences neuronal shape and is involved in neurite outgrowth (102, 103). It binds to a variety of cytoskeletal proteins, including kinesin, tubulin, actin and myosin (101). Immunoprecipitation of vimentin from fibroblasts co-precipitated torsinA, as well as α-tubulin, actin and kinesin, supporting that these proteins are forming a complex in these cells (76). Further-more, an association between torsinA and vimentin was observed in control and EOTD patient derived fibroblasts during perturbation of the cytoskeleton. Treatment with trypsin, nocodazole or overexpression of a dominant-negative domain of KLC1 led to the formation of aggregates that were immunopositive for torsinA and vimentin, while tubulin and PDI immunoreactivity remained unaffected. Interestingly, Hewett and colleagues (2006) observed that fibroblasts of EOTD patients show a distinct vimentin staining around the nucleus, which was not apparent in control fibroblasts. However, an alteration of torsinA staining was neither detected in control fibroblasts, nor in EOTD patient derived cells. In addition, Hewett and colleagues (2006) showed that overexpression of ΔE torsinA, but not wildtype torsinA, in neuroblastoma cells inhibited neurite extension in response to retinoic acid. In those cells the formation of torsinA- and vimentin-positive inclusions was observed.

In summary, these results suggest that the disease-associated ΔE torsinA may interfere with cytoskeletal dynamics, possibly mediated by impairing the movement of vimentin.

2.6.4 LAP1 and LULL1

TorsinA has been shown to be an ER-resident protein but several studies indicate that it is also present in the NE (70, 71). Additionally, ΔE torsinA has been observed to be abnormally enriched at the NE, indicating that torsinA may bind to substrates within this structure (70, 71, 112).

To confirm this hypothesis Goodchild and colleagues (2005) performed a screen in which they searched for NE substrates that alter localization of torsinA from the ER to the NE (91). They selected candidate proteins that normally reside in the NE and are suggested to have a potential functional role within the NE, as they are containing predicted lumenal domains. The lamina associated protein 1 (LAP1) was found to recruit torsinA to the NE in a perinuclear distribution reminding on the ATP hydrolysis mutant torsinA that functioned as a substrate trap (71). LAP1 is known to bind A- and B-type lamins, it contains a putative transmembrane and lumenal domain but its functional role is poorly understood (127, 128).

Co-immunoprecipitation and co-localization studies of the ATP hydrolysis mutant torsinA and ΔE torsinA, respectively, with LAP1 further supported an interaction with torsinA at the NE. Moreover, Goodchild and colleagues generated LAP1 variants that contain the isolated lumenal domain, which no longer concentrates in the NE but localizes in the ER. Overexpression of this lumenal domain altered the subcellular localization of both ΔE torsinA and the ATP hydrolysis mutant torsinA, by redistributing the proteins from the NE to the ER, indicating that this domain is responsible for the interaction with torsinA. Furthermore, co-immunoprecipitation of LAP1 with either the ATP hydrolysis mutant torsinA or wildtype torsinA showed a stronger binding of LAP1 to the hydrolysis mutant, suggesting that it is a torsinA substrate.

In addition, these researchers identified a novel transmembrane protein to interact with torsinA, which they called lumenal domain like LAP1 (LULL1) (91). This protein resides within the ER, has a single predicted transmembrane domain and as included in its name, contains a lumenal domain like LAP1. Overexpression of full-length LULL1 or only the lumenal domain of LULL1 also revealed a re-localization of ATP hydrolysis mutant torsinA from the NE to the ER.

Taken together, the authors suggest that LAP1 and LULL1 are substrates of torsinA either in the NE or the ER.

2.7 Objectives

2.7.1 Preliminary work

There is one interesting difference between torsinA and other AAA$^+$ proteins, namely the lack of an obvious substrate binding domain and other functional regions on either end of the ATPase domain. This complicates the search for torsinA interacting proteins and identifying the pathway(s) in which the torsin proteins function. In order to discover new interactors and to get more insights into the function of torsinA, a yeast two-hybrid screen in an adult human brain cDNA library has been conducted previously (66). Amino acids 251-332 of the C-terminus of human wildtype torsinA where used as bait, which contain the α-helical sensor 2 motif, spanning the region of the EOTD-causing glutamic acid deletion. 15 positive clones were identified and subdivided into three subgroups: ten encoded fragments of KLC 1, three the non-motor domain of unconventional myosin IX A, and two encoded hBex2 (human brain expressed X-linked protein 2).

In humans, *Bex2* belongs to a gene family clustered on the X-chromosome, which comprises *Bex1* (*REX3/NADE4*), *Bex2* (*NADE5*), *Bex3* (*HGR74/NADE*), *Bex4* and *Bex5*. The *hBex2* ORF consists of 375 bp, resulting in a peptide of 125 amino acids with a calculated molecular weight of 14.4 kD (129-134). Amino acid sequence analyses of hBex2 protein revealed the presence of a charged histidine-rich domain near the C-terminus (aa 114-117) and a C-terminal CAAX motif (CLMP, aa 122-125) (Fig. 6). The latter is a potential signal for posttranslational lipid modification and can mediate insertion of the target protein to cellular membranes (135). Additionally, hBex2 contains a stretch of positively charged amino acids (aa 46-58), corresponding to the requirement of a nuclear localization signal (136). Alignments show that the amino acid sequences of hBex1 and hBex2 are nearly identical (87% identical, 90% similar), whereas hBex3, 4 and 5 are more distantly related (Fig. 6). Interestingly, the C-terminal histidine-rich domain and the CLMP motif are highly conserved throughout all human Bex family members, except hBex4, and may therefore reflect an important functional domain (Fig. 6). Although several features of Bex proteins suggest that they might act as modulators in intracellular signaling pathways and may be involved in dopaminergic neuron differentiation, little is known about the specific cellular function of hBex2 (129-133).

```
hBex1 MESKEERALNNLIVENVNQENDEKDEKEQVANKGEPLALPLNVSEYCVPRGNRRRFRVRQPILQYRWDIMH
hBex2 MESKEKRAVNSLSMENANQENEEK---EQVANKGEPLALPLDAGEYCVPRGNRRRFRVRQPILQYRWDMMH
hBex3 -------------MANIHQENEEM---EQ-PMQNGEEDRPLGGGEGHQPAGNRR-GQARRLAPNFRWAIPN
hBex4 MESKEELAANNLNGENAQQENEGG---EQAPTQNEEESRHLGGGEGQKPGGNIRRGRVRRLVPNFRWAIPN
hBex5 ------------MENVPKENKVV---EKAPVQN--EAPALGGGEYQEPGGNVK-GVWAPPAPGFGEDVPN
                *  :**.     *:  . :.       *. .*   *  ** :       :   : :

hBex1 RLGEP--QARMREENMERIGEEVRQLMEKLREKQLSHSLRAVSTDPP-HHDHHDEFCLMP 128
hBex2 RLGEP--QARMREENMERIGEEVRQLMEKLREKQLSHSLRAVSTDPP-HHDHHDEFCLMP 125
hBex3 RQIN--DGMGGDGDDMEIFMEEMREIRRKLRELQLRNCLRILMGELSNHHDHHDEFCLMP 111
hBex4 RHIEH----NEARDDVERFVGQMMEIKRKTREQQMRHYMRFQTPEPD----NHYDFCLIP 120
hBex5 RLVDNIDMIDGDGDDMERFMEEMRELRRKIRELQLRYSLRILIGDPP-HHDHHDEFCLMP 111
            *  :       :::* :   :: ::  .* ** *:   :*    :        :* :***:*
```

Fig. 6: Amino acid sequence and structure predictions of the hBex2 protein.

A ClustalW sequence alignment of human Bex proteins 1, 2, 3, 4 and 5 is depicted (accession numbers AY833560, AF220189 (AY833561), AF187064, AY833563 and AY833564, respectively). Highlighted sequence in grey marks the region used for Bex2 antibody generation (aa 1-13). Yellow highlighted amino acids 46-58 mark the NLS, green highlighted amino acids 114-118 mark the histidine-rich charged region and orange highlighted amino acids 122-125 depict the CAAX prenylation motif.

2.7.2 Goals of this study

Although many hypotheses about the role of torsinA in neurons of the mammalian brain have emerged, its precise cellular function still remains unknown. Hence, the mechanism of how the GAG deletion in *DYT1* contributes to the development of EOTD is unsolved. One possibility to discover a piece of puzzle of torsinA's cellular function is the search for interactors and their related functions. hBex2 has been found to be a torsinA interacting protein in a previously performed yeast two-hybrid screen (66). Thus, the main focus of this study was the biochemical validation of the interaction between torsinA and hBex2. For this purpose an antibody against hBex2, which had been generated elsewhere (Xandra O. Breakefield, Massachusetts General Hospital, not published), was characterized with respect to its specificity and functionality.

At the beginning of this study little was known about the role of Bex2 in the mammalian brain. To gain more insights into the function of Bex2 and contribute to the understanding of torsinA function, this study further aimed at characterizing the subcellular localization of Bex2 and torsinA within compartments and a possible co-localization of both proteins in neurons of the mammalian brain.

The EOTD causing mutant torsinA variant was previously shown to be abnormally enriched at the NE and to re-locate wildtype torsinA from the ER to the NE in patient derived fibroblasts and neurons of ΔE torsinA transgenic mice (70). Additionally, ΔE torsinA was shown to influence localization of cytoskeletal vimentin, as an enrichment of vimentin at the NE has been observed in EOTD patient-derived

fibroblasts (76). Thus, it has been suggested that ΔE torsinA has altered substrate binding abilities (71, 91). For this reason, a possible effect of ΔE torsinA on Bex2 binding and localization was examined.

In the yeast two-hybrid screen the C-terminal amino acids 251-332 of human torsinA were used as bait, showing that the interaction between torsinA and hBex2 occurs within the region that contains the sensor2 motif of torsinA. To identify the torsinA-interacting domain of hBex2, several hBex2 deletion constructs were generated and the resulting truncated proteins were tested for their ability to bind torsinA. Furthermore, the relevance of predicted sequence motifs of hBex2, such as the NLS and CAAX, were proven by studying the subcellular localization of hBex2 deletion variants.

Given that Bex2 interacts with torsinA, it is likely that its expression is similar to torsinA. Hence, the expression of *Bex2* mRNA and Bex2 protein has been investigated in various tissues. Additionally, Bex2 protein expression has been assessed in a variety of neuronal cell lines and its distribution in the adult rat brain was examined, in comparison to torsinA expression patterns.

In summary, this study was undertaken to validate the torsinA-hBex2 interaction and to gain information about the functional relevance of torsinA binding.

3 RESULTS

3.1 Characterization of the polyclonal Bex2 antibody

Little has been known about the novel identified, torsinA-interacting protein Bex2. In order to study the functional role of this protein, a polyclonal antibody against amino acids 1-13 of human Bex2 was generated. It has to be mentioned that the N-terminal region of hBex2, used to generate the antibody, is highly similar to the corresponding region in the hBex1 homolog (77% identical). Therefore, it is likely that the Bex2 antibody recognizes both Bex1 and Bex2. As the Bex2 antibody has previously not been characterized or described, its specificity and functionality were investigated by performing immunoprecipitation (IP), immunoblotting (IB), immunocytochemistry (ICC) and immunohistochemistry (IHC).

First, the anti-Bex2 antibody was analyzed by IB, using Neuro-2A cell extracts, endogenously expressing Bex2 (Fig. 7A). An immunoreactive band at approximately 25 kD band was detected in these mouse cell extracts (Fig. 7A upper lanes). The antibody specificity was confirmed by preadsorption experiments, pre-incubating the Bex2 antibody with purified MBP-hBex2 fusion protein. Thus, specific binding of MBP-hBex2 fusion protein to the Bex2 antibody is expected to result in suppression of immunoreactive signals in the following experiments. Preadsorption of the Bex2 antibody completely supressed the 25 kD band (Fig. 7A, compare lower lanes), demonstrating that the Bex2 antibody specifically recognizes mouse Bex2 protein. As the calculated molecular weight of Bex2 is approximately 14 kD, appearance of a higher molecular weight band may indicate that Bex2 undergoes post-translational modification. Similar findings were previously reported by Koo and colleagues (2005) that demonstrated the existence of a 23 kD immunoreactive in CHO cells transfected with mouse Bex2 using an anti-Bex1 polyclonal rabbit antibody that also recognizes Bex2 (137).

Furthermore, specificity of the anti-Bex2 antibody was analyzed by IP. Therefore, mouse neuroblastoma cell lysate (Neuro-2A) was incubated with Bex2 antibody, bound to protein A beads. Subsequent IB analysis of the resulting protein eluate with the Bex2 antibody revealed a single immunoreactive band (Fig. 7B, first lane), which co-migrated with the 25 kD band in the cell extract (Fig. 7B, last lane). As a negative

control, rabbit immunoglobulin G was bound to protein A beads and incubated with mouse neuroblastoma cell lysates. No immunoreactive band was observed in the eluate from the control IP (Fig. 7A, middle lane), showing that precipitation of endogenous mouse Bex2 from Neuro-2A cells with the Bex2 antibody is specific.

In addition, the Bex2 antibody was tested to recognize overexpressed human Bex2 protein, which is N-terminal tagged to a FLAG epitope (Fig. 7C). Hence, overexpressed hBex2 can be detected with the Bex2 antibody, as well as an antibody directed against the FLAG epitope, the latter serving as a transfection control. Using the Bex2 antibody a 25 kD band was observed in both transfected and non-transfected mouse neuronal CAD cell lysates (Fig. 7C). In extracts of transfected cells an additional band was detected, migrating at approximately 23 kD. Both, the 23 kD and 25 kD species were also observed in transfected cell extracts by staining with the FLAG antibody, which reflects overexpressed human Bex2 (Fig. 7C). As the Bex2 antibody shows similar immunoreactive bands like the FLAG antibody, anti-Bex2 is assumed to specifically recognize overexpressed human Bex2. However, the detection of a lower 23 kD band is surprising, as overexpressed Bex2 carries a N-terminal FLAG epitope and would therefore be expected not to migrate lower than endogenous Bex2. Thus, it might be possible that overexpressed epitope tagged Bex2 is modified differently from the endogenous protein.

Finally, the antibody was tested to specifically recognize endogenous Bex2 in neurons of adult rat brain, by performing ICC and IHC experiments (Fig. 7D, E). Staining with the Bex2 antibody revealed strong intra-nuclear immunoreactivity (IR) in neurons of adult rat brain in both ICC and IHC (Fig. 7D, E, first panels). A significant reduction of IR was observed, by preadsorbing the Bex2 antibody with recombinant MBP-hBex2 protein (Fig. 7D, E), indicating that anti-Bex2 specifically detects endogenous rat Bex2.

Taken together, these results confirm that the antibody, which has been raised against the N-terminal region of human Bex2, specifically recognizes endogenous mouse and rat Bex2, as well as overexpressed human Bex2 in mammalian cell lines. The calculated molecular weight of Bex2 is approximately 14 kD, thus the presence of two immunoreactive species at 23 kD and 25 kD, respectively, may indicate that Bex2 is post-translational processed. Furthermore, the Bex2 antibody was shown to function in IP, IB, ICC and IHC.
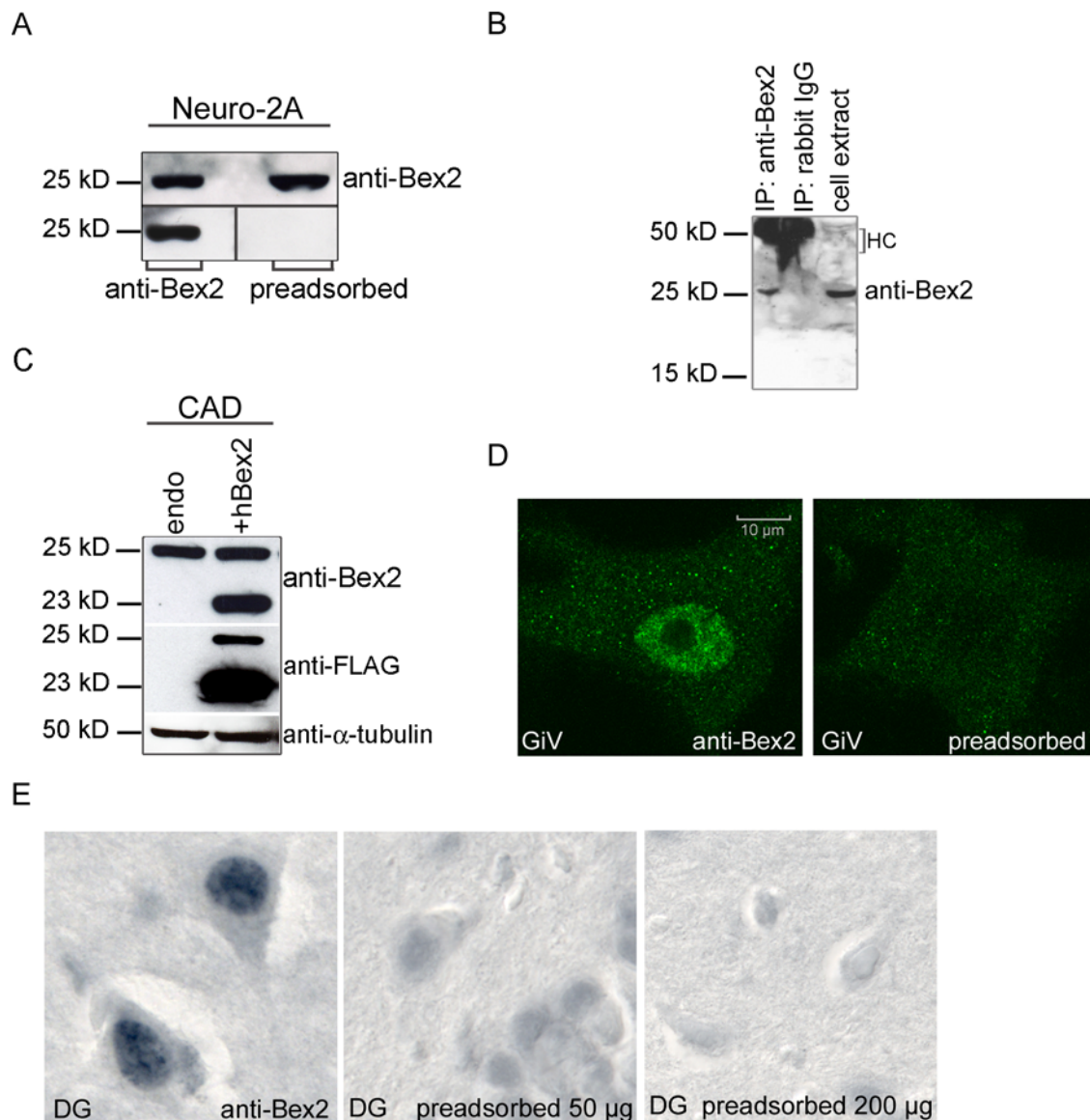
Fig. 7: Specificity of the polyclonal Bex2 antibody.

A) IB analyses of Neuro-2A cell extracts showed a 25 kD immunoreactive band using the Bex2 antibody, reflecting endogenous Bex2 (upper lanes). The membrane was cut and after stripping off antibodies, one strip was re-probed with the Bex2 antibody showing strong IR (lower left lane), whereas the other strip was incubated with Bex2 antibody preadsorbed with the MBP-hBex2 recombinant protein. Preadsorption of anti-Bex2 led to complete suppression of immunoreactive Bex2 signal (lower right lane). **B)** Endogenous Bex2 protein from mouse Neuro-2A cells was specifically immunoprecipitated with the Bex2 antibody, detected as a 25 kD band in IB using the Bex2 antibody (left lane). No IR was observed in the control IP with matched amounts of rabbit immunoglobulin G (middle lane). The same immunoreactive 25 kD band was observed in total cell extract, using the Bex2 antibody (right lane). *HC*, antibody heavy chain **C)** CAD cell extracts, either transfected with hBex2 that carries a N-terminal fused FLAG epitope or non-transfected, were used in IB analyses. Staining with the Bex2 antibody revealed a 25 kD band in non-transfected cells and an additional 23 kD band in hBex2 transfected cells (upper lanes). Use of an antibody specific to the FLAG epitope of hBex2, also detected the 25 and 23 kD bands in transfected cell extracts, but did not recognize any signal in non-transfected cells (middle lanes). Staining against α-tubulin shows loading of equal protein amounts (lower lanes). **D, E)** ICC and IHC analyses of adult rat brain neurons showed strong nuclear IR after staining with Bex2 antibody (first panels) and a significant reduction of Bex2 IR after preadsorption of the antibody. In IHC preadsorption of the Bex2 antibody with 200 µg recombinant MBP-hBex2 was sufficient to significantly reduce Bex2 IR (3rd panel), whereas some Bex2 signal remained after preadsorption with only 50 µg MBP-hBex2 (2nd). DG, dentate gyrus; GIV, gigantocellular reticular nucleus, ventral part

3.2 Expression of Bex2 and torsinA in mammalian tissues and cell lines

To get an idea about the function of Bex2, it is important to study its expression at the mRNA and protein level in different tissues. Recent studies described Bex2 to be primarily present in brain but absent in peripheral tissues, indicating that it is has a specialized function within the brain (133). This finding was confirmed at the transcriptional level by performing qRT-PCR using mRNA of various human tissues. Whereas hBex2 mRNA was detected within different brain regions of adult human brain and abundant in fetal brain, no signal was detected in lung and heart (Fig. 8). The examined mRNAs showed highest levels of hBex2 in the cerebellar cortex, cerebellum and putamen of adult human brain.
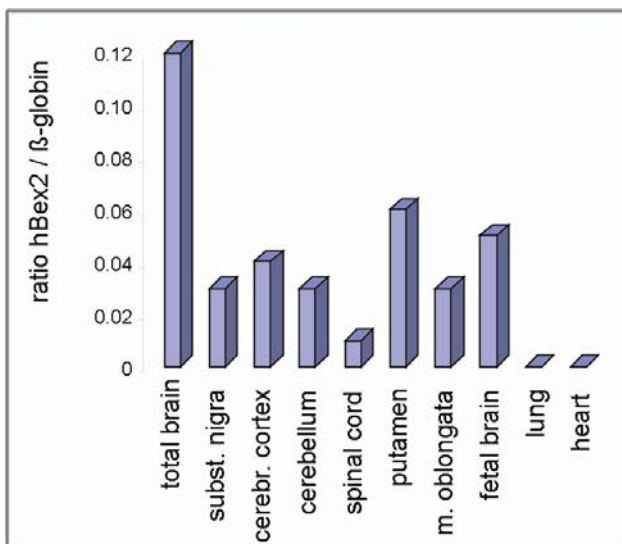
Fig. 8: Expression of hBex2 mRNA in human tissues.

qRT-PCR analyses showed ubiquitous expression of hBex2 mRNA throughout the human brain with highest levels in the cerebellar cortex, cerebellum and the putamen but was absent in peripheral tissues, such as lung and heart. hBex2 mRNA was also detected in mRNA of fetal brain.

To investigate the brain regional expression of Bex2 at the protein level, IB analyses of rat brain tissues were performed, using the Bex2 antibody (Fig. 9). Two distinct bands with molecular weights of 15 kD and 25 kD were apparent in all examined rat brain structures (Fig. 9A, left panel). IR of both, the 15 and 25 kD band, was almost completely omitted by preadsorption of the Bex2 antibody with recombinant MBP-hBex2 protein (Fig. 9A right panel), indicating that the antibody specifically detects the 15 kD and 25 kD band, probably reflecting Bex2 isoforms. To examine whether the presence of the 15 kD Bex2 isoform is rat specific, IB analyses with extracts from human, mouse and rat brain were performed (Fig. 9B). A 25 kD band was detected in rat and mouse brain, whereas the 15 kD band was only seen in rat brain extract,

indicating that this Bex2 isoform is rat specific. Surprisingly, no IR was observed in extracts of human cortex, cerebellum and brain stem. This may either be due to low antibody sensitivity to endogenous human Bex2 or due to protein degradation, as human post mortem tissue had been used. Staining against torsinA revealed weak IR in human brain tissue extracts, but no IR was detected in rat and mouse brain extracts (Fig. 9B).

Contradictory to previous findings, which showed that Bex2 is primarily expressed throughout the brain (133), in this study IB analyses with the Bex2 antibody also revealed Bex2 IR in non-neuronal peripheral rat tissues (Fig. 9C). Assuming that Bex2 is present in cells of the mammalian brain but not in non-neuronal tissues, this observation indicates that the Bex2 antibody also recognizes the highly similar Bex1 homolog. In fact, human *Bex1* gene expression has been shown to be high in the CNS, as well as in peripheral tissues, such as liver, kidney and heart (133).

Furthermore, Bex2 and torsinA expression were examined in several neuronal and non-neuronal mammalian cell lines, as well as primary rat cortical neurons (RCN), using antibodies against Bex2 and torsinA (Fig. 9D). Bex2 protein was detected in neuronal-like cells, such as mouse neuroblastoma CAD and Neuro-2A, human bone marrow neuroblastoma SH-SY5Y, rat pheochromocytoma PC-12 and RCN, but neither in SKN (human brain neuroblastoma) nor in non-neuronal HEK 293T (human embryonic kidney) cell lines (Fig. 9D). In neuronal-like cells Bex2 was detected as a 25 kD band, whereas in primary neurons from rat an additional 15 kD band was observed, similar to IB analyses of adult rat brain extracts (compare Fig. 9B and D). TorsinA IR was observed in neuronal as well as non-neuronal cells, but the IR was week in cell lines derived from mouse neuroblastoma and rat pheochromocytoma cells (Fig. 9D), suggesting that the anti-torsinA antibody preferentially recognizes human torsinA.

In summary, endogenous Bex2 protein is ubiquitously expressed through all rat brain structures examined in this study, present in mouse brain, as well as various mammalian neuronal cell lines. Unfortunately, the Bex2 antibody failed to recognize endogenous Bex2 from human brain tissues. Furthermore, using the monoclonal D-M2A8 anti-torsinA antibody, torsinA was detected in human brain extracts but neither in rat nor mouse brain tissues. Additionally, torsinA-positive IR in neuronal mouse and rat cells lines was weak, indicating that this antibody poorly detects

mouse and rat torsinA, respectively. Furthermore, as Bex2 is known to be primarily expressed in brain, it is very likely that the Bex2 antibody also recognizes Bex1, as immunoreactive bands were detected in extracts of non-neuronal rat tissues.
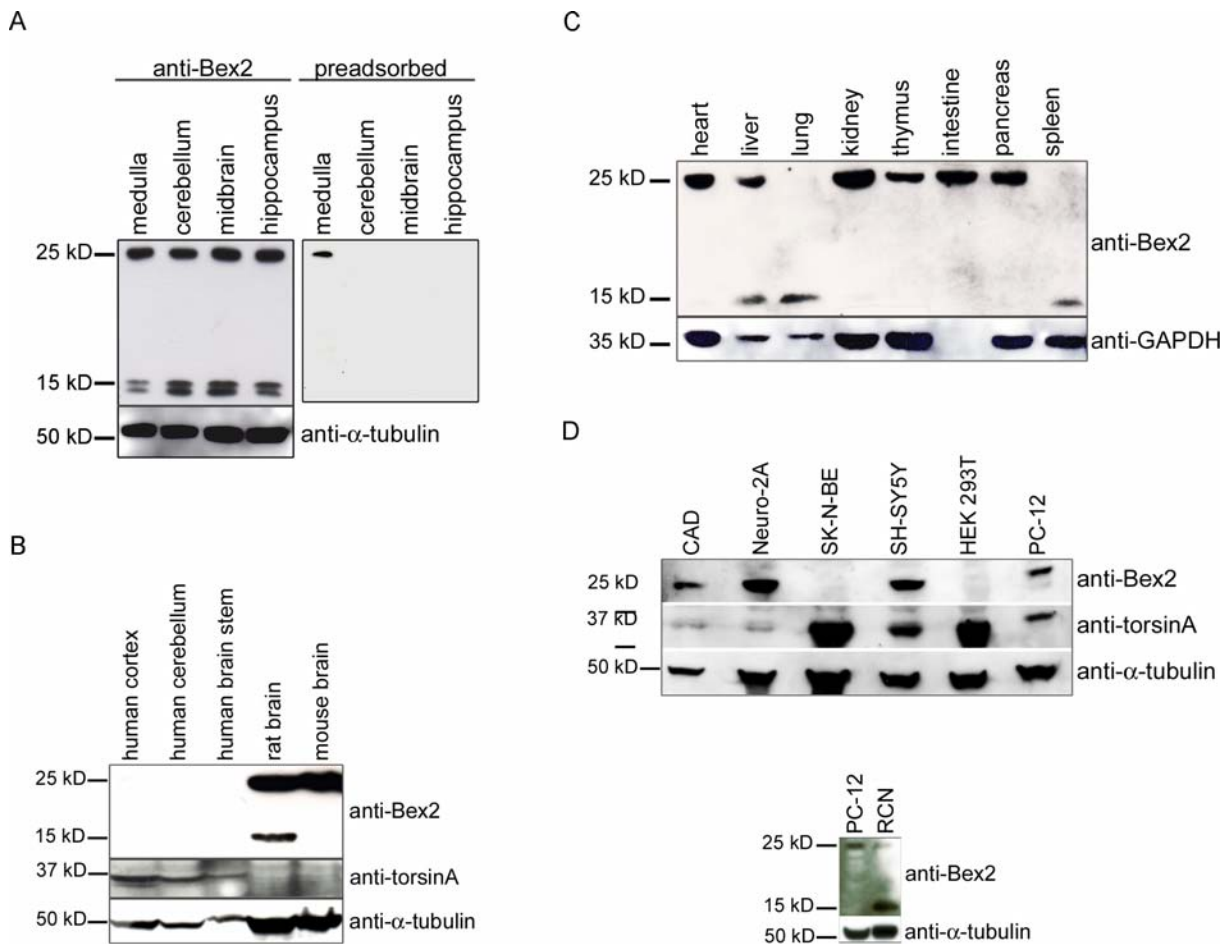
Fig. 9: Endogenous Bex2 and torsinA expression in mammalian tissues and cell lines.
A) Bex2 IR was detected in all examined rat brain structures, apparent as 15 and 25 kD bands. Preadsorption of the Bex2 antibody with the MBP-hBex2 fusion protein led to an almost complete supression of both immunoreactive species. Staining against α-tubulin shows equal loading of protein extracts. **B)** IB analysis of human, rat and mouse brain extracts with the Bex2 antibody revealed IR at 25 kD in rat and mouse, but no IR in the human cortex, cerebellum and brain stem. The 15 kD Bex2 isoform was only present in rat brain extracts. TorsinA staining showed IR in the examined human brain structures but no torsinA IR was observed in rat and mouse brain extracts. Staining against α-tubulin shows loaded protein amounts. **C)** IB analysis of peripheral rat tissues revealed the existence of a 15 and/or 25 kD band. Staining against GAPDH shows loaded protein amounts. **D)** Bex2 IR was observed in neuronal CAD, Neuro-2A, SH-SY5, PC-12 cells and RCN, whereas torsinA IR was detected in neuronal and in non-neuronal cell lines. α-tubulin staining shows even protein loading.

3.3   Bex2 and torsinA interact in *in vitro* affinity precipitation assays

hBex2 has been identified as a torsinA interacting protein in a yeast two-hybrid screen of a human brain cDNA library (66). Thus, the relevance of this association was further confirmed biochemically, by performing protein-protein-interaction assays (MBP-affinity precipitation) with torsinA and Bex2.

Furthermore, as the ATP hydrolysis mutant torsinA and the disease-associated ΔE torsinA are both enriched at the NE after overexpression in cell culture, some researchers suggest that torsinA may have specific substrates at the NE and that both mutant variants may display altered substrate binding abilities (71, 91). Thus, the binding behavior of Bex2 to the disease-associated ΔE torsinA was also studied in MBP-affinity precipitation assays.

In a first approach, HEK 293T cell lysates, containing either overexpressed human wildtype torsinA or ΔE torsinA protein, were incubated with purified MBP-hBex2 fusion protein (Fig. 10A). Both wildtype and mutant torsinA bound to MBP-hBex2, whereas no binding to the MBP control was observed. Affinity precipitation furthermore revealed two distinct species of ΔE torsinA that bound to Bex2, one band typically migrating at 35 kD and a second migrating higher at approximately 37 kD (Fig. 10A, arrows). Hence, this additional higher molecular weight band may reflect a ΔE torsinA variant that is differentially modified, possibly by glycosylation. Interestingly, another higher molecular weight band at approximately 40 kD was observed in cell extract, overexpressing ΔE torsinA, suggesting a third differently processed protein variant.

In the reverse order, when HEK 293T cell lysates containing overexpressed hBex2 were incubated with either recombinant MBP-torsinA or the mutant variant MBP-ΔE torsinA, hBex2 bound to both torsinA and ΔE torsinA (Fig. 10B). Only marginal binding to MBP alone was observed. In both assays it appeared that Bex2 has a slight tendency to bind stronger to ΔE torsinA, particularly the unmodified 15 kD variant (Fig. 10B, C).
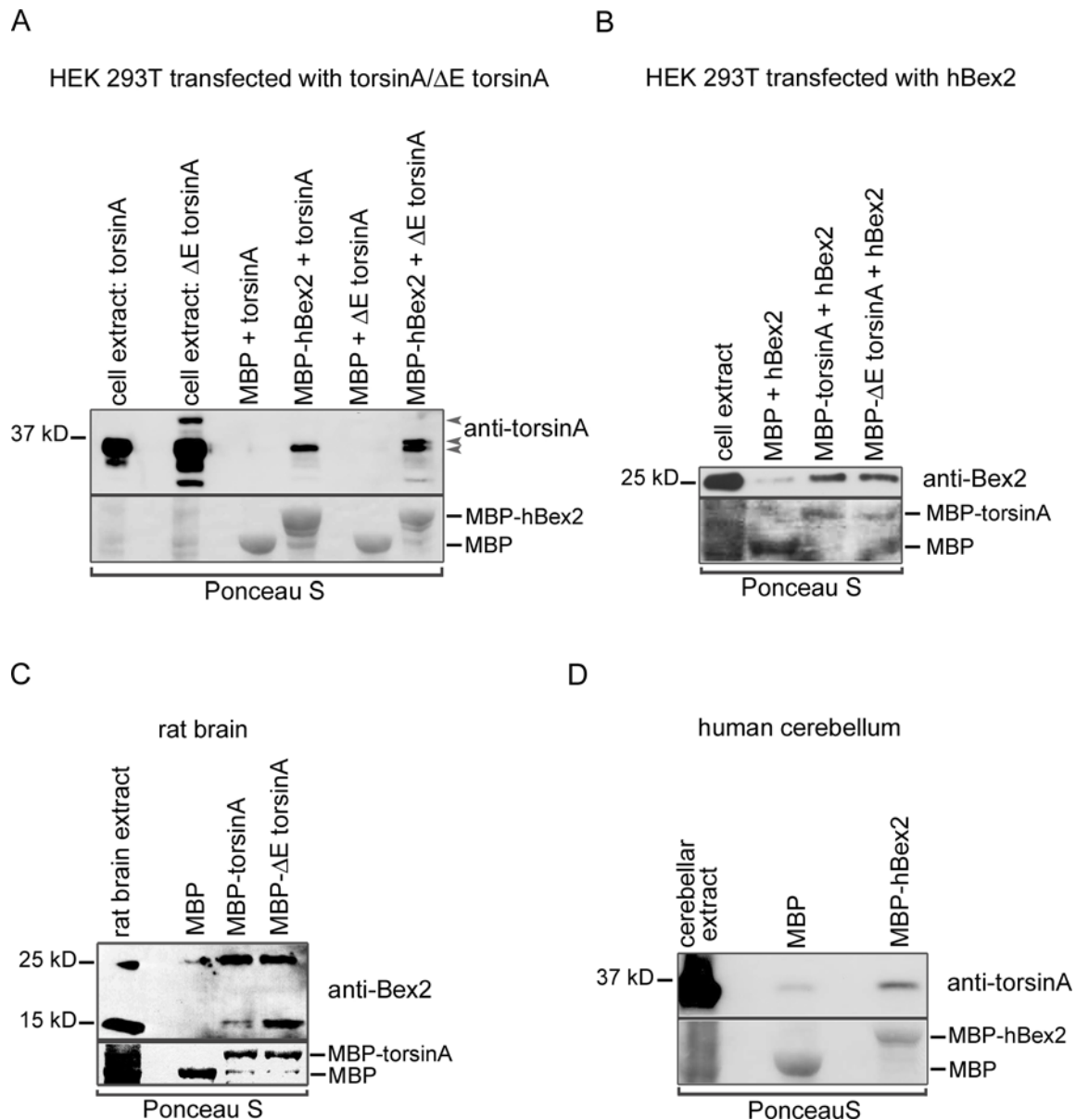
Fig. 10: Bex2 interacts with wildtype and mutant torsinA in *in vitro* affinity precipitation assays.
A) Overexpressed wildtype torsinA and ΔE torsinA proteins were affinity purified with MBP-hBex2 fusion protein, no binding to MBP alone was observed. Different species of ΔE torsinA bound to Bex2, which migrated at 35 kD and 37 kD, respectively (lower grey arrows), indicating the presence of post-translational modified forms of ΔE torsinA. A third higher molecular weight band was observed in ΔE torsinA overexpressing cell extract (upper grey arrow). **B)** Overexpressed hBex2 binds to wildtype and mutant MBP-torsinA. Binding of hBex2 to MBP was marginal. **C)** Two distinct endogenous iso-forms of Bex2 (15 kD and 25 kD) were affinity purified from rat brain with both recombinant MBP-torsinA and MBP-ΔE torsinA. No binding to the MBP control was observed for the 15 kD isoform, whereas the 25 kD isoform slightly bound to the control. **D)** Endogenous torsinA from human cere-bellum was affinity purified with MBP-hBex2, with only slightly binding to MBP.

A second approach addressed the question whether endogenous brain-derived Bex2 and torsinA, respectively, also interact with the appropriate MBP fusion protein. Incubation of rat brain lysate with either MBP-torsinA or MBP-ΔE torsinA resulted in precipitation of two distinct Bex2 immunoreactive species, migrating at 15 kD and 25 kD, respectively (Fig. 10, compare B and C), which have already been detected in

prior IB analysis of rat brain extracts (Fig. 9B). Thus, affinity precipitation confirmed that both isoforms are interacting with torsinA. No binding of the 15 kD Bex2 isoform to MBP was observed, whereas the 25 kD isoform slightly bound to the MBP control (Fig. 10C). Moreover, the 15 kD Bex2 isoform seemed to bind stronger to ΔE torsinA than to wildtype torsinA. In contrast, this effect has not been observed for the 25 kD isoform. In the reverse experiment human cerebellar lysate was incubated with recombinant MBP-hBex2, which revealed binding of endogenous human torsinA to hBex2 (Fig. 10D). Only marginal binding of torsinA to the MBP control was detected. Taken together, these results show that wildtype and mutant torsinA bind Bex2 *in vitro*, either overexpressed in cells or endogenous from mammalian brain. Moreover, affinity precipitation assays indicate, that Bex2 tends to bind ΔE torsinA with higher affinity than wildtype torsinA. Furthermore, both the 15 kD and 25 kD Bex2 isoforms were affinity precipitated from rat brain extracts, suggesting the existence of monomeric (15 kD) and/or dimeric (25 kD) Bex2 isoforms or post-translational modification of Bex2.

Affinity precipitation assays demonstrated the interaction between torsinA and Bex2. Hence, another question to be resolved was whether torsinA – Bex2 complexes can be identified *in vivo*, using a different protein-protein interaction assay that co-precipitates complexed proteins.

IP was performed with an immobilized antibody against torsinA, which was subsequently incubated with adult rat brain extract. This analysis revealed specific precipitation of torsinA from rat brain extracts, as well as co-precipitation of Bex2 (Fig. 11A). However, using immobilized mouse IgG as a control also precipitated Bex2, indicting that a significant amount of Bex2 binds unspecifically to beads and/or IgG (Fig. 11A).

Although no torsinA IR was observed in the rat brain extract, torsinA immunopositive signal was detected after enrichment in the IP, showing that torsinA is poorly detected in rat brain extract (Fig. 11A). Hence, co-IP with human brain extract was performed, resulting in precipitation of torsinA with immobilized monoclonal and polyclonal torsinA antibodies, respectively (Fig. 11B, upper panel). However, co-precipitation of Bex2 with either of these antibodies failed or could not be detected with the Bex2 antibody in subsequent IB due to cross reactivity with eluted antibody chains (Fig. 11B, lower panel).
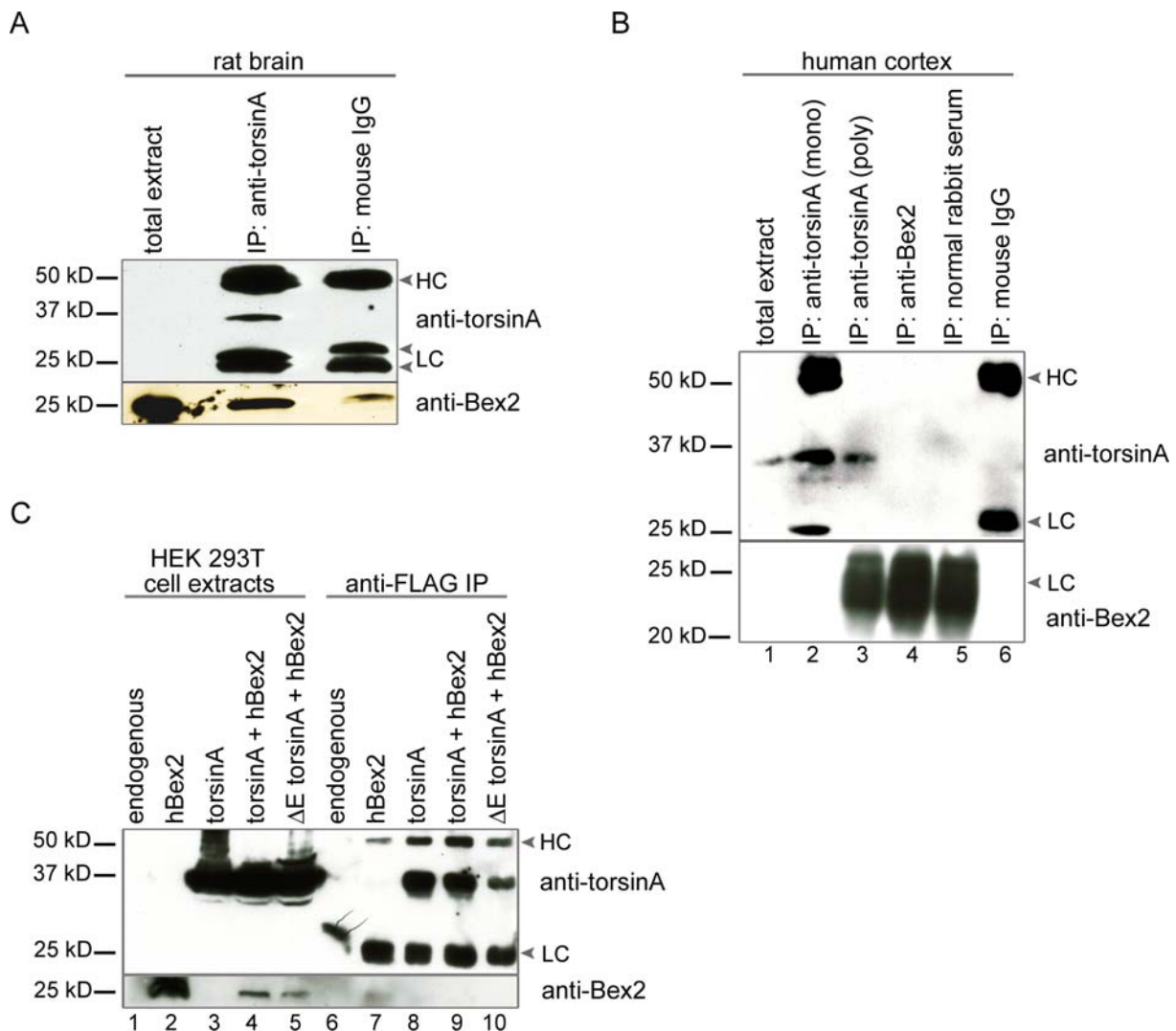
Fig. 11: Analyses of torsinA-Bex2 complexes using co-IP.

A) Anti-torsinA and mouse IgG were non-covalently coupled to protein G beads and subsequently incubated with rat brain extracts. Eluted proteins were analysed by IB, using antibodies directed against torsinA and Bex2, respectively. TorsinA was specifically precipitated (middle lane), as no IR was observed in the mouse IgG control IP (last lane). Staining against Bex2 showed IR in both the anti-torsinA IP and mouse IgG control IP, indicating non-specific binding of Bex2 to beads and/or IgG. Arrows point at antibody heavy (HC) and light chains (LC), respectively. **B)** Mouse monoclonal (mono) and rabbit polyclonal (poly) torsinA antibodies, Bex2 antibody, normal rabbit serum and mouse IgG were bound to beads, followed by incubation with extracts from human cortex. Anti-torsinA IP resulted in precipitation of torsinA (upper panel, lane 2 and 3), but did not co-precipitate Bex2 protein (lower panel, lane 2). Intense crossreactivity of eluted antibody chains was detected after staining with the secondary antibody (lower panel, lanes 3-5), thus precluding detection of possible Bex2 IR. Arrows point at antibody heavy (HC) and light chains (LC), respectively. **C)** HEK 293T cells overexpressing hBex2 and torsinA, respectively or both hBex2 and torsinA (either wildtype or ΔE torsinA) were used in anti-FLAG IPs. N-terminal FLAG-tagged hBex2 binds to a immobilized FLAG specific antibody. The lower panel shows overexpressed (lane 2, 4 and 5) and precipitated hBex2 (lane 7). The upper panel shows staining against torsinA. TorsinA IR was also observed in the negative control IP (lane 8), indicating that torsinA binds non-specifically to beads. Thus, the apparent co-precipitation of wildtype and ΔE torsinA in lanes 9 and 10 may reflect unspecific binding of both variants to the beads. Arrows point at antibody heavy (HC) and light chains (LC), respectively.

To circumvent crossreactivity of the secondary antibody with eluted antibody chains in IB analyses and to enhance Bex2 binding to an antibody in IP, FLAG IPs were

performed (Fig. 11C). Thus, HEK 293T cells either single transfected with FLAG-tagged hBex2 and torsinA, respectively, or co-transfected with hBex2 and torsinA variants were used in FLAG IPs. Slight precipitation of hBex2 was detected in hBex2 single transfected cells, overexpressing the highest amount of hBex2, indicating that the protein binds to the FLAG antibody (Fig. 11C, lower panel, lane 7). Cells overexpressing torsinA served as a control in the FLAG-IP to test for unspecific binding of torsinA to beads. Indeed, although no FLAG-tagged protein was present in extracts of the control IP, precipitation of torsinA was observed, indicating that torsinA binds non-specifically to beads (Fig. 11C, upper panel, lane 8). Thus, the detected torsinA IR in the FLAG IP with hBex2/torsinA co-transfected cell lysates reflects non-specific binding of torsinA to beads rather than specific binding to Bex2 (Fig. 11C, lanes 9 and 10).

In summary, none of the performed co-IPs resulted in precipitation of the torsinA-Bex2 *in vivo* complex, as several limitations complicated its identification (see discussion). Nevertheless, these analyses do not exclude the presence of such an *in vivo* complex.

3.4 Bex2 and torsinA co-localize at the NE and in processes of neuron-like cells

Having confirmed the biochemical interaction between Bex2 and torsinA, their subcellular localization and a possible co-localization of both proteins was investigated by performing ICC in neuronal mouse neuroblastoma cells (Neuro-2A). Endogenous Bex2 IR in Neuro-2A cells was observed in a punctuated pattern throughout the cytoplasm and within the nucleus, as indicated by staining with nucleoporin p62, a subunit of the nuclear pore complex (Fig. 12A-C). ICC confirmed the finding of previous IB analyses (Fig. 9D), revealing weak expression of endogenous torsinA in Neuro-2A cells (data not shown). To investigate the subcellular localization of torsinA, Neuro-2A cells were transfected with torsinA. Overexpressed torsinA was observed throughout the cytoplasm and at the NE, as indicated by nucleoporin p62 marker staining (Fig. 12D-F). Similar findings have been reported in previous studies, also showing an enrichment of torsinA at the NE of transfected BHK21 cells (hamster fibroblasts) and in infected Gli36 cells (70, 112). Previous studies furthermore demonstrated an abnormal high concentration of ΔE torsinA at the NE of EOTD

patient-derived fibroblast and cultured neurons (70, 71, 85). Indeed, Neuro-2A cells overexpressing ΔE torsinA showed distinct enrichment of mutant torsinA at the NE, even more abundant than overexpressed wildtype torsinA (Fig. 12G-I). Moreover, previous cell culture studies demonstrated the existence of large spheroid, intracellular torsinA inclusions in cells transiently transfected with ΔE torsinA (56, 57, 82). These findings could be confirmed in Neuro-2A cells overexpressing ΔE torsinA, which showed intracellular inclusions immunopositive for torsinA (Fig. 12G-I).

Moreover, in torsinA overexpressing cells endogenous Bex2 IR appeared to be perinuclear, where it partially co-localized with torsinA (Fig. 12J-L, arrows). Hence, Neuro-2A cells were co-transfected with torsinA and hBex2 to examine the site of their co-localization in more detail. ICC analyses revealed strong IR for both proteins throughout the cytoplasm, with partial punctuate co-localization of Bex2 and torsinA (Fig. 12M-R). Additionally, high Bex2 IR was detected within the nucleus but more remarkable, was slightly enriched around the nucleus, where it co-localized with torsinA (Fig. 12M-R, arrows), suggesting that both proteins reside at the NE.

A similar effect was observed in cells, overexpressing ΔE torsinA and hBex2, in which hBex2 was also abundant within the nucleus and enriched at the NE, where it partially co-localized with ΔE torsinA (Fig. 12S-U, arrows). Thus, ΔE torsinA did not affect the localization of hBex2 and the enrichment of hBex2 around the nucleus was similar to cells overexpressing wildtype torsinA. In contrast to the co-localization of hBex2 and ΔE torsinA at the NE, torsinA-positive inclusions were devoid of hBex2 IR. Moreover, overexpression of hBex2 did not alter localization or size of ΔE torsinA inclusions.

In summary, ICC studies in Neuro-2A cells showed that Bex2 is expressed in a punctured pattern throughout the cytoplasm and the nucleus, whereas overexpression led to an enrichment of hBex2 in and around the nucleus. Moreover, Bex2 partially co-localized with torsinA in the cytoplasm and most probably at the NE, as both proteins were enriched around the nucleus. Similarly, perinuclear co-localization of ΔE torsinA and hBex2 was observed in discrete punctuated structures. These findings lead to the assumption that both torsinA and Bex2 are NE-resident proteins and that they may form complexes at the NE or at vesicle-like compartments throughout the cytoplasm. Moreover, presence and co-localization of hBex2, torsinA and ΔE torsinA, respectively, at the NE suggests Bex2 to be a NE-specific substrate for torsinA.
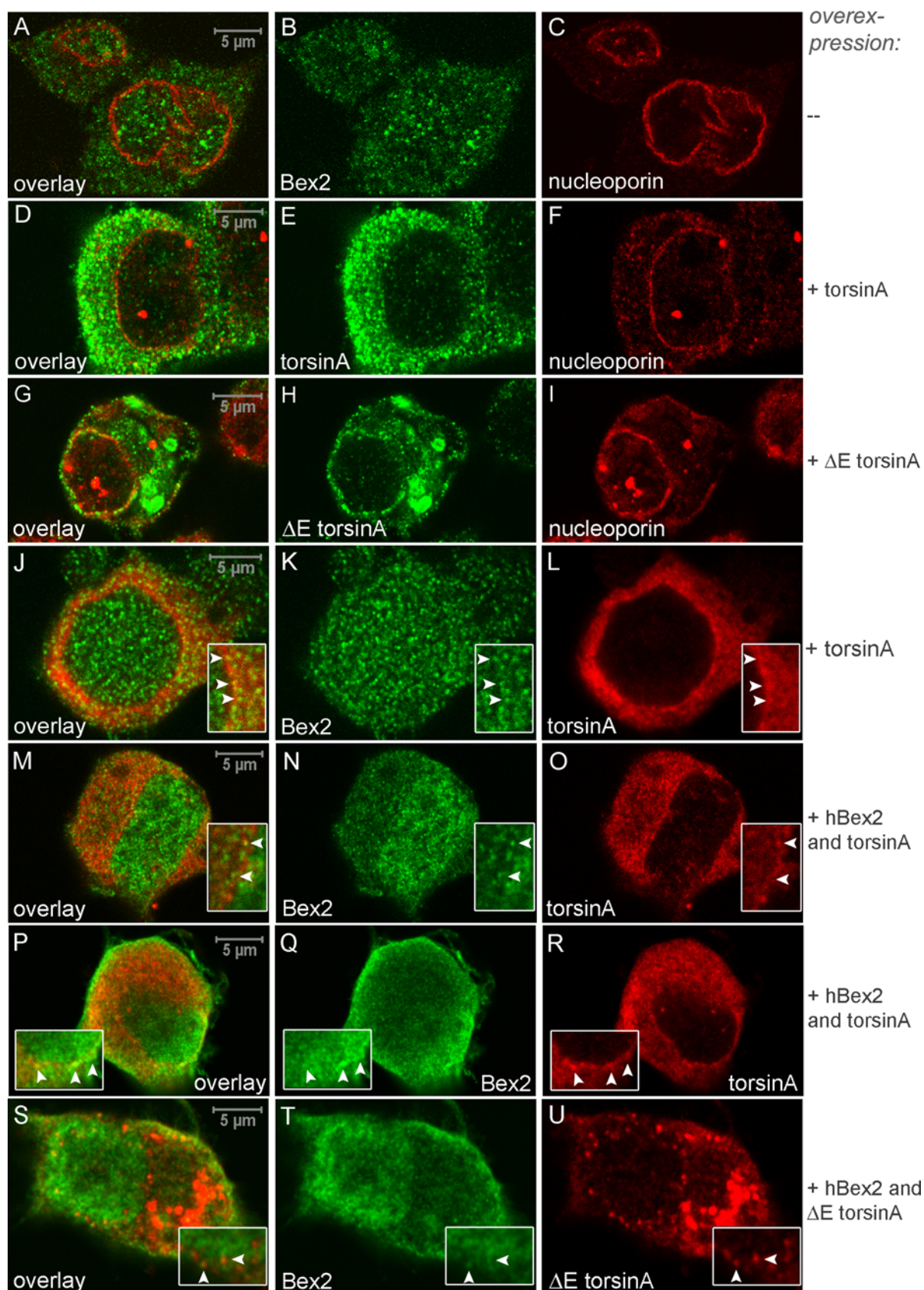
Fig. 12: Bex2, wildtype and mutant torsinA are enriched at the NE of Neuro-2A cells.

A-C) Endogenous Bex2 IR (green) was detected throughout the cytoplasm and within the nucleus. The NE is marked by staining with an antibody against nucleoporin p62 (red). **D-F)** Overexpressed wildtype torsinA IR (green) was observed in a punctuate pattern throughout the cytoplasm and at the NE, as marker staining against nucleoporin p62 revealed (red). **G-I)** TorsinA-positive intracellular inclusions were observed in cells overexpressing ΔE torsinA (green). Marker staining against

nucleoporin p62 (red) revealed an enrichment of ΔE torsinA at the NE. **J-L)** Endogenous Bex2 IR (green) was observed around the nucleus of torsinA (red) overexpressing cells. Arrows mark regions of co-localization. **M-R)** Overexpressed hBex2 (green) and torsinA (red) are present in the cytoplasm in a punctuate pattern and are both enriched at the NE, where they partially co-localize (arrows). Overexpression of hBex2 led to a predominant nuclear localization. **S-U)** Cells overexpressing hBex2 (green) and ΔE torsinA (red) showed enrichment of both proteins around the nucleus with partial co-localizing speckles (arrows). In contrast, ΔE torsinA-positive inclusions were devoid of Bex2.

Previous IB analyses revealed that Bex2 and torsinA are endogenously expressed in rat PC-12 cells (Fig. 9D). Hence, further ICC studies were conducted in PC-12 cells. To examine the localization of endogenous Bex2 and torsinA in processes, PC-12 cells were induced to differentiate by treatment with NGF. The observed expression pattern for Bex2 in differentiated PC-12 cells differed from that of Neuro-2A cells, as high IR for endogenous Bex2 was observed within nucleus, excluding the nucleolus (Fig. 13). Moreover, Bex2 and torsinA showed a similar punctuate expression throughout the cytoplasm and within processes, where discrete co-localization between both proteins was observed. The punctuate pattern and the abundance of Bex2 and torsinA in processes indicates an association of both to vesicular compartments, which are possibly transported along neurites.
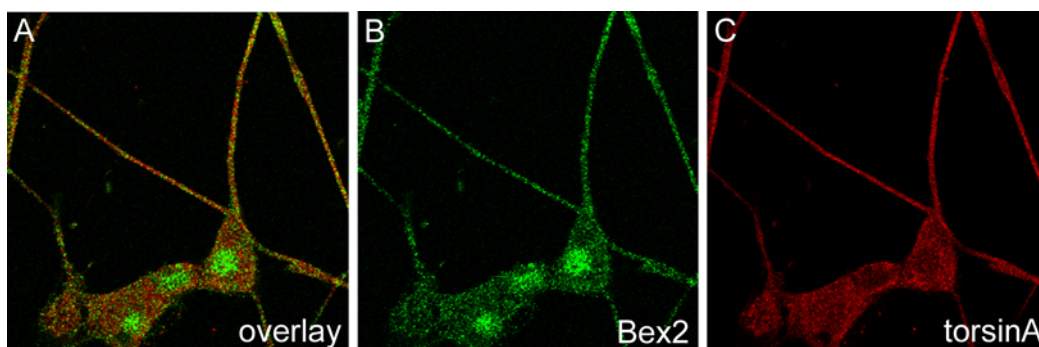
Fig. 13: Expression of endogenous Bex2 and torsinA in differentiated PC-12 cells.
A-C) The expression of endogenous Bex2 (green) and torsinA (red) was similarly throughout the cytoplasm and within processes, where partial co-localization of both proteins was observed.

3.5 Bex2 and torsinA accumulation in the membranous fraction of mouse neuroblastoma cells

ICC analyses of Neuro-2A cells revealed that overexpressed hBex2 and torsinA are both enriched around the nucleus, most prominently at the NE, where co-localization between both proteins was observed. Furthermore, studies in differentiated PC-12 showed Bex2 and torsinA expression in the cytoplasm and within neurites in a punctuate pattern, possibly reflecting vesicular structures. To elucidate whether these

findings reflect association of Bex2 and torsinA to nuclear or vesicular membranes, subcellular localization of both proteins was examined in more detail, with biochemical fractionation methods.

In a first approach protein extracts of mouse neuroblastoma CAD cells, co-transfected with hBex2 and torsinA, were analyzed in a linear 0.32-1.9 M sucrose gradient. hBex2, torsinA and the transmembrane ER marker protein calnexin were found to peak in fractions 15-17 (Fig. 14A). Likewise, the synaptosomal-associated protein 25 (SNAP-25) was highest enriched in these fractions (14-16), indicating that these fractions correspond to ER-derived and synaptosomal membranes. Interestingly, torsinA also showed enrichment in fractions 3-7, corresponding to light membranes.

Having shown that Bex2 and torsinA co-fractionate in sucrose density gradients of cultured cells, it was furthermore analyzed to which subcellular compartment/s these proteins are localized. Thus, fractionation was carried out, using the Qproteome cell compartment kit (Roche), which allows sequential isolation of proteins from different compartments by applying various extraction buffers to the cell extract. This results in separation of soluble cytoplasmic proteins (Cyto), proteins of plasma and organelle membranes, proteins from the lumen of organelles (Mem), as well as soluble, membrane-bound nuclear proteins (Nuc) and residual, mostly cytoskeletal proteins (Csk) .

Fractionated Neuro-2A cells, co-transfected with hBex2 and torsinA (Fig. 14B), showed an enrichment of both hBex2 and torsinA in the membranous fraction (Mem). Additionally, hBex2 and torsinA were detected in the cytosolic fraction (Cyto), whereas cytosolic hBex2 migrated at 23 kD, which was lower compared to the 25 kD hBex2 of the membranous fraction. In contrast to Bex2, overexpressed torsinA was additionally detected in the nuclear fraction, indicating that torsinA is not only present in membranes derived from organelles, such as the ER, but also localizes to nuclear membranes or is present in the nucleus. However, contamination of ER proteins in the nuclear fraction can not be excluded, as staining against calnexin, an ER marker protein, also revealed IR in the nuclear fraction.

Subcellular fractionation experiments of non-transfected Neuro-2A cells confirmed the co-localization of Bex2 and torsinA in the membranous fraction (Fig. 14C).

A
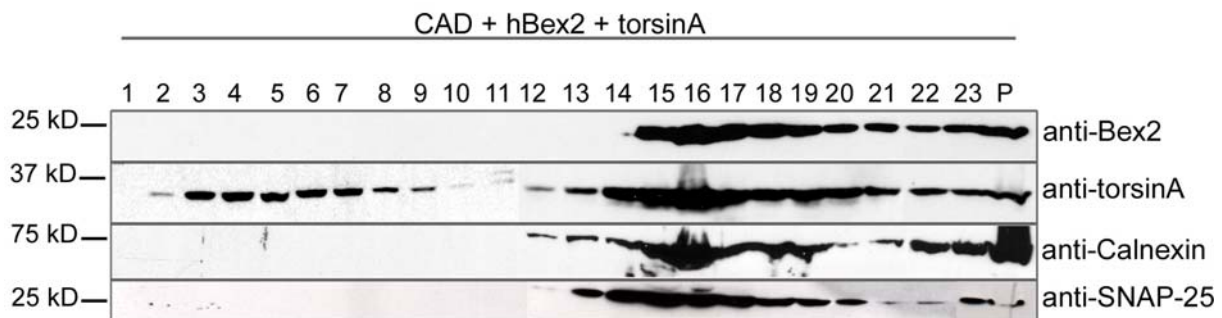
B
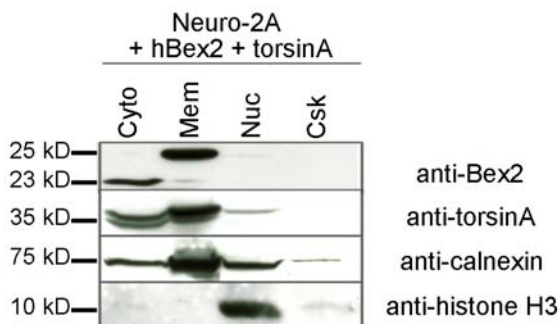
C
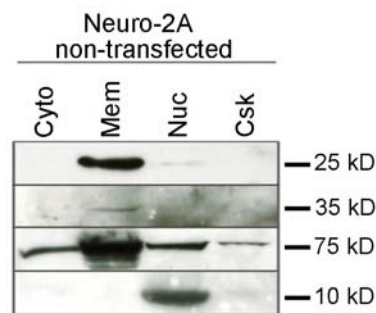
Fig. 14: Bex2 and torsinA are both enriched in the membranous fraction of cultured cells.
A) Linear 0.32-1.9 M sucrose density fractionation with CAD cell extracts, overexpressing hBex2 and torsinA, showed enrichment of both proteins in overlapping fractions 15-23 with a peak in fractions 15-19, similar to the ER marker protein calnexin. SNAP-25, a synaptosomal membrane marker protein, was enriched in fractions 14-17. None of the proteins, except torsinA, was observed in fractions 1-11. *P*, pellet. **B)** Fractionation of Neuro-2A cells, transfected with hBex2 and torsinA revealed an enrichment of Bex2 and torsinA in the membranous fraction (Mem), which contains proteins from organelle and plasma membranes as well as lumenal organelle proteins. Additionally a 23 kD band was detected in the cytosolic fraction (Cyto). Overexpressed torsinA was also found in the cytosolic fraction (Cyto) and to a lower extent in the nuclear membrane and protein containing fraction (Nuc). Neither Bex2 nor torsinA were present in the cytoskeletal protein fraction (Csk). **C)** Endogenous Bex2 and torsinA from non-transfected Neuro-2A cells were enriched in the membranous fraction. Staining against calnexin (ER marker) and histone H3 (chromatin marker) show separation of proteins from different compartments.

However, expression of endogenous torsinA in Neuro-2A cells was weak, as it has already been observed in previous IB analyses (Fig. 9D). No Bex2 IR was observed in the cytosolic fraction of non-transfected cells, which are simply expressing endogenous Bex2. Separation of compartments was checked by marker staining against histone H3, a chromatin binding protein, which was enriched in the nuclear fraction. Calnexin, a transmembrane ER-resident protein was predominantly enriched in the membranous fraction, but also detected in the cytoplasmic and nuclear fraction.

Taken together, biochemical fractionation of Neuro-2A cells showed co-fractionation of Bex2 and torsinA, with an enrichment of both proteins in membrane containing fractions. Thus, it has to be solved, whether these findings indicate tethering of both proteins to similar organelle membranes.

3.6 Bex2 and torsinA are associated with synaptosomal membranes in the mammalian brain

As shown by subcellular fractionation of cultured neuronal cells, Bex2 and torsinA are abundant in membranous fractions (Fig. 14). To elucidate whether this indicates the presence of both proteins in plasma and/or organelle membranes or whether Bex2 resides within the lumen of specific organelles, subcellular fractionation of adult rat brain by differential centrifugation was carried out. This technique allows a distinct separation of membranes and organelles in cells derived from tissue.

Fractionation of adult rat brain revealed an enrichment of Bex2 in fractions, corresponding to nuclei, heavy mitochondria and cell debris (P1), mitochondria, lysosomes, Golgi membranes, crude synaptosomal membranes (P2) and synaptosomal membranes (LP1), respectively (Fig. 15A). Thus, presence of Bex2 in fractions P1 and LP1 may reflect an association with nuclear and/or synaptosomal membranes. No Bex2 IR was present within the soluble protein containing fractions S2, S3, LS1 and LS2, indicating that Bex2 is insoluble as it is tightly associated with membranes.

KHC, another torsinA interactor was enriched in fraction P3 and LP2, showing association to microsomes and synaptic vesicles but also present in the soluble fractions S3 and LS1 and LS2. Only a slight co-fractionation of KHC with Bex2 was observed in the LP1 fraction, indicating that some KHC is also present in synaptosomal membranes.

SNAP-25, which predominantly localizes on the cytoplasmic face of the synaptosomal plasma membrane and on secretory vesicles (138), was enriched in the microsomal fraction P3 and particularly synaptic vesicle fraction LP2, showing a clear separation of synaptic vesicles. Further, the integral synaptic vesicle protein synaptophysin (139) was found in fractions LP1 and LP2, as expected. Calnexin, which is an ER resident transmembrane protein was enriched in fractions P3, LP1 and LP2, indicating that the ER extends into the synapse.
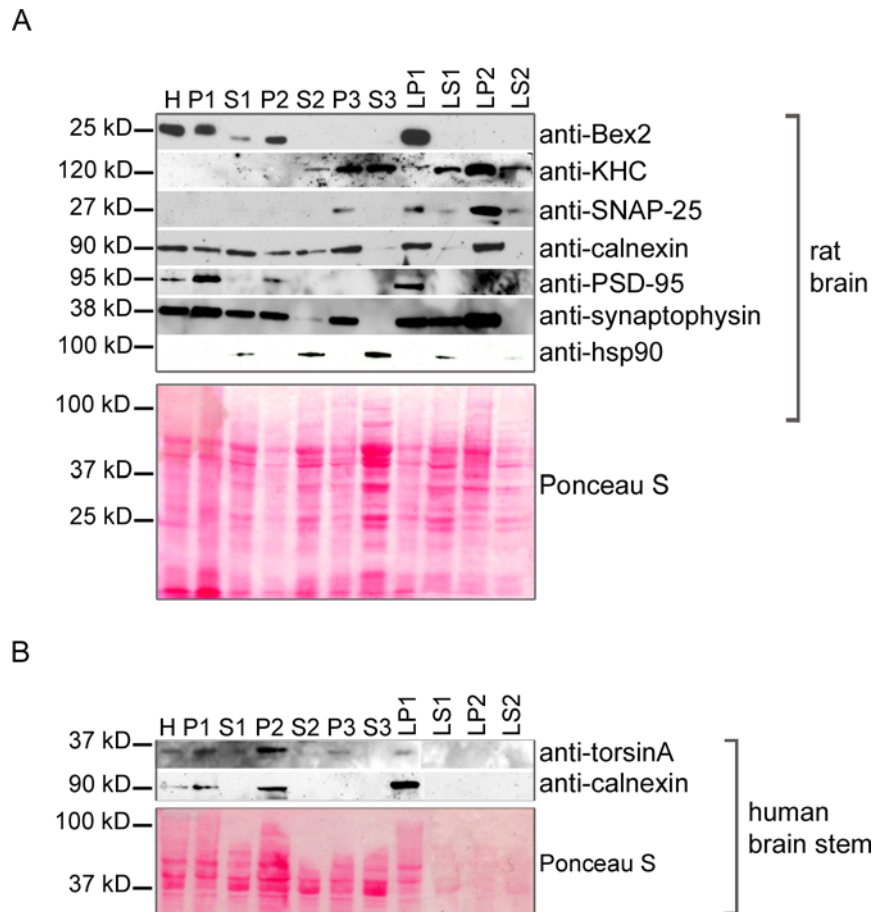
Fig. 15: Bex2 and torsinA are enriched in nuclear and synaptosomal membrane fractions of the mammalian brain.

A) Differential centrifugation of adult rat brain homogentae showed enrichment of Bex2 in nuclear (P1) and synaptosomal (LP1) membranes. KHC was enriched in microsome and synaptosomal membrane containing fractions and in soluble fractions S3 and LS1. SNAP-25 protein was found in the synaptic vesicle-enriched fraction LP2, PSD (postsynaptic density protein)-95 in the synaptosomal membrane fraction LP1 and synaptophysin fractionated with synaptosomal (LP1) and synaptic vesicle (LP2) membranes, indicating a clear separation of all fractions. Calnexin was observed within all membrane-containing fractions but excluded soluble fractions S3, LS1 and LS2. In contrast, the cytosolic protein hsp90 was exclusively detected in fractions, containing soluble proteins. **B)** Differential centrifugation of human brain stem lysate revealed torsinA within nuclear, microsomal and synaptosomal fractions. Calnexin was found to be enriched similarly, except the P3 fraction. H (homogenate), P1 (nuclear fraction), P2 (crude synaptosomal membranes), P3 (microsomes), LP1 (synaptosomal membranes), LP2 (synaptic vesicle enriched fraction).

PSD-95 is a marker for the postsynaptic density and was enriched in the synaptosome-containing fraction as expected. Hsp90, a marker for cytosolic proteins was only detected in soluble fractions. Additionally, Ponceau S staining shows equal loading of protein amounts.

Staining with antibodies against torsinA did not reveal any immunoreactive signals, due to low sensitivity of those antibodies against endogenous rat torsinA. Nevertheless, previous fractionation studies of human brain by Augood and colleagues (2003) reported an enrichment of torsinA in nuclear and synaptosomal membrane fractions (61), indicating that both torsinA and Bex2 are present within similar

compartments. Thus, subcellular fractionation was additionally performed with human brain stem tissue. In fact, torsinA was present in the nuclear and synaptosomal membrane containing fractions, similar to the ER marker protein calnexin (Fig. 15B). Staining with the Bex2 antibody could not confirm the findings of subcellular fractionation in rat brain, as the antibody does not detect endogenous Bex2 from human brain tissue.

In summary, these results indicate that Bex2 and torsinA are both associated with nuclear and synaptosomal membranes in the mammalian brain, which suggests a role for both proteins in these organelles.

3.7 Bex2, torsinA and kinesin-I co-localize in primary cortical rat neurons

Preceding fractionation studies revealed localization of Bex2 and torsinA to synaptosomal and nuclear membranes. Furthermore, ICC in neuronal cell lines confirmed the association of Bex2 and torsinA with nuclear membranes, as both proteins were concentrated around in the NE, where they showed discrete co-localization. Additionally, Bex2 and torsinA IR was observed to co-localize in neurites of differentiated PC-12 cells. To elucidate the precise localization of Bex2 in neurons and a possible association to torsinA, subsequent ICC examinations were performed in primary rat cortical neurons (RCN), using confocal microscopy.

Immunolabeling of Bex2 and torsinA revealed IR of both proteins throughout the cytoplasm and within neurites, where both proteins showed a punctuated staining pattern (Fig. 16A-F). Co-localization between Bex2 and torsinA was observed in discrete spots within the cytoplasm and along processes (Fig. 16A, D), presumably reflecting vesicular structures. Higher magnifications show the vesicular pattern of Bex2 and torsinA. Regions of co-localization appear to be restricted to the perinuclear area, possibly referring to the nuclear membrane.

As already observed for endogenous Bex2 in differentiated PC-12 cells (Fig. 13), an intense signal of the protein was detected within the nucleus, shown by double staining with the NE marker nucleoporin p62 (Fig. 16G-I).
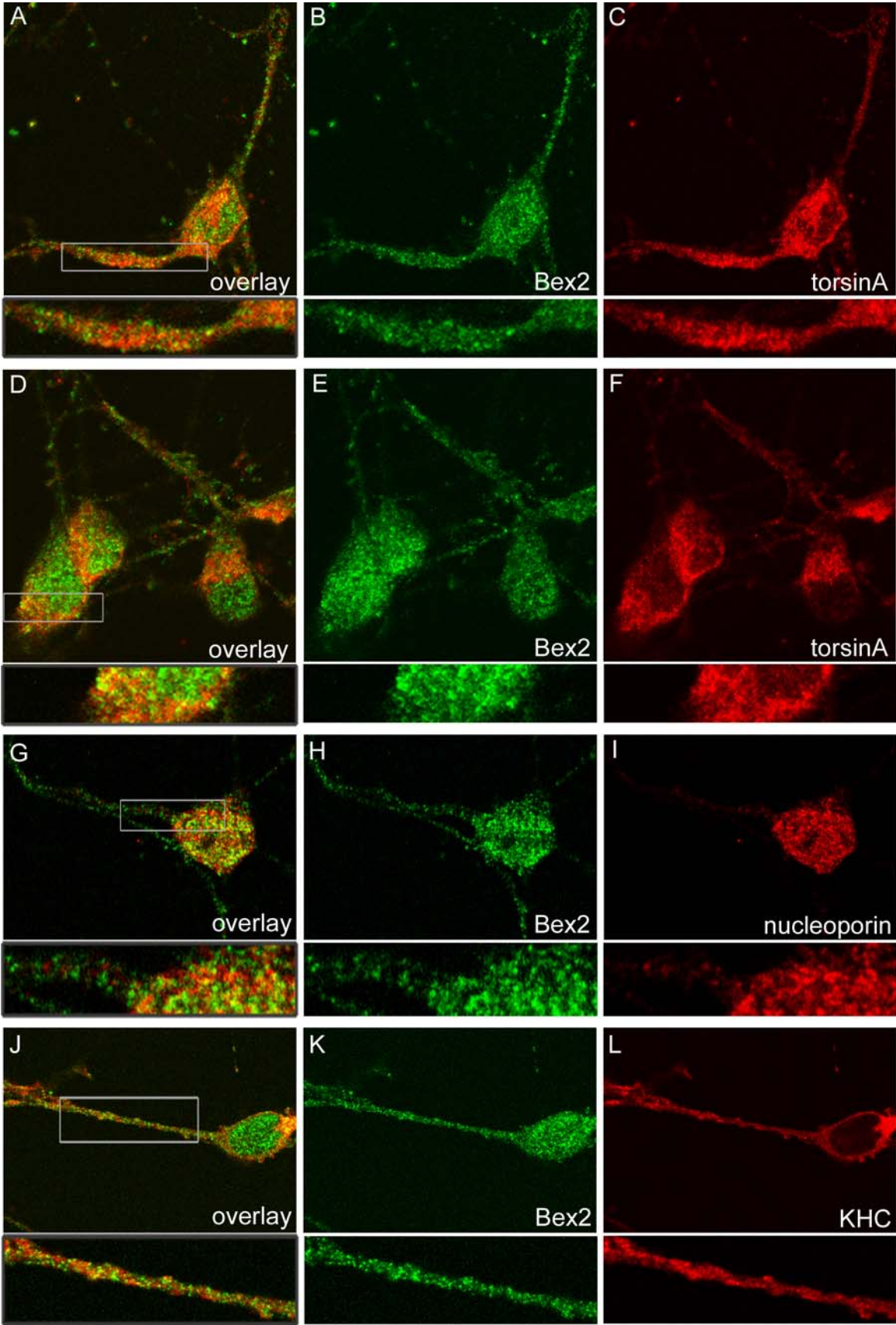
Fig. 16: Bex2 partially co-localizes with torsinA, nucleoporin p62 and KHC in RCN.

A-F) ICC staining against Bex2 (green) and torsinA (red) revealed partial co-localization of both proteins especially in processes and the cytoplasm of neurons (overlay A, D). Higher magnifications that are depicted below each image show the vesicular pattern of Bex2 and torsinA IR. **G-I)** Bex2 (green) is abundant in the nucleus and partially co-localizes with nucleoporin p62 (red), as double

staining against the NE marker indicate. A weaker Bex2 signal was observed within processes and the cytoplasm. **J-L)** Staining against Bex2 (green) and KHC (red) also showed a vesicular distribution pattern of both proteins, partially co-localizing in the cytoplasm and along neurites.

Surprisingly, in RCNs staining with nucleoporin p62 did not show the typical rim-shaped structure, but was more diffusively distributed throughout the nucleus and weakly extending into neurites, which may be due to non-specific staining. Partial co-localization between nucleoporin p62 and Bex2 demonstrate the presence of Bex2 in the NE (Fig. 16G).

Interestingly, partial co-localization of Bex2 and the torsinA interacting motor protein kinesin-I (KHC) was observed within processes and cytoplasm of primary neurons in a punctured pattern (Fig. 16J-L). Thus, leading to the assumption that Bex2 may be associated with vesicular structures and moreover may exist in a complex, including torsinA and KHC. However, a possible interaction between KHC and Bex2 may only be transiently and the binding of both proteins weak, since biochemical fractionation indicated KHC to be a soluble and Bex2 a membrane-bound protein.

To further study the subcellular localization of Bex2 in RCN, double-labeling ICC with Bex2 antibody and antibodies against marker proteins of several cellular compartments, such as early endosomes, mitochondria and synaptic vesicles were performed. Additionally, Bex2 was stained together with F-actin and the microtubule associated protein 2 (MAP2), respectively. These analyses revealed that the expression pattern of endosomes and mitochondria, stained with the EEA 1 antigen and mitotracker, respectively, greatly differed from Bex2 IR (Fig. 17A-C and D-F, respectively), indicating that endosomal and mitochondrial membranes are not the site of action of Bex2. Bex2 showed a punctuate staining pattern like the vesicle associated protein synaptophysin, but no co-localization of Bex2 and synaptophysin IR was observed as most labeled spots were clearly separated from each other (Fig. 17G-I). Furthermore, F-actin, a component of the cytoskeleton, involved in intracellular transport of organelles, showed a diffuse distribution in processes, where Bex2 IR was observed to partially co-localize with F-actin (Fig. 17J-L). An antibody against MAP-2, which is present in dendrites and somata of neurons and associates with microtubules, was used as a neuronal marker. Bex2 IR was observed in MAP-2-positive as well as MAP-2-negative processes, indicating that Bex2 is not exclusively expressed in dendritic processes (Fig. 17M-O).
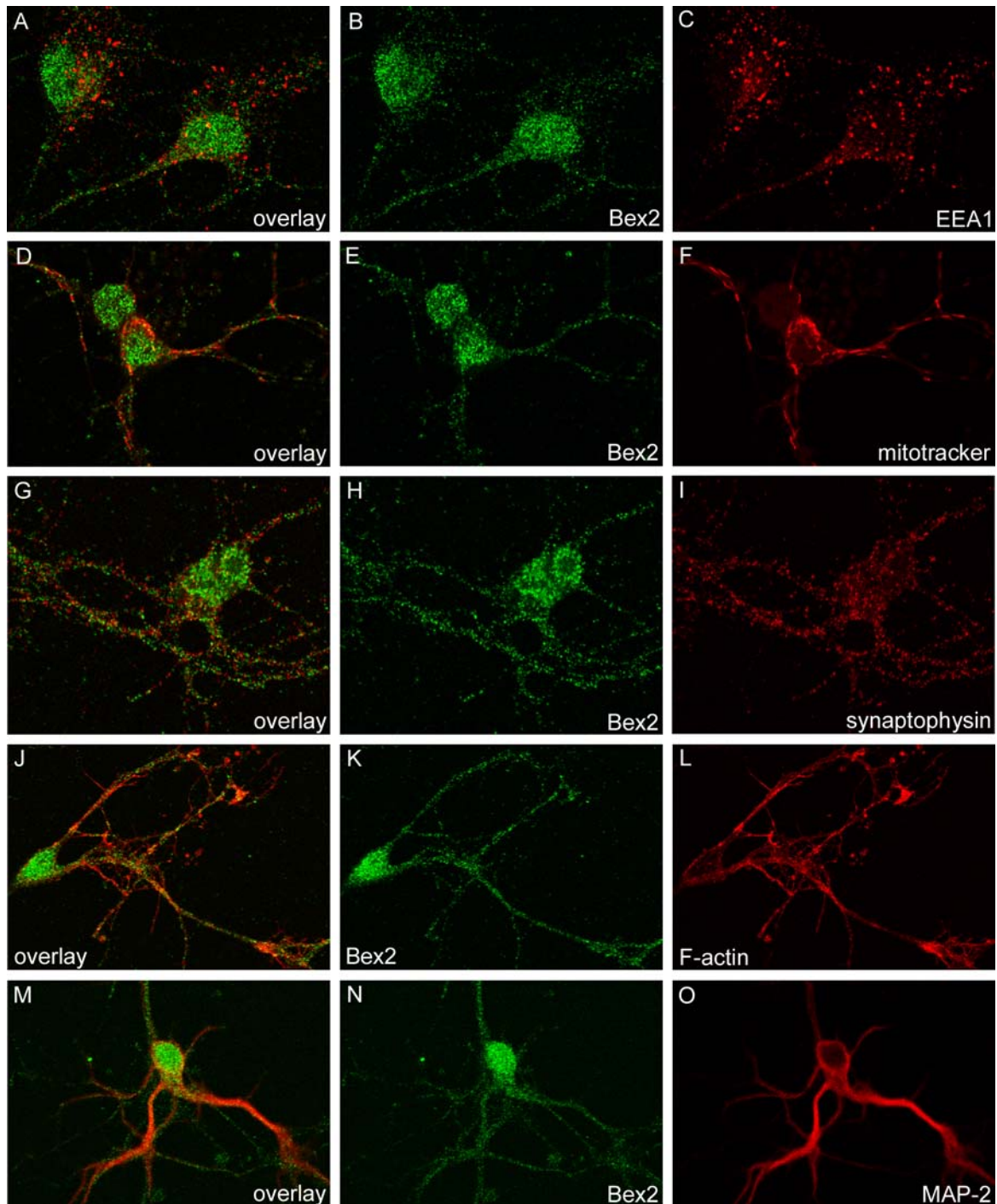
Fig. 17: Subcellular localization of Bex2 in RCN.

A-C) Staining against early endosomes (EEA 1, red) and Bex2 (green) revealed no association of Bex2 with these organelles. **D-F)** Likewise, labeling of mitochondria (red) showed a different pattern to Bex2 IR (green). **G-I)** IR of synaptophysin (red) was similar to Bex2 IR (green) but did not reveal any co-localization. **J-L)** The distribution of cytoskeletal components, such as F-actin (red), and Bex2 (green) were similar and both proteins showed overlapping IR. **M-O)** MAP-2 (red) staining revealed Bex2 (green) IR in dendritic processes.

In summary, these results provide further evidence for an association between torsinA and Bex2, as partial co-localization of both proteins and an obvious similar expression pattern was observed in primary neurons of rat. Furthermore, this

association appeared to be most prominent around the nucleus, most probably reflecting co-localization of both proteins at the NE. Staining against KHC and synaptophysin indicate that Bex2 may be associated with vesicles. Discrete co-localization between Bex2 and kinesin-I was observed and it may therefore be hypothesized that Bex2, torsinA and kinesin-I exist in a complex, associated with vesicular structures, which may be transported along actin filaments or microtubules.

3.8   Characterization of hBex2 deletion variants

Affinity precipitation assays showed that torsinA and Bex2 are interacting *in vitro*. Moreover, the domain that mediates binding of torsinA to Bex2 is most likely located in the C-terminus of torsinA (amino acid 251-332), since this region was used as bait in the yeast two-hybrid screen. It contains the α-helical sensor2 motif and spans the region of the glutamic acid deletion, found in EOTD patients.

To elucidate the torsinA binding domain of Bex2, several hBex2 deletion constructs were generated to analyze their binding ability to torsinA in MBP affinity precipitation assays. The deletion constructs, either N-terminal tagged with MBP or the FLAG epitope, are depicted in Fig. 18. Three constructs comprise the N-terminal hBex2 sequence (ΔhBex2_1-20, 1-50 and 1-70) and two the C-terminus (ΔhBex2_71-121 and 71-125). To elucidate whether the C-terminal CAAX prenylation motif is the site of protein binding, one construct lacks this sequence (ΔhBex2_1-121).

To decipher the torsinA binding domain of Bex2, affinity precipitation was performed by incubating purified recombinant MBP-ΔhBex2 deletion variants with HEK 293T cell extracts containing overexpressed wildtype torsinA. Interestingly, all deleted protein variants were found to bind to torsinA (Fig. 18B), suggesting that there is no specific protein binding domain in hBex2 and that the entire protein interacts with torsinA. This binding was specific as torsinA did not bind to MBP alone. However, it remains to be elucidated whether some hBex2 domains show higher affinity to torsinA, which could not be clarified in affinity precipitation analyses, due to unequal loading of MBP-ΔhBex2 fusion proteins (Fig. 18B, Ponceau S).

A
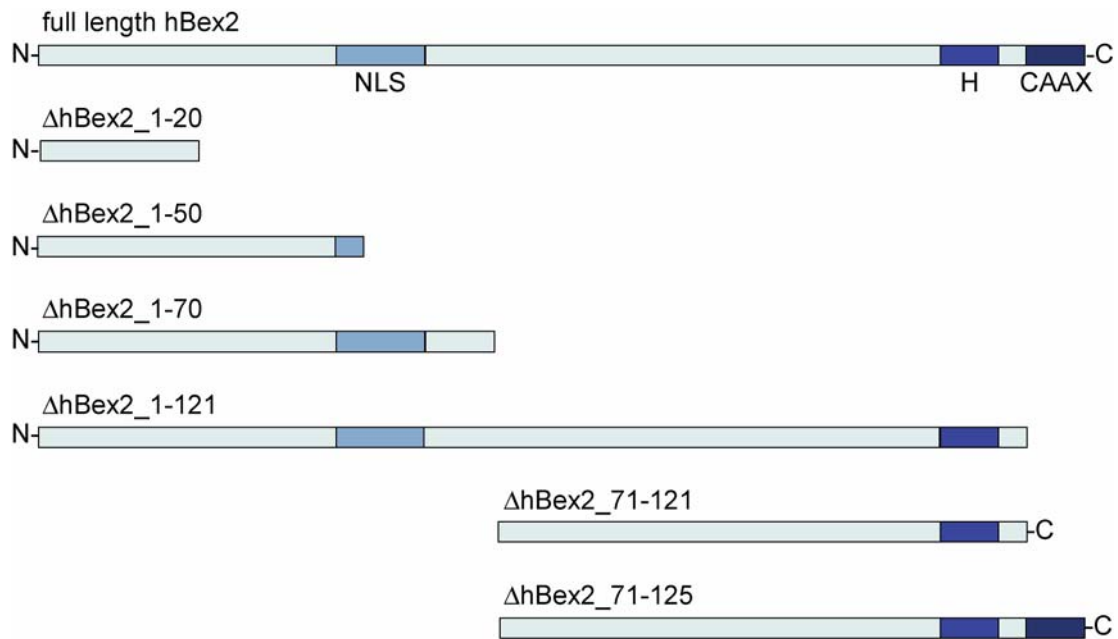
B
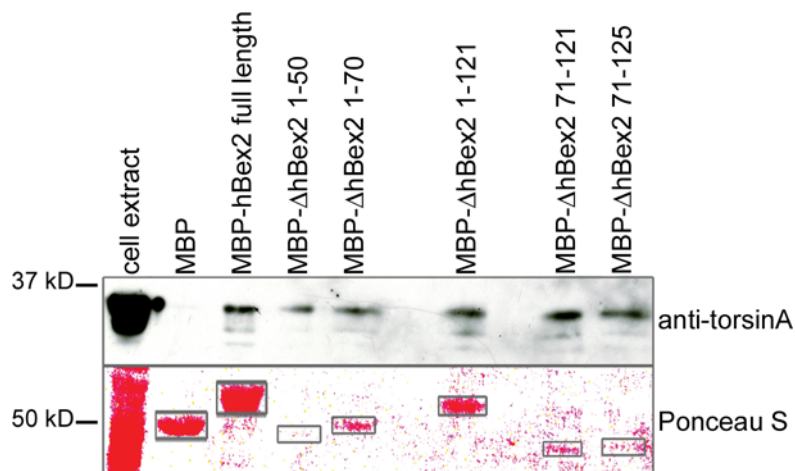
Fig. 18: Human Bex2 deletion variants bind to torsinA in *in vitro* affinity precipitation assays.

A) Full length hBex2 is contains a putative NLS, a histidine-rich sequence (H) and a prenylation motif (CAAX). N-terminal ΔhBex2_1-20 lacks the NLS, P, H and CAAX. ΔhBex2_1-50 is similar to the former variant but contains 4 amino acids of the putative NLS. N-terminal ΔhBex2_1-70 is devoid of all putative motifs but contains the NLS and ΔhBex2_1-121 only lacks the putative prenylation site. C-terminal ΔhBex2_71-121 misses NLS and CAAX motifs and ΔhBex2_71-125 lacks the NLS. **B)** MBP-affinity precipitation assays were performed by binding MBP-ΔhBex2 variants to the beads, followed by incubation with HEK 293T cell extracts overexpressing torsinA. Protein eluate was subsequently analyzed by IB analyses. Staining with anti-torsinA revealed that torsinA binds to all MBP-ΔhBex2 variants, but not to the MBP control, suggesting that binding is specific. Ponceau S staining shows loading of MBP-ΔhBex2 fusion proteins. MBP-ΔhBex2 1-50 and MBP-ΔhBex2 71-125 amounts are low, as they could barely be detected using this method.

To study the functional relevance of predicted hBex2 domains, expression and localization of the deletion variants were analyzed in IB and ICC, respectively. Interestingly, the N-terminally deleted variants (ΔhBex2_71-12 and ΔhBex2_71-125) and the shortest variant ΔhBex2_1-20 were not detectable in IB, which may be due to low transfection efficiency, instability or insolubility of the truncated proteins (Fig. 19). Expression of the N-terminal containing but CAAX motif deleted hBex2 variants (ΔhBex2_1-50, 1-70 and 1-121) was proven, since detection with antibodies against the FLAG epitope and Bex2, respectively, showed IR at distinct molecular weights. However, similarly to full-length Bex2 the truncated protein variants ΔhBex2_1-50 and ΔhBex2_1-121 did not migrate at their calculated molecular weights of approximately 6 kD and 13 kD, respectively, but were detected at higher molecular weights (15 kD and 20/25 kD, respectively). In contrast, ΔhBex2_1-70 was detected at approximately 8 kD, reflecting the calculated protein size.
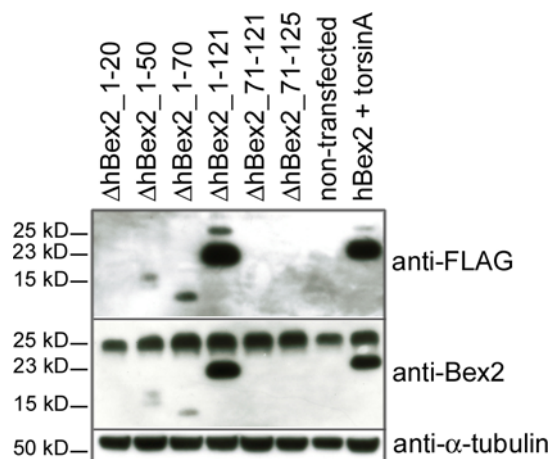
Fig. 19: Expression of hBex2 deletion variants in transfected Neuro-2A cells.

Cells extracts of Neuro-2A overexpressing the appropriate hBex2 deletion variant (ΔhBex2_1-20, 1-50, 1-70, 1-121, 71-121 and 71-125) were analyzed by IB using an antibody directed against the N-terminal FLAG epitope (upper panel) or against Bex2 (middle panel). ΔhBex2_1-50 and 1-70 were detected at approximately 15 kD and 8 kD, whereas ΔhBex2_1-121 showed IR at approximately 20 kD and 25 kD. No IR was observed for ΔhBex2_1-20, 71-121 and 71-125. Staining against α-tubulin shows equal protein loading (lower panel).

To investigate the subcellular localization of the appropriate hBex2 deletion variants ICC in transfected Neuro-2A cells was performed. The CAAX prenylation site lacking variants were analyzed in respect to their ability to associate with membranes (ΔhBex2_1-20, 1-50, 1-70, 1-121 and 71-121). Variants with deletions in the putative NLS were analyzed with respect to possible alterations in nuclear localization

(ΔhBex2_1-20, 1-50, 71-121, 71-125). ICC revealed immunoreactive signals of all truncated proteins (Fig. 20), although cells that overexpressed ΔhBex2_1-20, 71-121 and 71-125 showed a lower transfection rate (data not shown), as already indicated by IB analyses (Fig. 19).
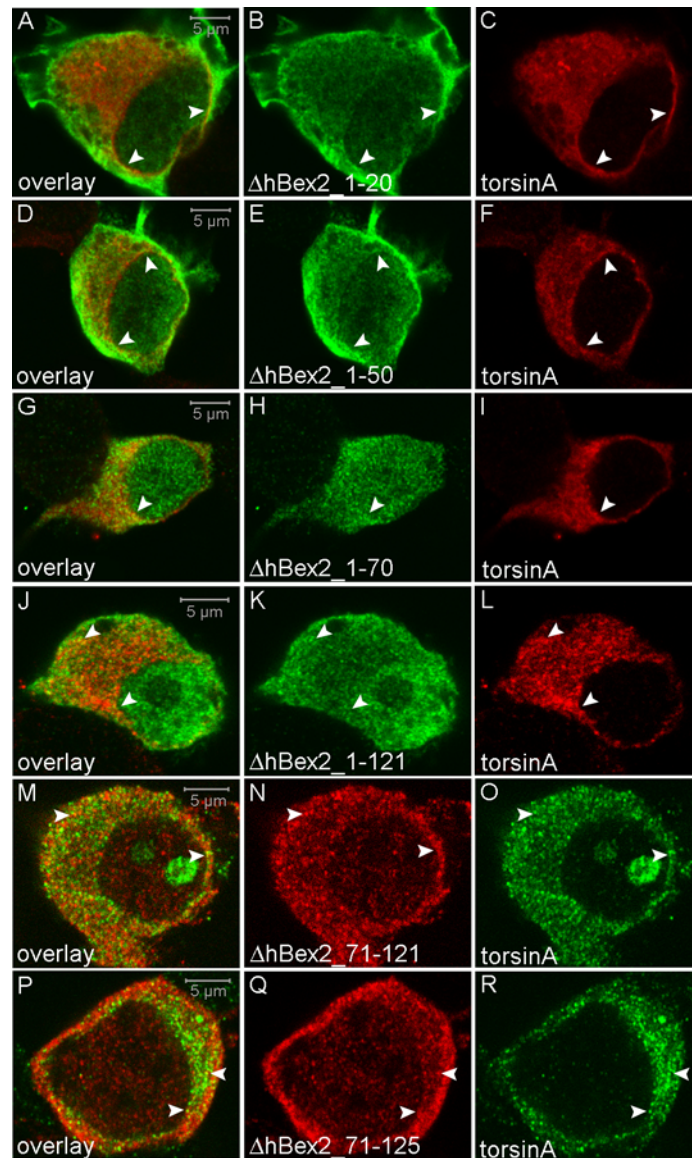
Fig. 20: Subcellular localization of hBex2 deletion variants in Neuro-2A cells.

Neuro-2A cells were co-transfected with an N-terminal FLAG tagged ΔhBex2 deletion construct and torsinA and subsequently analyzed by ICC. **A-C)** ΔhBex2_1-20 (green) IR was detected throughout the cytoplasm and weaker within the nucleus. ΔhBex2_1-20 (green) and torsinA (red) were both enriched around the nucleus, where they partially co-localized (arrows). **D-F)** Similar findings were observed in cells overexpressing ΔhBex2_1-50 (green) and torsinA (red). **G-I)** ΔhBex2_1-70 (green) showed stronger expression within the nucleus, compared to ΔhBex2_1-20 and 1-50. Co-localization with torsinA (red) was detected within the cytoplasm and around the nucleus (arrows). **J-L)** ΔhBex2_1-20 (green) showed highest expression in the nucleus and throughout the cytoplasm, resembling the expression of full length hBex2. Co-localization with torsinA (red) was observed in the cytoplasm and around the nucleus (arrows). **M-R)** ΔhBex2_71-121 and ΔhBex2_71.125 (red) were detected with an antibody against the FLAG epitope, since both variants are lacking the N-terminal region, recognized by the Bex2 antibody. Both variants showed a predominant cytoplasmic expression and co-localized with torsinA (green) in the cytoplasm and around the nucleus (arrows).

Furthermore, the NLS deletion variants ΔhBex2_1-20 and ΔhBex2_1-50 were expressed throughout the cytoplasm and to a lower extent in the nucleus, suggesting that deletion of the putative NLS does not completely inhibit nuclear transport (Fig. 20A-F). However, ΔhBex2_1-70 and ΔhBex2_1-121 that are containing the putative NLS showed a stronger expression within the nucleus (Fig. 20G-L) and the ΔhBex2_1-121 expression pattern resembled that of full length hBex2. Moreover, N-terminal truncated hBex2 (ΔhBex2_71-121 and 71-125) was expressed throughout the cytoplasm but weak IR was observed in the nucleus, indicating that the N-terminal region, including the NLS, is essential for nuclear import (Fig. 20M-R). Lack of the C-terminal CAAX motif did not reveal an obvious alteration of the overall localization of ΔhBex2_1-121 and 71-121. Consistent with the findings in affinity precipitation assays (Fig. 18) all hBex2 deletion variants co-localized with torsinA. This co-localization was observed in the cytoplasm and partially around the nucleus (Fig. 20, arrows).

3.9   Bex2 and torsinA are similarly distributed throughout adult rat brain

In vitro analyses in cell culture and primary cortical rat neurons showed similar distribution patterns and co-localization of torsinA and Bex2 (Fig. 12, Fig. 13 and Fig. 16). To investigate the expression and distribution of endogenous torsinA and Bex2 in the mammalian brain, immunohistochemical analyses on fresh frozen adult rat brain sections were conducted.

TorsinA and Bex2 immunopositive signals were widely distributed throughout grey matter and showed a highly similar distribution (Fig. 21 and Fig. 22). Hence, absence of Bex2 and torsinA from white matter indicates neuronal expression of both proteins. Fig. 21 shows Bex2 and torsinA IR in sagital sections of rat brains. Highest immunopositive signals for both proteins were observed in the hippocampal formation (CA1-CA3), the cerebellar cortex, and the olfactory bulb.

Similar observations were made in coronal sections of rat brain, furthermore revealing high expression of Bex2 and torsinA in the substantia nigra, dorsal cochlear nucleus, vestibular nucleus, interposed cerebellar nucleus, and piriform cortex (Fig. 22A-C and D-F, respectively). Specificity of the Bex2 antibody was verified by preadsorption with purified MBP-hBex2 protein, resulting in a significant reduction of

immunoreactive signal (Fig. 22G, H). Levels of torsinA and Bex2 IR in the examined rat brain structures are compared in table 3.
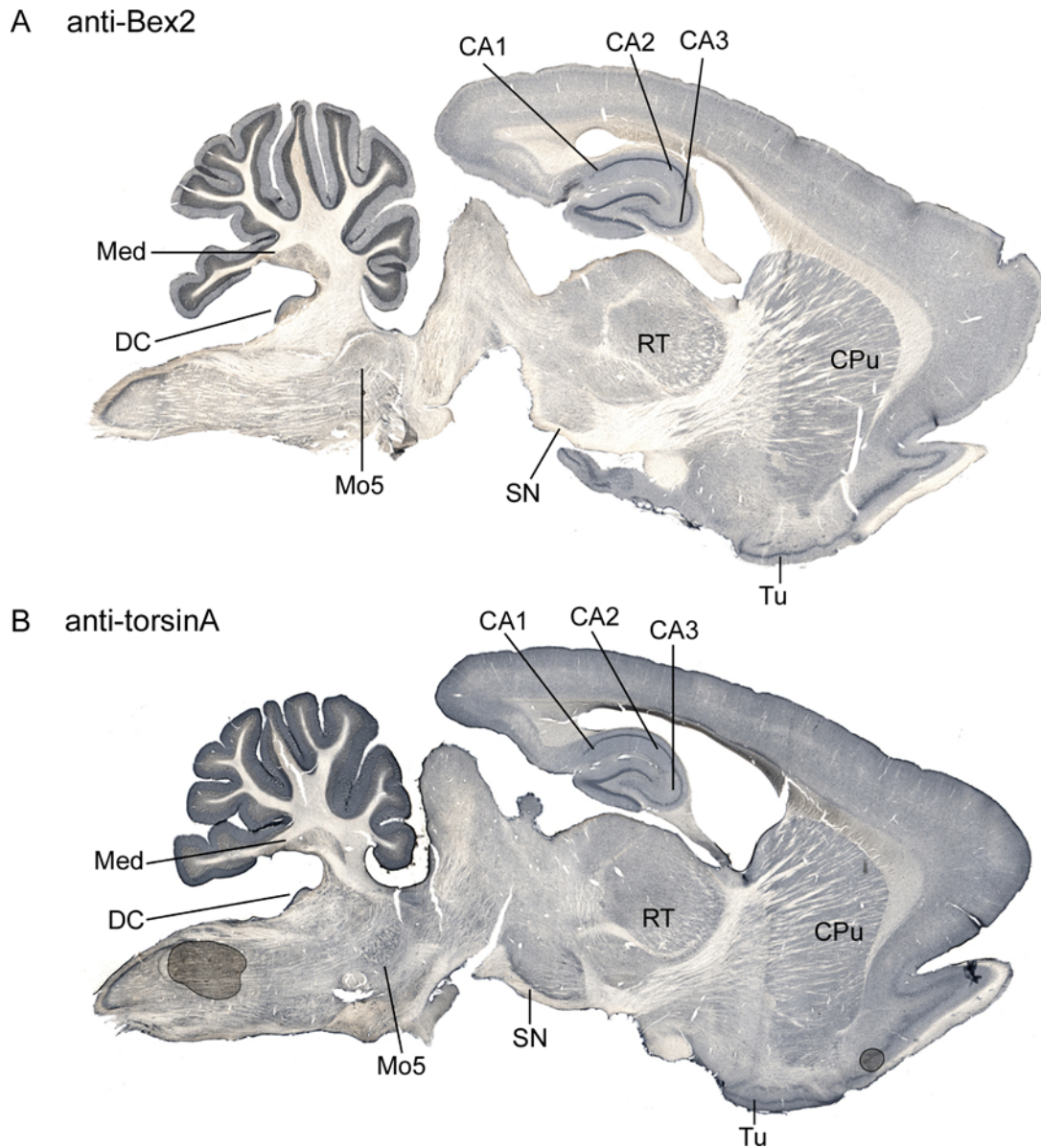
Fig. 21: Bex2 and torsinA have a similar distribution pattern throughout the grey matter of adult rat brain.

A) Immunostaining against Bex2 shows a widespread distribution, with highest IR in the medial cerebellar nucleus (MED), dorsal cochlear nucleus (DC), olfactory tubercle (Tu), olfactory bulb, cerebellum and CA1-3 of the hippocampus. Moderate labeling was observed in substantia nigra (SN), motor trigeminal nucleus (Mo5), caudate putamen (CPu, striatum), reticular thalamic nucleus (RT) and cortex. **B)** Immunostaining against torsinA revealed a similar widespread expression, with IR in identical structures.
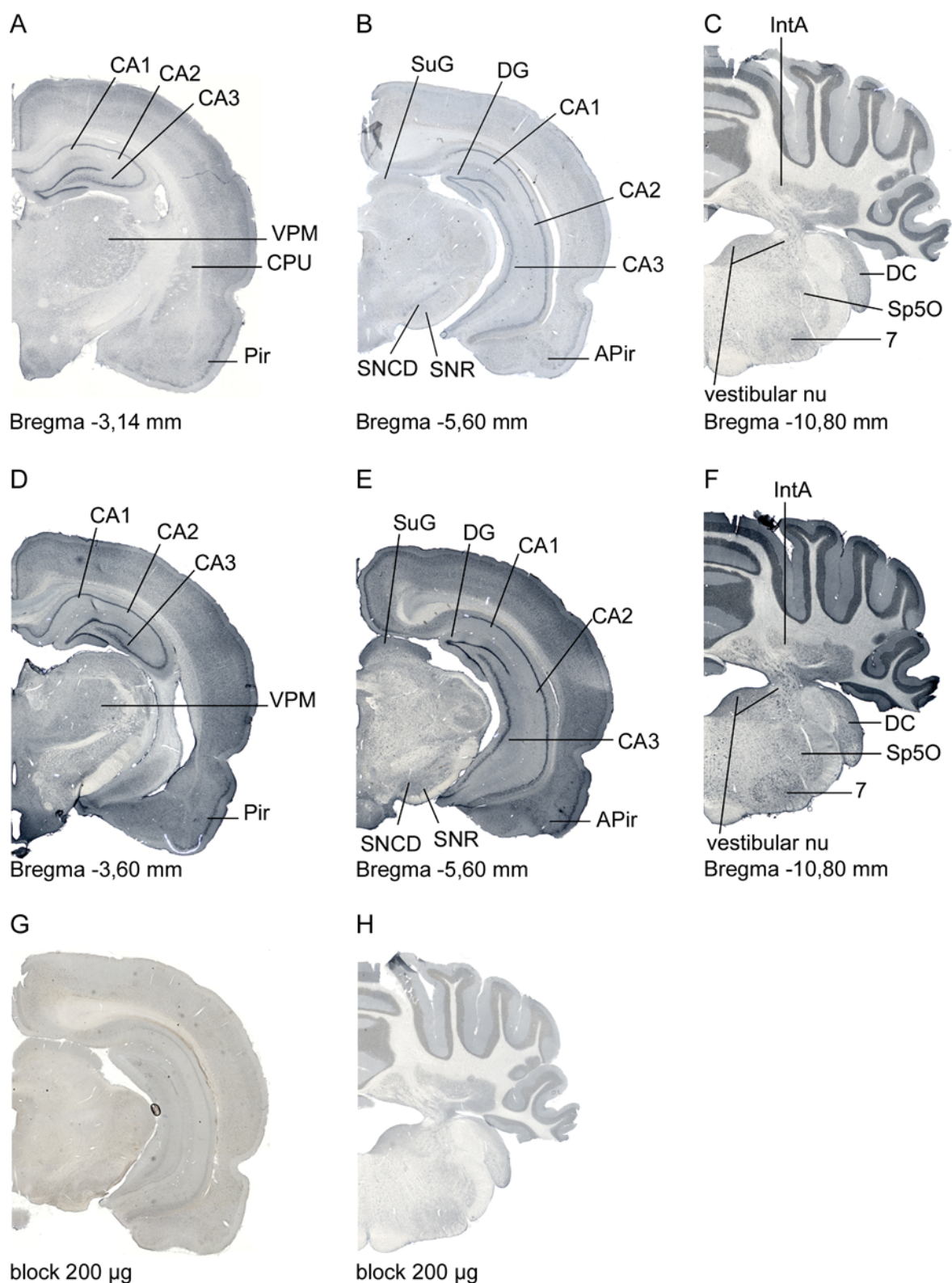
Fig. 22: Similar expression pattern of torsinA and Bex2 in coronal rat brain sections.

A-C) Bex2 IR was highest in dorsal cochlear nu (DC), substantia nigra reticular part (SNR), the hippocampal formation (CA1-CA3), cerebellar cortex, vestibular nu, interposed cerebellar nu (IntA), and piriform cortex (Pir). D-F) The pattern of torsinA IR was similar to Bex2, with somewhat stronger staining in the substantia nigra, reticular part (SNR). G,H) Preadsorption of the Bex2 antibody with recombinant MBP-hBex2 protein significantly reduced Bex2 IR. 7, facial nu; CPu, caudate putamen (striatum); DC, dorsal cochlear nu; DG, dentate gyrus; IntA, interposed cerebellar nu, anterior; Lat, lateral cerebellar nu; MGP, medial globus pallidus; Pir, piriform cortex; APir, amygdalopiriform transition area; PPy, parapyramidal nu; SNCD, substantia nigra, compact part, dorsal tier; SNR, substantia nigra, reticula part; Sp5O, spinal 5 nu, oral part; SuG, superficial gray layer of sup coll; VPM, ventral posteromedial thalamic nu;

Table 3: Intensity of Bex2 and torsinA immunoreactive signal in adult rat brain structures.

brain structure	torsinA level	Bex2 level
medial cerebellar nu	+++	+++
dorsal cochlear nu	+++	+++
substantia nigra reticular part	+++	+++
substantia nigra compact part	+++	++
hippocampus (CA1-CA3)	+++	+++
cerebellar cortex (stratum granulosum)	+++	+++
vestibular nu	+++	+++
piriform cortex	+++	+++
olfactory tubercle	+++	+++
olfactory bulb	+++	+++
retucular thalamic nu	++	++
caudate putamen	++	++
facial nu	++	++
motor trigeminal nu	++	++
dorsal cochlear nu	++	++
interposed cerebellar nu	++	++
lateral cerebellar nu	++	++
ventral posteromedial nu	++	++
spinal 5 nu	++	++
amygdalopiriform transition area	++	++

At the cellular level, all analyzed rat brain regions showed neurons immunopositive for both Bex2 and torsinA protein (Fig. 23). Bex2 signal was found throughout the cytoplasm and in processes, but stronger within nuclei of neurons (Fig. 23A-D).
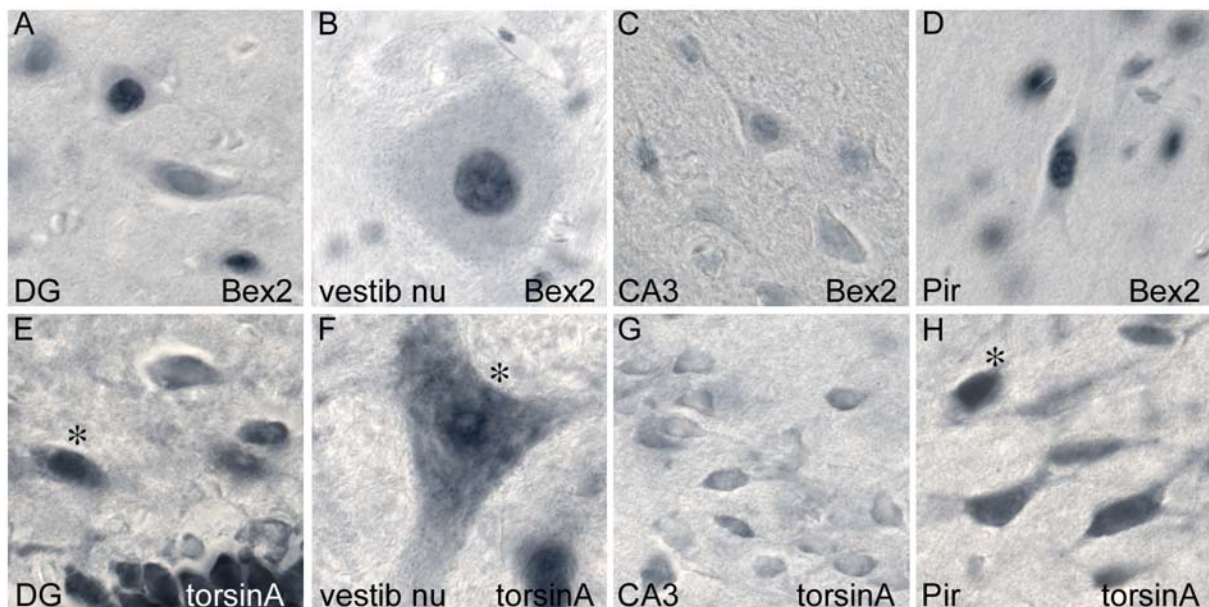
Fig. 23: Immunohistochemical analysis of neurons from different rat brain structures.

A-D) Immunostaining against Bex2 showed a strong immunoreactive signal within the nuclei of neurons and to a lesser extent in the cytoplasm and processes. **E-H)** TorsinA immunostaining varied between neurons. Labeling was mostly detected within the cytoplasm and processes, some neurons showed torsinA IR within the nucleus (asterisks). DG, dentate gyrus; vestib nu, vestibular nucleus; CA3, CA3 region of hippocampus; Pir, piriform cortex

In contrast, torsinA IR was found to be variable but was primarily observed within the cytoplasm and neurites, most frequently excluding the nucleus (Fig. 23E-H). However, there were some neurons in almost all regions examined, which showed intra- or perinuclear torsinA IR, excluding the nucleolus (Fig. 23E, F, H asterisks).

3.10 TorsinA and Bex2 co-localization in neurons of adult rat brain

Since IHC analyses revealed similar expression patterns of torsinA and Bex2, ICC analyses on adult rat brain sections were conducted to elucidate a possible association of torsinA and Bex2 in neurons of adult rat brain by performing double staining against both proteins (Fig. 24). Several rat brain structures were examined and showed both torsinA and Bex2 IR in the cytoplasm and processes of neurons (Fig. 24A-F). However, a clear co-localization of Bex2 and torsinA could not be confirmed, as labeling for Bex2 was weak throughout the cytoplasm and processes and furthermore impaired by an intense background staining.

Consistent with preceding ICC analyses, a very intense Bex2 IR was observed within the nucleus, excluding the nucleolus, partially co-localizing with the NE protein nucleoporin p62 (Fig. 24G-I). As previously described in immunohistochemical analysis of rat brain (Fig. 24E, F, H), torsinA immunopositive signal was again detected within the nucleus of some neurons, where partial co-localization with Bex2 signal was observed (Fig. 24, arrows B, E).

Taken together, distribution and localization of torsinA and Bex2 proteins in neurons of adult rat brain was found to resemble that of *in vitro* cultured differentiated PC-12 cells, as well as primary RCN. However, one major difference was the presence of torsinA immunopositive signal within the nucleus of rat brain neurons, which had never been detected in cell cultures.
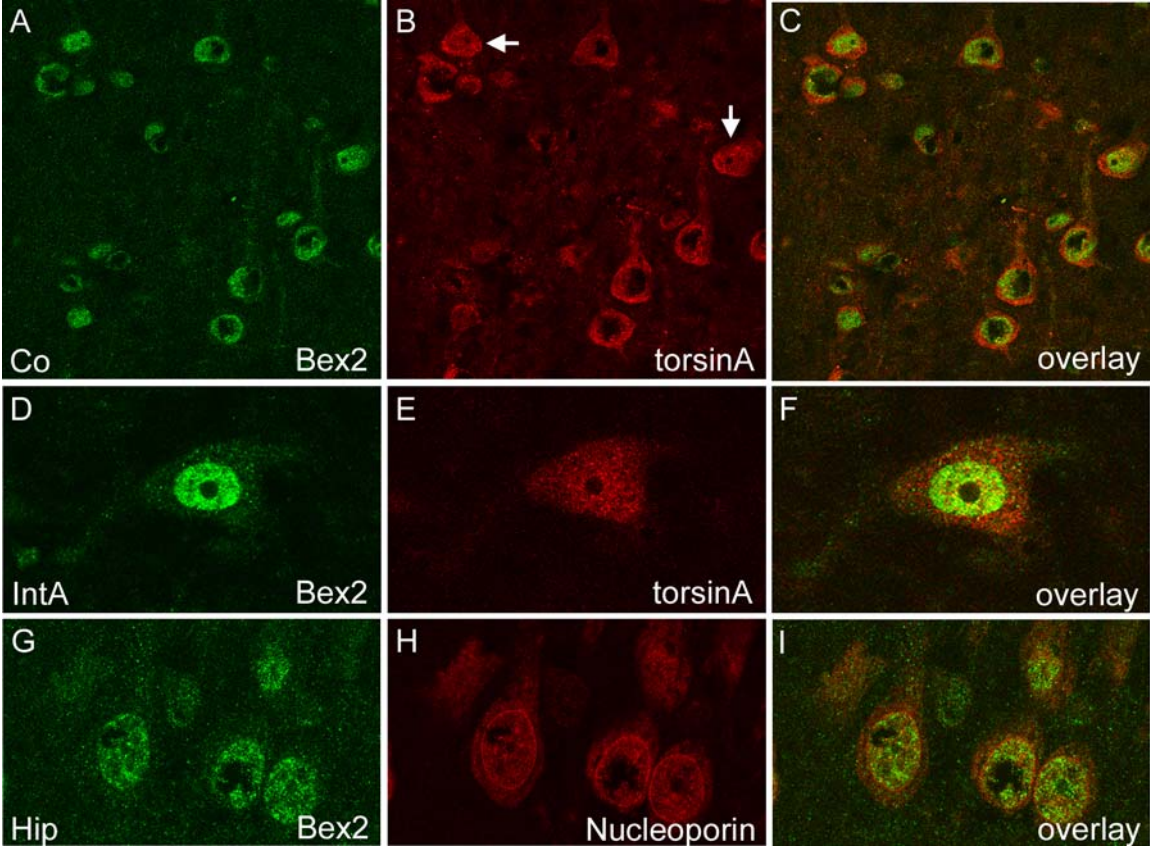
Fig. 24: Co-localization of Bex2 and torsinA in neurons of the adult rat brain.

A-F) ICC analyses revealed a prominent Bex2 IR (green) within the nucleus, but a weaker signal in the cytoplasm and processes of neurons from different rat brain structures. TorsinA IR (red) was primarily detected in the cytoplasm and processes of neurons and in some neurons torsinA staining was also observed in the nucleus (arrows B, E). In those neurons partial co-localization of Bex2 and torsinA IR was detected mainly in the nucleus. **G-I)** Staining against the NE protein Nucleoporin p62 (red) and Bex2 (green) showed partial co-localization in the nucleus. Co, cortex; IntA, interposed cerebellar nu; Hip, Hippocampus

4   DISCUSSION

4.1   The polyclonal Bex2 antibody specifically recognizes Bex2

To characterize Bex2, a novel polyclonal antibody, directed against the first 13 amino acids of human Bex2, had been generated and was tested in this study. Preadsorption analyses in different applications such as IB, ICC and IHC demonstrated the specificity of the Bex2 antibody. Furthermore, IP analyses with this antibody revealed specific precipitation of Bex2 protein from mouse Neuro-2A cells as a single 25 kD band. The presence of a 25 kD band is contradictory to the calculated molecular weight of Bex2, which is approximately 14 kD. However, using a polyclonal antibody, which had been generated against recombinant purified Bex1 protein and that recognizes Bex1 and Bex2, Koo and colleagues (2005) also demonstrated the existence of a single immunoreactive band at approximately 23 kD in brain extracts of young and adult mice, and of differentiated and undifferentiated F9 cells. Similarly, these researchers detected a 23 kD band in extracts of CHO cells, transfected with Flag-tagged Bex1 or Bex2 (137). Thus, the appearance of higher molecular weight bands may indicate that Bex2 is posttranslationally modified, possibly by sumoylation or ubiquitination. Sumoylation is a reversible coupling of small ubiquitin-related modifier (SUMO) proteins to cellular targets, which modulates protein-protein or protein-DNA interactions. Furthermore, SUMO binding is known to alter localization of the target protein, mostly by mediating nucleocytoplasmic trafficking, and to protect from ubiquitin-mediated degradation (140-142). SUMO proteins are approximately 100 amino acids long with a molecular weight of approximately 11 kD and covalent binding of SUMO results in a molecular weight shift of the target protein on SDS-PAGE. Thus, the observed 25 kD high molecular weight band of Bex2 might reflect sumoylated protein. Most known SUMO targets contain a minimal consensus motif for sumoylation (aaKxE/D, a is an aliphatic residue), however, other conjugation sites are beginning to emerge (143). Analyzing Bex1 and Bex2 amino acid sequences, using Abgent SUMOPlot™ to search for putative SUMO motifs revealed that mouse and rat Bex2, as well as mouse, rat and human Bex1 contain motifs with a low probability for SUMO binding (Fig. 25). However, no motif was found in the hBex2 amino acid sequence, but as new motifs begin to appear hBex2 may contain a

different one. To verify sumoylation of Bex2, IP with an antibody against SUMO should elucidate whether Bex2 can be immunoprecipitated from cell extracts containing endogenous or overexpressed Bex2, which would demonstrate reversible binding to SUMO.

Alternatively, the 25 kD band may reflect Bex2 splicing variants or may indicate that Bex2 forms dimers, although the latter is quite unlikely, since proteins should be denatured under the reducing conditions of SDS-PAGE. Nevertheless, dimerization of Bex2 could be facilitated, as it exhibits a CAAX motif at the very end of the C-terminus (Fig. 25), which is a site for post-translational modification with geranyl-geranyl or farnesyl substituents (prenylation). Prenylation enables reversible association of a protein with lipid bilayers, but there is also considerable evidence that prenylation mediates protein-protein interactions as shown for proteins of the Rab and Ras family, respectively (135, 144, 145).

```
hBex1  MESKEERALNNLIVENVNQENDEKDEKEQVANKGEP-LALPLNVSEYCVPRGNRRRFRVRQPILQY
rBex1  MESK-DQGAKNLNMENDHQKKEEKEEKPQDTIKREPVVAPTFEAGKNCAPRGGRRRFRVRQPISHY
mBex1  MESK-DQGVKNLNMENDHQKKEEKEEKPQDTIRREPAVALTSEAGKNCAPRGGRRRFRVRQPIAHY
hBex2  MESKEKRAVNSLSMENANQENEEK---EQVANKGEP-LALPLDAGEYCVPRGNRRRFRVRQPILQY
rBex2  MESKVEQGVKNLNMENDHQEKEEKEEKPQDANKREPVVALPFEAGEYYVPRGSRRRFRVRQPIAHY
mBex2  MESKVEQGVKNLNMENDHQEKEEKEEKPQDASKRDPIVALPFEAGDYYVPRGGRRRFRVRQPIVHY

hBex1  RWDIMHRLGEPQARMREENMERIGEEVRQLMEKLREKQLSHSLRAVSTDPPHHDHHDEFCLMP 128
rBex1  RWDLMHRVGEAQGRMRDENVQRFGEDMRHLMGKLRERQLSHSLRAVSTDPPHHDHNDEFCLMP 128
mBex1  RWDLMQRVGEPQGRMREENVQRFGGDVRQLMEKLRERQLSHSLRAVSTDPPHHDHHDEFCLMP 128
hBex2  RWDMMHRLGEPQARMREENMERIGEEVRQLMEKLREKQLSHSLRAVSTDPPHHDHHDEFCLMP 125
rBex2  RWDLMHRVGEPQGRMREENVQRFGEDMRQLMEKLRERQLSHSLRAVSTDPPHHDHHDEFCLMP 129
mBex2  RWDLMHRVGEPQGRMREENVQRFGDDVRQLMEKLRERQLSHSLRAVSTDPPHHDHHDEFCLMP 129
```

Fig. 25: ClustalW amino acid sequence alignment of mouse, rat and human Bex proteins.
Depicted are putative sumoylation motifs (highlighted in blue) and the CAAX motifs (highlighted in green), the latter are present in Bex1 and Bex2 of all three species.

Furthermore, IB and preadsorption analyses showed that the Bex2 antibody specifically recognizes endogenous mouse, rat and human Bex2 in cultured cells, with an apparent molecular weight of 25 kD. In contrast, Bex2 was not detected in tissue extracts of human brain, which may most probably be due to protein degradation, as post mortem tissue was used. However, Bex2 from mouse and rat brain tissue was specifically detected with anti-Bex2, migrating at 25 kD. Interestingly, an additional 15 kD immunoreactive band was apparent in rat brain extracts and extracts of RCN, which could be suppressed by pre-incubation of anti-Bex2 with recombinant MBP-hBex2. The presence of an additional 15 kD band suggests the existence of rat-specific Bex2 splicing variants or may represent a monomeric form of rat Bex2.

Moreover, the Bex2 antibody was successfully tested to recognize overexpressed hBex2. However, IB analyses of hBex2 overexpressing cell extracts revealed not only the presence of an immunoreactive 25 kD band, but an additional signal at 23 kD. This finding is astonishing, as the overexpressed hBex2 carries an N-terminal Flag epitope and would therefore be expected not to migrate lower than 25 kD. One explanation for a reduction in size may be endoproteolytic cleavage of a C-terminal portion of overexpressed hBex2, mediated by prenylation. Such a processing mechanism has been shown for lamin A, a major component of the nuclear lamina in mammalian cells (146). The lamin A protein is synthesized as a higher molecular mass precursor protein, prelamin A (~70 kD), which undergoes farnesylation (147, 148). Farnesylation is required for subsequent endoproteolytic cleavage of 15 amino acid residues upstream of the farnesylated cysteine, resulting in the mature lamin A protein, which migrates at a lower molecular weight (149-151). Thus, it might be possible that the abundance of overexpressed hBex2 promotes C-terminal processing mediated by prenylation. Alternatively, a decrease in protein size in SDS-PAGE may be due to the N-terminal FLAG epitope, which might alter the confor-mation of hBex2 by changing chemical properties and thus leading to a different behavior of hBex2 in SDS-PAGE.

Taken together, anti-Bex2 was shown to specifically recognize Bex2 in cultured cells, as well as in mouse and rat brain and was furthermore demonstrated to detect overexpressed FLAG-tagged hBex2. Additionally, different Bex2 isoforms seem to exist among species, as varying molecular weight bands were recognized with the Bex2 antibody (table 4).

Table 4: The Bex2 antibody recognizes different Bex2 species.

System	Bex2 species	Localization
mouse cell lines (CAD, Neuro-2A)	25 kD	vesicular throughout cytoplasm and nucleus
rat pheocytochroma cells (PC-12), non-differentiated	25 kD	vesicular throughout cytoplasm and processes, enriched in the nucleus
human neuroblastoma (SH-SY5Y)	25 kD	not examined
rat primary cortical neurons (RCN)	25 kD 15 kD	vesicular throughout cytoplasm and processes, enriched in the nucleus
adult rat brain	25 kD 15 kD	vesicular throughout cytoplasm and processes, enriched in the nucleus
adult mouse brain	25 kD	not examined
overexpressed hBex2 (N-terminal Flag epitope)	25 kD 23 kD	vesicular throughout cytoplasm, enriched in the nucleus

Furthermore, IB analyses in this study revealed that the Bex2 antibody recognizes a 15 kD and 25 kD band, respectively, in extracts of peripheral rat tissues. However, qRT-PCR data of this study and previous subtractive hybridization analyses (133) showed expression of hBex2 mRNA exclusively in the brain but not peripheral tissues. In contrast, the Bex1 homolog was shown to be expressed in neuronal as well as non-neuronal tissues (136). Given these findings and the fact that the region in Bex2 used for antibody generation is highly similar (77% identity) to the corresponding amino acid sequence in Bex1, it is possible that the antibody also detects Bex1. To prove this assumption, future experiments have to be performed. First, human Bex1-5 should be single transfected into cultured cells and subsequential protein extracts analyzed by immunoblotting, using anti-Bex2, as well as antibodies against other Bex family members. A second approach would require knocking down endogenous and overexpressed Bex2 in cell culture, using the RNAi system. Subsequent IB and ICC analyses with anti-Bex2 should then elucidate whether the antibody detects Bex1.

4.2 Bex2 interacts with wildtype and EOTD-causing torsinA *in vitro*

The first hint for an interaction between torsinA and Bex2 originates from a yeast two-hybrid screen, in which the C-terminal amino acids 251-332 of human torsinA were used to screen an adult human brain cDNA library, resulting in the identification of two positive hBex2 encoding clones (66).

In this study, *in vitro* MBP affinity precipitation assays confirmed the interaction of overexpressed Bex2 and torsinA in cells, as well as endogenous Bex2 and torsinA in rat and human brain. Using this assay, it was shown that Bex2 also binds the disease-associated mutant ΔE torsinA. Moreover, Bex2 seemed to have a higher affinity for the mutant variant, though this observation has to be considered with care and future experiments have to validate this possible effect more precisely. Nevertheless, it has been suggested that ΔE torsinA, as well as the ATP hydrolysis mutant E171Q-torsinA, have altered interaction abilities through tighter binding to their substrates (71, 91). Both mutant variants had a slower fluorescence recovery at the NE as compared to wildtype torsinA, suggesting an abnormal interaction with an immobilized transmembrane substrate (91). Moreover, ΔE torsinA was found to be

abnormally enriched at the NE of EOTD patient-derived fibroblasts, in cultured neurons and cells, indicating that torsinA may bind to substrates at the NE (70, 71, 85). Thus, it is likely that Bex2 binds ΔE torsinA tighter than wildtype torsinA and as ICC analyses showed that both proteins reside in the NE, this may indicate that Bex2 is a NE-specific substrate of torsinA.

Interestingly, Bex2 was found to bind different forms of ΔE torsinA, since two distinct immunoreactive bands were affinity precipitated with MBP-hBex2, migrating at approximately 35 kD and 37 kD, respectively. This finding suggests the presence of different post-translationally modified ΔE torsinA variants. TorsinA is known to be N-linked glycosylated at asparagines 143 and 158, respectively (56, 57). Recently, one study that used a cell free translation system demonstrated generation of four distinct membrane-associated torsinA products, migrating approximately between 30 kD and 37 kD. Two of these variants were either single or double glycosylated, as they migrated at higher molecular weights than two other non-glycosylated variants (77). Thus, different post-translationally modified variants of torsinA have been shown to exist *in vitro*. However, it should be considered that the proportion of double glycosylated torsinA is higher *in vivo* than in *in vitro* experiments. Nevertheless, it is supposable that the two distinct affinity precipitated bands observed in this study may reflect single and double glycosylated ΔE torsinA, respectively. Remarkably, although single glycosylated torsinA is considered to be represented at lower levels than double glycosylated in *in vivo* cell extracts, Bex2 appears to bind both variants equally in affinity precipitation assays.

Interestingly, an additional ΔE torsinA-immunopositive band was observed in trans-fected HEK 293Tcell extracts, migrating at approximately 40 kD. Taking into account that the localization of ΔE torsinA differs from wildtype torsinA in cell culture models, in terms of forming inclusions and abnormal enrichment at the NE, it is likely that overexpressed ΔE torsinA undergoes differential post-translational modifications. Thus, the 40 kD band may reflect the existence of higher glycosylated ΔE torsinA variants in transfected cells. Nevertheless, further experiments have to be performed to exclude the possibility of cell culture-derived artifacts.

In addition, co-IP studies were conducted to investigate the existence of an *in vivo* torsinA-Bex2 complex. So far, using this approach, an *in vivo* complex could not be confirmed, since Bex2 and torsinA were observed to bind non-specifically to beads and/or IgG. However, co-IP is an assay with some limitations: strong washing steps

that have to be used to circumvent unspecific binding of proteins to beads lead to disruption of weak interactions and co-IP is highly dependent on the specificity of the applied antibody. Moreover, isolation of protein complexes tightly bound to cellular membranes is rather sophisticated. Thus, association of torsinA and Bex2 with membranes may have impeded these analyses. Hence, it remains to be elucidated whether torsinA and Bex2 directly interact in an *in vivo* complex.

In summary, it was demonstrated that Bex2 and torsinA interact *in vitro*, either over-expressed in cultured cells or endogenously expressed in mammalian brain. Furthermore, Bex2 was shown to interact with different variants of ΔE torsinA, indicating the existence of ΔE torsinA isoforms, possibly differing in glycosylation states. However, future glycosylation studies with eluates of affinity purification assays should be performed in future to confirm the presence of differentially glycosylated ΔE torsinA. Moreover, the observation that Bex2 tended to bind stronger to ΔE torsinA than to wildtype torsinA indicates that the binding behavior of ΔE torsinA to target proteins is changed. Although this finding should be proven in further experiments, this data strengthens the hypothesis that EOTD may be caused by altered substrate binding of ΔE torsinA.

4.3   Bex2 and torsinA co-localize at the NE of neuronal-like cells

Immunocytochemical co-localization studies in differentiated rat PC-12 cells, RCN and adult rat brain neurons demonstrated a very similar subcellular localization of torsinA and Bex2, since both proteins showed a punctuate expression pattern throughout the cytoplasm and within processes of neurons. Additionally, endogenous Bex2 IR was shown to be abundant within the nucleus, sparing the nucleolus. In undifferentiated mouse Neuro-2A cells endogenous Bex2 IR was also observed in a punctuate pattern throughout the cytoplasm and within the nucleus. However, expression differed from PC-12 cells, RCN and neurons, as Bex2 IR was not enriched in the nucleus, indicating that Bex2 localization may be dependent on differentiation.

Single transfection of wildtype and mutant torsinA in Neuro-2A cells resulted in an enrichment of both proteins at the NE, whereas ΔE torsinA enrichment was observed to be even higher. These findings are consistent with previous studies showing that

torsinA is present in the NE, suggesting interaction with NE substrates. The particular high concentration of ∆E torsinA at the NE has been described in EOTD patient-derived fibroblasts, cultured neurons and cells, indicating that torsinA may have specific functions in the NE (70, 71, 85). Remarkably, overexpression of hBex2 resulted in predominantly nuclear localization and notably enrichment around the nucleus. Thus, it was investigated whether the NE is the site of the torsinA-Bex2 interaction. In fact, overexpressed torsinA and Bex2 were not only found to co-localize in the cytoplasm of Neuro-2A cells, but even more strikingly were enriched at the NE, where an intense co-localization of both proteins was observed. Thus, results of this study support preceding findings of an interaction between torsinA and Bex2 and moreover points to a role of both proteins at the NE.

Furthermore, a possible effect of ∆E torsinA on Bex2 localization was investigated, as previous studies indicated that ∆E torsinA re-localizes wildtype torsinA from the ER to the NE in neurons of ∆E torsinA transgenic mice (70). Additionally, the type III inter-mediate filament protein vimentin was found to be enriched in the NE due to overex-pression of ∆E torsinA (76). However, these findings do not apply for Bex2, since overexpression of ∆E torsinA did neither alter the subcellular localization of endogenous (data not shown) nor overexpressed hBex2. Nevertheless, overex-pressed Bex2 and ∆E torsinA were shown to be enriched at the NE, where some co-localization between both proteins was observed. Bex2 enrichment at the NE was equal to the enrichment observed in wildtype torsinA overexpressing cells, indicating that ∆E torsinA does not enhance localization of Bex2 to the NE.

Furthermore, the typical and manifold described ∆E torsinA-positive inclusions (56, 57, 64), also observed in this study, did not show IR for Bex2, suggesting that Bex2 is not a component of those inclusions. This is reasonable, since ICC and electron microscopic studies demonstrated that these ∆E torsinA-positive inclusions arise from the ER membrane (56) and Bex2 has not been shown to reside in the ER. However, it should be considered that the functional consequences of ∆E torsinA-positive inclusions are yet not clear and it remains to be elucidated whether these inclusions represent an artifact, resulting from very high expression levels in transfected cells (112). As a matter of fact, most previous studies did not detect torsinA-immunoreactive inclusions by light microscopy in brains of EOTD patients (43, 63). So far, only one study demonstrated the presence of ubiquitin/torsinA-

immunoreactive inclusions in neurons of the pedunculopontine nucleus, cuneiform nucleus and periaqueductal grey in brains of DYT1 patients (44).

Taken together, this study confirms the interaction between torsinA and Bex2, as both proteins were found to co-localize in the cytoplasm and in processes. Furthermore, co-localization and enrichment of torsinA and Bex2 were observed at the NE, which leads to the assumption that both proteins may have particular functions at the NE and that Bex2 may be a NE-specific substrate for torsinA.

4.4 Bex2 and TorsinA are associated with synaptosomal membranes

ICC studies in RCN revealed a possible association of Bex2 with vesicular structures, as staining against kinesin-I and synaptophysin, which are vesicle associated proteins, showed a very similar expression pattern. Moreover, Bex2 was observed to co-localize with torsinA and kinesin-I in discrete structures within the cytoplasm and processes. TorsinA is known to be an ER resident protein that is presumably peripherally associated with ER membranes (22, 46, 56, 57) and kinesin-I has been shown to interact with torsinA (66). Furthermore, kinesin-I is known to transport membranous organelles anterogradely along microtubules (78, 115, 116). Thus, as co-localization of torsinA and kinesin was observed within processes and growth cones, it has been suggested that torsinA may be transported by kinesin-I, presumably involving trafficking of ER-derived membranes. *In silico* analyses of Bex2 revealed the presence of a C-terminal CAAX motif, known to be a potential signal for posttranslational lipid modification and to mediate insertion of the target protein to cellular membranes (135). Considering these findings it was hypothesized that both Bex2 and torsinA may tightly be tethered to similar organelle membranes and binding to kinesin-I may facilitate their transport along microtubules.

To test this hypothesis, different subcellular fractionations were carried out. Analyses revealed an enrichment of Bex2 and torsinA in membranous fractions, containing proteins of plasma and organelle membranes, as well as proteins from the lumen of organelles. In addition, Bex2 and torsinA were enriched in the synaptosomal membrane fraction, in which also a low amount of kinesin-I was detected. This finding provides strong evidence that Bex2, torsinA and presumably kinesin-I are associated

with synaptosomes. However, the synaptosomal membrane fraction also contains debris, mitochondrial-, ER- and Golgi-derived membranes. Hence, Bex2 and torsinA may also be associated with those membranes.

TorsinA was additionally found in the microsome enriched fraction that represents fragmented ER membranes, confirming the association of torsinA with the ER. Also calnexin and PDI, both transmembrane ER proteins, were enriched in similar fractions as torsinA. Interestingly, calnexin was also detected in synaptosome- and synaptic vesicle-enriched fractions of rat brain, respectively, indicating that the ER extends into dendrites. Indeed, previous studies have shown that calnexin and the ER lumenal protein BiP are expressed in the ER of Purkinje cells, with distribution from the cell body to dendrites and dendritic spines (152). Recent studies even suggest the presence of a neuronal secretory pathway, as live cell imaging and ICC in cultured rat hippocampal neurons showed cargo budding from the ER at specialized ER exit sites, which are located in the soma and dendrites, and trafficking to the neuronal Golgi (153). Unfortunately, our antibodies did not detect torsinA in rat brain and the corresponding fractions in human brain could not be investigated due to low protein amounts. Thus, the presence of torsinA in synaptic vesicle-enriched fractions could not be confirmed in this study.

In conclusion, immunocytochemical studies and subcellular fractionations support the hypothesis of Bex2 and torsinA association to cellular membranes and indicate that both proteins are acting in similar compartments. Those compartments most probably include the NE and, as both proteins co-localized to vesicular structures and were enriched in synaptosomal membranes, further include a yet unspecified compartment. However, whether kinesin-I transports these compartments along microtubules remains to be elucidated. Moreover, Bex2 and torsinA were shown to be enriched at the NE in immunocytochemical analyses and to be enriched in the nuclear membrane-containing fraction after subcellular fractionation. Thus, these findings point to a role for both proteins at the nuclear membrane.

4.5 Expression of Bex2 and torsinA in neurons of the adult rat brain

The overall Bex2 and torsinA protein expression pattern in the adult rat brain was shown to be very similar for both proteins. Bex2 and torsinA showed a widespread distribution throughout the grey matter of rat brain, with especially high levels in the cerebellar cortex, cerebellum, hippocampus and olfactory bulb. These findings are consistent with qRT-PCR analyses in this study that revealed high Bex2 mRNA levels in the cerebellar cortex, cerebellum and moreover in the putamen of human brain tissue. Additionally, Koo and colleagues (2005) also demonstrated high levels of Bex2 mRNA in the cerebellum, hypothalamus and olfactory bulb of young and adult mice (137). Furthermore, a Human Multiple Tissue Expression Array, probed with oligonucleotides specific for human Bex1 and Bex2, respectively, revealed high expression levels of human Bex1 and Bex2 in the cerebellum, temporal lobe and pituitary (133).

The preferential expression of torsinA and Bex2 within the grey matter of rat brain indicates that both proteins are expressed in neurons. Examination of single rat brain neurons by IHC and ICC confirmed the findings of ICC analyses in cultured PC-12 cells and RCN in this study, since torsinA and Bex2 IR was present throughout the cytoplasm and within processes, partially co-localizing in the perinuclear region. Likewise, increased Bex2 IR was detected within the nucleus, excluding the nucleolus. Similar findings have been reported by Koo and colleagues (2005). By conducting ICC in mouse brain neurons using an antibody that recognizes Bex1 and Bex2, they observed Bex IR in dendritic processes and axon bundles, as well as in cell bodies, which were intensely labeled in the perinuclear region (137).

In contrast to ICC studies in cultured cells torsinA IR in rat brain neurons was additionally detected within the nucleus of some neurons, where strong co-localization with Bex2 was observed. TorsinA neuronal localization was previously described to vary between and within different brain structures, also depending on the antibody used. Using a rabbit polyclonal antibody, torsinA IR was detected in the cytoplasm and neurites but also within the nucleus in a vast majority of neurons in rat and human brain (58, 63). It has been suggested that torsinA contains a bipartite nuclear localization sequence **KK**IILNAVFGFINNP**K**P**KK** (basic amino acids in bold)

at amino acid residues 76 to 94 (58). In contrast, Augood and colleagues observed torsinA IR in the neuropil of human and maquaqe brain, which completely excluded the cell body (61), using the the same mouse monoclonal torsinA antibody as applied in this study. Similarly, intranuclear localization of torsinA in mammalian neurons could not be confirmed in studies using different anti-torsinA antibodies (43, 114, 154, 155). Thus, it remains controversially whether torsinA is present within the nucleus and it still has to be clarified if torsinA may have functions within this compartment.

4.6   hBex2 deletions

It has recently been shown that the subcellular localization of Bex family members differs, as expression ranged from predominantly nuclear (rat Bex1) or cytoplasmic (rat Bex3, human Bex5, and mouse Bex6) to diffuse, with some of the proteins found in both the nucleus and cytoplasm (rat Bex2 and rat Bex4) (133). Hence, these differences in the subcellular localization may reflect the presence of nuclear localization signals or nuclear export motifs in these proteins. Indeed, Bex3 contains a leucine-rich nuclear export sequence and nuclear export signal mutant Bex3 was shown to remain in the nucleus (132). Furthermore, treatment with leptomycin B, which inhibits the Crm1-mediated leucine-rich nuclear export (156), resulted in nuclear and cytoplasmic localization of Bex3, confirming the existence of a nuclear export signal (133). Thus, as Bex2 was predicted to contain a NLS that could facilitate nuclear import (136), hBex2 NLS-deletion variants (ΔhBex2_1-20 and 1-50) were overexpressed in Neuro-2A cells to analyze their subcellular localization. However, ICC analyses revealed that both variants were expressed in the cytoplasm as well as in the nucleus, although nuclear staining of NLS-deletion variants was not as strong as observed for overexpressed full-length Bex2. Similar results were obtained by Alvarez and colleagues (2005), who showed that mutation of two basic lysine amino acids in Bex1 that correspond to a putative nuclear localization motif did not alter Bex1 protein distribution (133). These independent findings indicate that a different mechanism than active nuclear transport through the presence of a NLS cause nuclear localization of Bex1 and Bex2. As mentioned earlier, sumoylation facilitates nuclear transport of a target protein and thus, covalent binding to SUMO might enable Bex1 and Bex2 to enter the nucleus. However, since hBex2 does not

contain a conserved sumoylation motif there might be a different mechanism allowing the protein to enter the nucleus. Considering that Bex2 is a small protein with a calculated molecular weight of approximately 14 kD, it is very likely that it passively diffuses through nuclear pore complexes, which have an exclusion size of approximately 50 kD (157).

Furthermore, deletion variants lacking the putative CAAX prenylation motif (ΔhBex2_1-121) and N-terminal amino acids (ΔhBex2_71-125) or both (ΔhBex2_71-121) were analyzed. N-terminal deleted variants were expressed throughout the cytoplasm of Neuro-2A cells, but showed a decreased nuclear IR, suggesting that nuclear import of these variants is impaired. Thus, the N-terminal NLS including region seems to be important for a nuclear localization. Indeed, this assumption was confirmed by overexpression of N-terminal containing variants ΔhBex2_1-17 and ΔhBex2_1-121, respectively, as both truncated proteins were observed within the nucleus of Neuro-2A cells. Remarkably, ΔhBex2_1-121 was found to resemble the expression pattern of full-length hBex2, as it was exceedingly high expressed in the nucleus. Moreover, all variants were shown to co-localize with torsinA in the cytoplasm and partially around the nucleus, thereby confirming previous affinity precipitation assays, in which torsinA bound to all MBP-hBex2 deletion variants.

IB analyses of ΔhBex2 variant overexpressing cell extracts revealed no IR for the N-terminally deleted variants ΔhBex2_71-12 and ΔhBex2_71-125, respectively, as well as for the short N-terminal variant ΔhBex2_1-20. Hence, such low protein levels may either be due to low transfection efficiencies of these constructs or instability of the resulting protein variants. Alternatively, truncated proteins may have been insoluble in the applied lysis buffer. To test the latter, proteins should be extracted from cells using a lysis buffer with a different detergent or a higher concentration of detergent.

In conclusion, these findings suggest that binding of Bex2 to torsinA is not mediated by a particular domain in Bex2. Thus, it is more likely that the whole Bex2 protein is capable of interacting with torsinA. Moreover, the putative NLS does not seem to be functional, since NLS deletion variants are localized in the nucleus. However, variants that contain amino acids 1-70 of the N-terminal region of hBex2 are predominantly nuclear localized, indicating that the N-terminus is essential for intra-nuclear transport. It is not clear whether the C-terminal CLMP sequence undergoes prenylation, but it lack lack of the CAAX motif did not alter the subcellular localization of truncated hBex2 protein variants. Further experiments will be required to elucidate

the relevance of the CAAX motif. One such experiment could include overexpression of CAAX-deletion variants, followed by subcellular fractionation assays to determine whether CAAX-lacking hBex2 proteins are still enriched in membrane containing fractions and hence are able to associate with cellular membranes.

4.7 The role of Bex1 in neurotrophin signaling, the cell cycle and neuronal differentiation – putative functions for Bex2?

Several indices are leading to the assumption that Bex1 and Bex2 are closely related proteins and may therefore possess similar functions (Fig. 26A). The first hint originates from amino acid sequences analyses showing that Bex1 and Bex2 are highly homologous proteins (hBex1 and hBex2 share 87% identity, 90% similarity), which share identical motifs, such as the putative NLS, kinase C phosphorylation site, the histidine-rich sequence and the C-terminal CAAX sequence. Furthermore, both proteins are expressed throughout the human CNS with very similar expression patterns (133) and have been reported to interact with the olfactory marker protein (OMP), a possible modulator component of the olfactory signal detection/transduction cascade (73, 136, 137). Moreover, whole-genome micro array analysis of epigenetic silencing identified *Bex1* and *Bex2* as candidate tumor suppressor genes in malignant glioma, implicating both proteins in a novel signaling pathway which regulates apoptosis (158). However, little is known about Bex2 function, as only two interacting proteins have been described so far, OMP and LMO2, the latter playing a role in hematopoetic stem cell differentiation and is a subunit of a DNA-binding protein complex (159, 160). Thus, Bex2 has been suggested to be involved in olfactory signaling and regulating embryonic development through modulation of the E-box sequence-binding DNA complex, respectively (137, 161).

In contrast to Bex2, more knowledge has been gathered about the function of Bex1 in the mammalian brain. Evidence emerged that implicates Bex1 in neuronal differentiation, as it has been identified in a screen for genes that are regulated by retinoic acid (130). Retinoic acid signalling is supposed to be important for the development of the olfactory system in mammals (162-164). Moreover, Bex1 was shown to be down regulated in proliferating neural stem cells of the subventricular zone of postnatal rats upon differentiation and overexpression of Bex1 in these precursors inhibited their differentiation into neurons (165, 166).

Furthermore, Bex1 has been shown to interact with the p75 neurotrophin receptor (p75^{NTR}), involved in neurotrophin signalling by mediating neuronal cell survival, differentiation and neurite outgrowth (165, 167). Neuronal and glial cell survival, growth and differentiation are mediated by the binding of nerve growth factor (NGF), as well as other neurotrophins, to two different types of cell surface receptors – the Trk tyrosine kinases and the p75 neurotrophin receptor (p75^{NTR}). Bex1 was shown to have a nucleocytoplasmic localization in p75^{NTR} expressing cells. Upon stimulation with NGF Bex1 rapidly re-localized from the nucleus to the cytoplasm, which has not been the case in TrkA expressing cells (165). Thus, a two-way communication has been proposed, in which two neurotrophin receptors work together – TrkA stabilizes Bex1 and p75^{NTR} translocates Bex1 out of the nucleus (Fig. 26B). Moreover, Bex1 levels were observed to oscillate during cell cycle and NGF treatment of differentiated PC-12 cells overexpressing Bex1 prevented them from cell cycle exit and differentiation, whereas knocking down of Bex1 accelerated PC-12 cell differentiation in response to NGF. Hence, Bex1 was suggested to represent a distinct class of intracellular modulators of neurotrophin receptors, linking neurotrophin signalling to the cell cycle.

In summary, these results point to a fundamental role of Bex1 protein in neuronal differentiation, development and function of the nervous system. As Bex1-shuttling between nucleus and cytoplasm seems to be important for cell proliferation and cell-cycle arrest, some authors even speculate that Bex1 might have an influence of the transcription of cell-cycle regulators (166).

Given the similarities between Bex1 and Bex2, it might be likely that Bex2 accomplishes related functions and it should therefore be investigated whether Bex2 also plays a role in neuronal differentiation and development of the nervous system. In this context it should be considered that the phenotype of EOTD only affects movement control within a narrow temporal window of symptom-onset, corres-ponding to a developmental period of synaptic plasticity associated with motor learning. Thus, further studies have to be conducted to investigate a possible role for Bex2 in neuronal development and synaptic plasticity. Moreover, examination of the relevance of the interaction between Bex2 and torsinA in this context may contribute to the understanding of the molecular pathogenesis of EOTD.

A
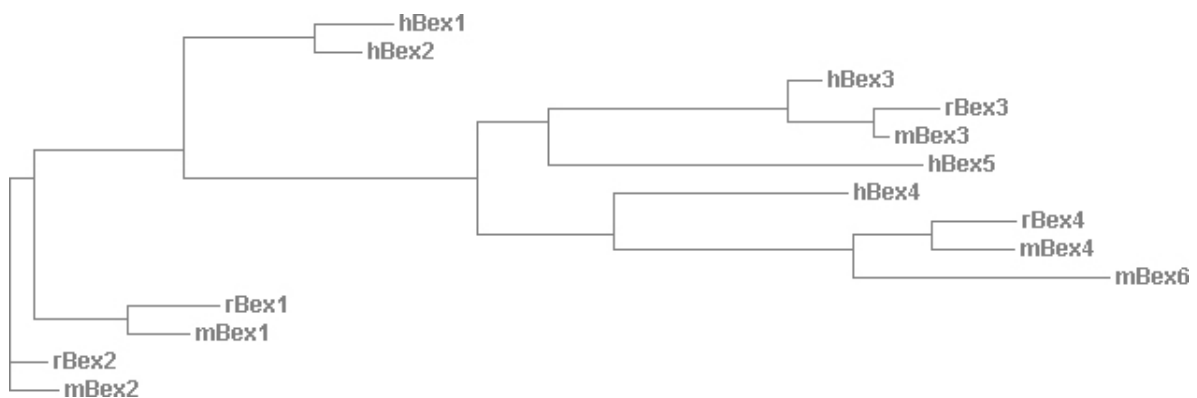
B
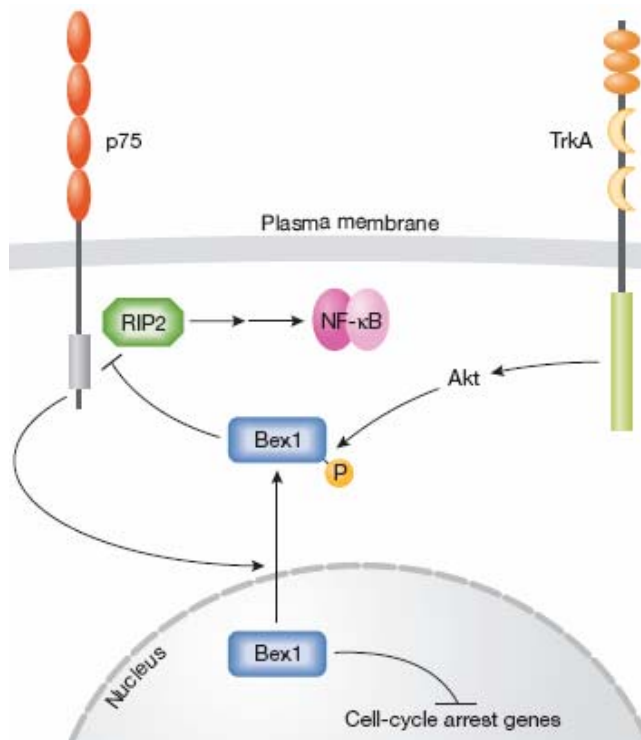
Fig. 26: Bex1 and Bex2 are closely related proteins, possibly comprising similar functions.

A) Phylogenetic tree of mouse, rat and human Bex family members (ClustalW) shows the close relation between hBex1 and hBex2. **B)** Bex1 localization and stability is regulated by neurotrophins. Binding of neurotrophin to TrkA stabilizes Bex1 through Akt-mediated phosphorylation. Simultaneously binding of neurotrophin to p75 promotes Bex1 nuclear export, which subsequently blocks the NF-κB pathway, resulting in cell-cycle arrest. RIP2, receptor interacting protein 2; Akt, serine/threonine kinase

From Carter (2006) (166)

4.8   Orientation of Bex2 and torsinA at cellular membranes

Several recent studies suggest torsinA to be primarily located in the ER lumen, where it is thought to associate with proteins in the ER membrane and binds to ER resident proteins like the transmembrane protein LULL1 and the primarily lumenal located homolog torsinB (45, 56, 57, 74, 107, 111, 168, 169). Over the past few years, increasing evidence emerged that torsinA also plays a crucial role at the NE, since the disease causing GAG deleted variant of torsinA and the ATP binding mutant (E171Q-torsinA) were found not only to be enriched at the NE, but also altered the morphology of the NE when overexpressed (70-72, 85, 107). Moreover, torsinA binds to LAP1, which spans the inner nuclear membrane and its overexpression recruits torsinA to the NE (91).

Nevertheless, several other torsinA-interacting proteins have been discovered, neither located in the ER nor the NE. These include kinesin-I, a motor protein mediating anterograde transport (66, 117, 118), and the cytoskeletal type III intermediate filament vimentin (75, 76, 99-103). Hence, there is also a significant fraction of torsinA functioning outside the NE and the ER or that is presumably localized at the cytoplasmic face of membranes. This would imply the presence of multiple torsinA isoforms, differing in ER and/or NE membrane orientation. In fact, recent *in vitro* membrane association studies provide evidence for the existence of differentially processed torsinA variants, thereby indicating that the mature torsinA is not a *bona fide* integral membrane protein but instead peripherally associated to ER membranes (170).

The present study demonstrates Bex2 as a novel torsinA-interacting protein, which was shown to be associated with nuclear and synaptosomal membranes. Interaction between both proteins was observed around the nucleus, most likely at the NE and in discrete vesicular compartments distributed throughout the cytoplasm and processes. Hence, four possible mechanisms are conceivable, how the interaction between Bex2 and torsinA may occur (Fig. 27).

I) Both proteins are peripherally associated to membranes with a cytoplasmic orientation - torsinA is tethered to the membrane via its N-terminal hydrophobic domain and Bex2 via C-terminal prenylation, whereas the C-terminal region of torsinA interacts with Bex2.

II) Both proteins interact in the lumen of a compartment and are peripherally associated to membranes: Bex2 flips within the lipid bilayer to achieve a lumenal orientation or is transported into the lumen of the appropriate compartment and subsequently tethers to the membrane, where it binds to the C-terminus of torsinA.

III) Both proteins are lumenal orientated, Bex2 is peripherally associated to membranes, but torsinA is integrated into the membrane.

IV) Interaction between Bex2 and torsinA is not direct and formation of a protein complex that includes Bex2 and torsinA is mediated via binding to other proteins such as LAP1.
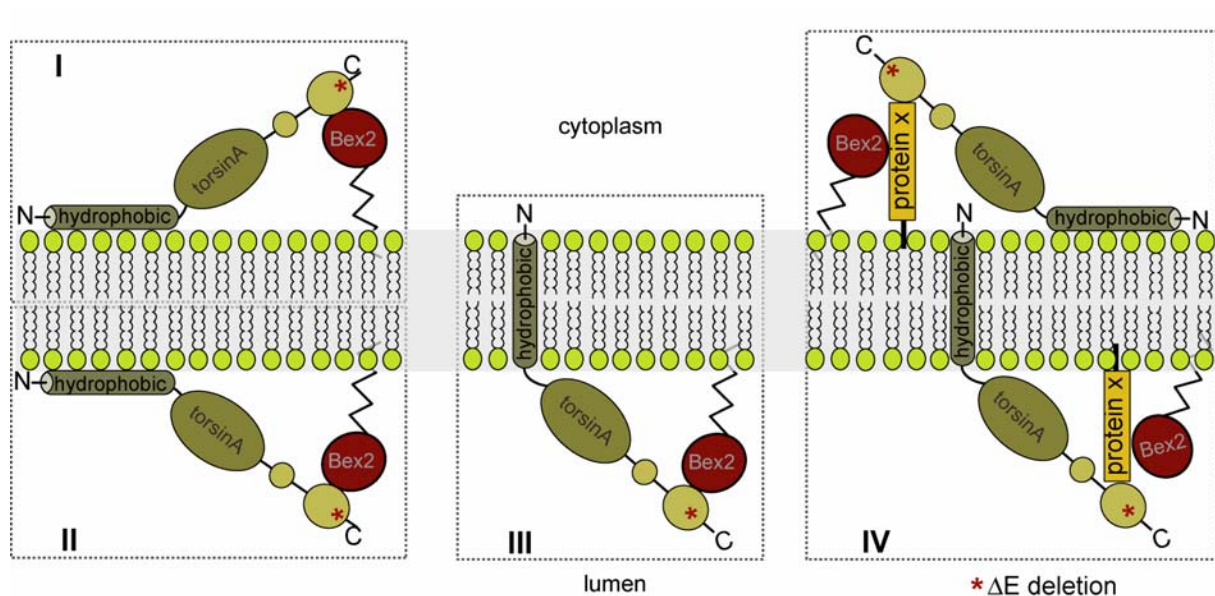
Fig. 27: Model for the localization of Bex2-torsinA complexes at cellular membranes.

Model I suggests a direct interaction of Bex2 and torsinA with cytoplasmic orientation and peripheral association to membranes. In model II both proteins interact directly and are peripherally associated to the lumen of a membrane. Model III also proposes a direct interaction of Bex2 and torsinA, whereas both proteins are lumenal orientated and torsinA is integrated into the membrane via its hydrophobic N-terminal domain. Model IV depicts a condition, in which Bex2 and torsinA are not directly interacting but are part of a membrane tethered complex including additional proteins.

4.9   Conclusion

This study demonstrates that Bex2 and torsinA are interacting *in vitro*, that they are co-localized in the cytoplasm, processes and especially around at the NE and that both proteins are associated with membranes of similar compartments. Hence, these findings are leading to the assumption that Bex2 and torsinA form a complex or are part of a protein complex, which is tethered to nuclear as well as synaptosomal membranes. The orientation of this complex at cellular membranes remains to be elucidated, but four different models have been described in the preceding chapter.

The Bex2-torsinA complex may include further proteins, previously shown to interact with torsinA. On the one hand this could include LAP1, which is tethered to the nuclear membrane and binds to B-type lamins and was shown to interact with torsinA at the NE (91, 127, 128). On the other hand, this complex may include kinesin-I, which had previously been shown to interact with torsinA (Fig. 28) (66). A first hint for the existence of the latter complex is a strong co-localization between Bex2 and kinesin-I, observed in discrete compartments within the cytoplasm and processes of primary neurons. Thus, it might be hypothesized that Bex2, torsinA and kinesin-I including complexes are associated with a yet unspecified compartment that is transported along microtubules through kinesin-I (Fig. 28).

Hence, Bex2 and torsinA may play a role in vesicular trafficking and/or may be involved in the neuronal secretory pathway. Indeed, a role for torsinA in vesicular trafficking or docking within pre-synaptic nerve terminals has already been proposed by Augood and colleagues (2003), who investigated the ultrastructural localization of torsinA in human and Macaque striatum and showed torsinA association with synaptic vesicles within axons and pre-synaptic terminals (61). Recently, also Hewett and colleagues (2007) suggested a role for torsinA as an ER chaperone that facilitates processing of proteins through the secretory pathway (171).
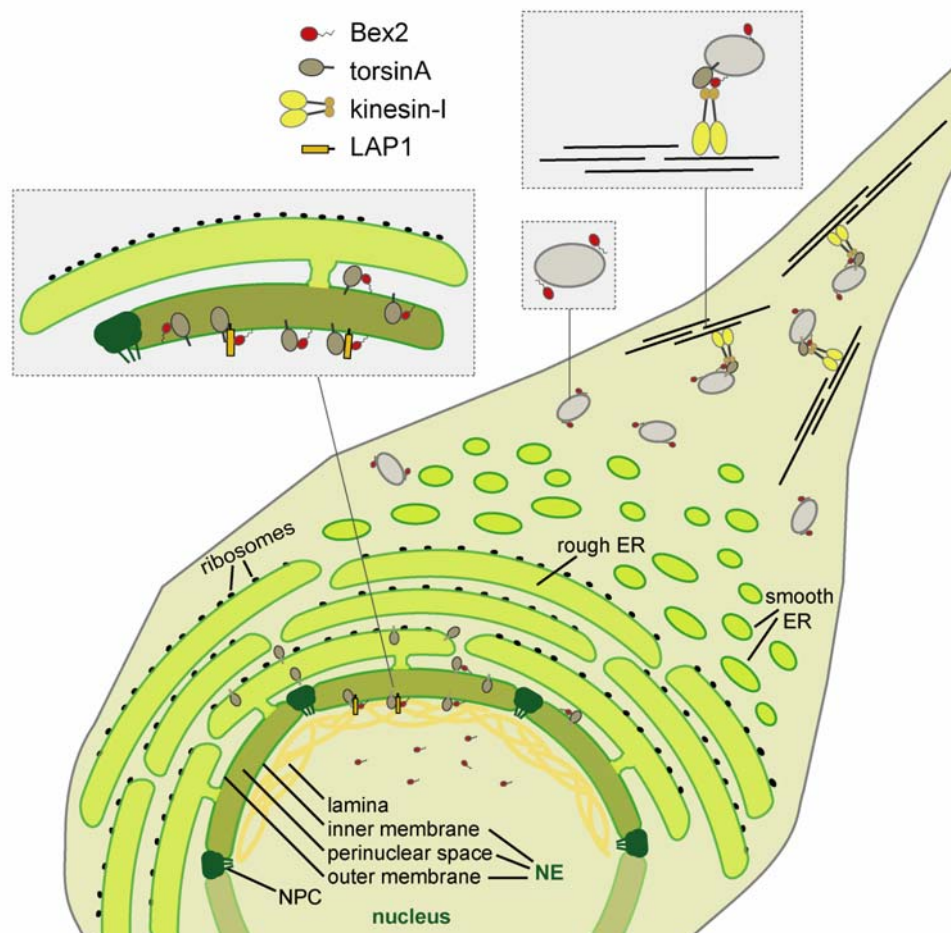
Fig. 28: Hypothetical model for the existence of Bex2-torsinA complexes at distinct cellular membranes.

Miscellaneous scenarios for the localization of different Bex2-torsinA complexes are imaginable. Bex2-torsinA complex might be associated with the inner and/or outer membrane of the NE, thereby possibly interacting with NE-resident proteins like LAP1. Moreover, Bex2-torsinA complex might be tethered to membranes of vesicular compartments, which may be transported along processes through binding to the motor protein kinesin-I.

4.10   Outlook

The present study provides evidence for the interaction between torsinA and Bex2 at the NE and therefore points to a role for both proteins at the nuclear membrane. Moreover, the finding that Bex2 also co-localizes with ΔE torsinA around the nucleus and that Bex2 appeared to have a slight tendency to bind tighter to mutant torsinA in *in vitro* affinity precipitation assays supports the hypothesis that altered substrate binding of mutant ΔE torsinA at the NE may lead to the development of EOTD. However, to confirm a possible altered binding behaviour of ΔE torsinA to Bex2, highly sensitive and quantitative protein-protein interaction assays, such as surface plasmon resonance (BIA*core*) that measures biomolecular interactions in real time (172-174) and bimolecular fluorescence complementation (BiFC), may be performed.

The former method can facilitate quantification of ΔE torsinA-Bex2 versus wildtype torsinA-Bex2 binding affinities *in vitro*, whereas the latter visualizes protein interactions *in vivo* (175). In the BiFC assay proteins of interest are tagged with fragments of a fluorescent protein (e.g. eYFP, Venus, Cerulean) (175). Direct interaction of the proteins of interest brings fluorescent protein fragments in close proximity, resulting in complex formation of fluorescent fragments, which increases fluorescence that can be analyzed and measured by fluorescence microscopy. As BiFC assays can also be performed in living cells, this method does not only allow the study of protein complex formation, but also their subcellular localization and transport (175). Hence, torsinA-Bex2 and ΔE torsinA-Bex2 complexes, respectively, could be studied *in vivo* in respect to their subcellular localization and ability to be transported within a cell. However, Bragg and colleagues (2004) demonstrated that high expression levels of mutant torsinA led to formation of torsinA-positive inclusions, whereas low expression led to a predominant perinuclear localization of ΔE torsinA (112). High level and drug dose-dependent expression of wildtype and mutant torsinA were achieved by generating two types of viral vectors (herpes simplex virus type 1 amplicon): either an amplicon under control of a strong constitutive viral promotor or a tetracycline-regulated amplicon under a drug-regulated promotor (112). A similar viral-based system could be used in combination with BiFC to study wildtype and mutant torsinA-Bex2 complex formation, respectively, under high level or low level expression in living cells.

This study furthermore hypothesized that Bex2, torsinA and kinesin-I may exist in a complex, in which Bex2 and torsinA are associated with a yet unspecified compartment that is transported along microtubules through kinesin-I. To verify this theory co-IP and/or affinity precipitation assays have to be peformed to prove binding of Bex2 to kinesin-I. Additionally, the aforementioned BiFC assay may also be conducted with Bex2 and kinesin-I constructs, tagged with the appropriate fluorescent protein fragment, to confirm complex formation and to elucidate in which compartments both proteins are localized. Moreover, this assay can be applied in living RCN to investigate whether kinesin-I-Bex2 and kinesin-I-torsinA complexes are transported along processes.

Furthermore, this study showed localization of Bex2, torsinA and kinesin-I, respectively, to punctuate presumably vesicular structures, distributed throughout the cytoplasm and within processes of RCN. Thus, it has to be investigated where these yet

unspecified compartments originate from. It is known that smooth ER is transported anterogradely via a distinct mechanism by the fast axonal transport system (176, 177). Moreover, it has been reported that a sub-compartment of the ER exists in a large, vesicular structure that is rapidly bi-directional moved along dendrites (178). It would therefore be interesting to study whether Bex2, torsinA and kinesin-I are components of this ER sub-compartment. Furthermore, it has been shown that movement of ER sub-compartments along dendrites was highly dependent on the integrity of kinesin, as overexpression of dominant-negative kinesin or knock-down with RNAi both yielded reduction of the velocity of vesicular movement (178). Hence, it should be investigated whether torsinA-Bex2 complexes and/or torsinA- and Bex2-positive vesicular-like structures are affected by overexpression of dominant-negative kinesin or antisense oligonucleotide treatment. These analyses would facilitate verification of the hypothesized interaction between Bex2, torsinA and kinesin-I and moreover, would shed light on a possible kinesin-I-dependent transport of Bex2-torsinA complexes along processes.

To elucidate the relevance of the Bex2-torsinA interaction in EOTD and a possible impairment of cellular processes through binding of mutant torsinA to Bex2, it is important to conduct further studies to enlighten cellular functions of Bex2. Thus, to study this protein's function in more detail, it would be essential to generate hBex2 transgenic mouse models and/or Bex2 knockout mice. Additionally, since Bex2 is highly similar to the close-related homolog Bex1, it should be investigated whether Bex2 accomplishes similar functions as Bex1, including neurotrophin signalling, cell cycle regulation and neuronal differentiation.

Moreover, only 30-40% of the *DYT1* mutation carriers develop EOTD, thus several other genetic modifications may contribute to the development of the disease and it should therefore be examined whether hBex2 may be such a modifier. One possibility is the search for polymorphisms within the *hBex2* gene and the performance of association studies to elucidate a possible genetic divergence between EOTD patients and healthy controls.

5   MATERIALS AND METHODS

5.1   Equipment and consumables

5.1.1   Molecular biology

equipment/materials	manufacturer
agarose gel electrophoresis chamber	Peqlab
cuvette, electroporation (gap 0.2 cm)	Biorad
E. coli Pulser™ transformation apparatus	Biorad
gel documentation system/UV monitor	Vilber Lourmat
incubator	Binder (Multimed)
Light Cycler	Roche
Light Cycler capillaries	Roche
microwave	Panasonic
pipettes	Gilson
pipettor	Hirschmann Laborgeräte
power supply	Consort
reaction tubes (0.5 ml, 1.0 ml, 2.0 ml)	Eppendorf
reaction tubes (15 ml, 50 ml)	Falcons
table top micro centrifuge 5415D	Eppendorf
table top centrifuge 5810R	Eppendorf
thermo cycler	Biozym Scientific GmbH
thermo mixer	Eppendorf

5.1.2   Protein biochemistry

equipment/materials	manufacturer
blotting chamber, semi-dry	Peqlab
blotting chamber, wet	Biorad
developer	Fujifilm
Econo-Pac column	Biorad
ELISA reader	Biorad
gel drying frames	Sigma
Hybond-P PVDF membrane	Amersham Biosciences
nitrocellulose transfer membrane	Amersham Biosciences
rotor, fixed angle F-34-6-38	Eppendorf
rotor TH-641, swinging-bucket	Amersham Biosciences
scale	Ohaus
SDS-PAGE chamber	Sorvall
shaker	Heidolph Instruments
sonicator	Bandelin
spectrophotometer	Amersham Biosciences
ultracentrifuge	Sorvall
Whatman blotting paper	Schleicher und Schuell

5.1.3   Cell biology

equipment/materials	manufacturer
autoclave	Systec
cell culture dishes (24 well, 6 well)	Corning
cell culture dishes (5 cm, 10 cm)	Becton Dickinson
cell culture flasks (75 cm^2, 175 cm^2)	Corning
cell scraper	Corning
cell strainer	BD Biosciences
chamber slides Super-Frost®	R. Langenbrinck
confocal fluorescence microscope and camera	Zeiss
counting chamber (Neubauer)	Roth
coverslips, 12 mm	Roth
cryopreserving tube	Greiner
dissecting scope	Leica
fluorescence microscope and camera	Zeiss
incubator, Heracell	Heraeus
freezing container (freezing of cells)	Nalgene
laminar flow	Heraeus/Kendro
microtome	Leica
Parafilm® M	Brand
reaction tubes (0.5 ml, 1.0 ml, 2.0 ml)	Eppendorf
reaction tubes (15 ml, 50 ml)	Greiner Bio-one
waterbath	Medingen

5.2   Chemicals and solutions

chemicals	manufacturer
40% Acrylamid/Bis solution 19:1	Biorad
all trans-Retinoic Acid	Sigma
Ammonium persulfate (APS)	Sigma
Amphotericin B	Sigma
Ampicillin	Sigma
Amylose resin	NEB
B-27 serum-free supplement	Gibco
Bacto-Agar	Becton Dickinson GmbH
Biorad protein assay (Bradford)	Biorad
Bovine Serum Albumin (BSA) for blocking solution	Sigma
Bovine Serum Albumin (BSA) as protein standard	NEB
Bromphenol blue sodium salt	Merck
Collagen type I, rat tail	Chemicon
Complete® protease inhibitor cocktail	Roche
Desoxynucleotide-5'-triphosphate (dNTP), 10 mM each	Qiagen
Dimethyl pimelimidate·2HCl (DMP)	Pierce
1,4-Dithiothreitol (DTT)	Roth
Dimethylsulfoxide (DMSO)	Sigma
DMEM (Dulbecco's minimal essential medium)	Biochrom

DMEM/HAM's-F12	Biochrom
DNA 100 bp ladder	NEB
DNA 1 kb ladder	NEB
DNA T4 Ligase (1U/µl)	Roche
DNA T4 Ligase buffer (10x)	Roche
EDTA	Sigma
EGTA	Sigma
Entellan® rapid mounting medium	Merck
Ethanol	Merck
Ethidium bromide	Merck
Fetal bovine serum gold	PAA
Fluorescence mounting medium	DakoCytomation
FuGENE 6 transfection reagent	Roche
Gel code blue stain R-250 (Coomassie)	Pierce
Glycerol	Sigma
Glycin	Roth
HBSS, 10x (Hanks' balanced salt solution)	Sigma
Hepes	Sigma
Hydrochloric acid (HCL)	Merck
Hydrogen peroxide (H_2O_2)	Sigma
Immun-Star HRP substrate	Biorad
Kanamycin	Sigma
L-glutamine (200 mM)	Gibco
Lipofectamine™ 2000	Invitrogen
ß-Mercaptoethanol	Merck
Methanol	Merck
2-Methylbutane	Roth
N,N,N',N'-Tetramethylethylendiamine (TEMED)	Merck
Nerve growth factor (NGF), mouse 25S, grade I	Alamone Labs
Neurobasal™ medium	Gibco
Non fat milk powder	Sucofin (Edeka)
Normal Goat Serum	Sigma
Normal Horse Serum	Invitrogen
NP-40/Igepal CA-630)	Sigma
One Shot® TOP10Electrocomp™*E. coli*	Invitrogen
Optimem	Gibco
Paraformaldehyde (PFA)	Sigma
Penicillin	Gibco
Pfu DNA polymerase	Stratagene
Pfu DNA polymerase buffer (10x)	Stratagene
Poly-D-lysine hydrobromide (PDL)	Sigma
Ponceau S Staining Solution	Sigma
Rabbit serum	Sigma
Potassium chloride (KCL)	Merck
Potassium dihydrogen phosphate (KH_2PO_4)	Merck
Precision Plus Protein Standard, prestained	Biorad
2-propanol	Merck
Protein A- and G-agarose	Roche
Random hexamer primers	Roche
Restriction endonucleases	Roche/Fermentas
Restriction endonuclease buffers	Roche/Fermentas

RNaseOUT (40 U/μl)	Invitrogen
S.O.C. medium	Invitrogen
Sodium azide (NaN$_3$)	Sigma
Sodium chloride (NaCl)	Merck
Sodium deoxycholate	Sigma
Sodium dodecyl sulfate (SDS)	Sigma
Sodium hydroxide (NaOH)	Merck
Sodium phosphate dibasic heptahydrate (Na$_2$HPO$_4$-7 H$_2$O)	Merck
Streptomycin	Gibco
Sucrose	Sigma
Taq DNA polymerase	Qiagen
Taq DNA polymerase buffer (10x)	Qiagen
TO-PRO®-3 iodide	Molecular probes
Transcriptor Reverse Transcriptase	Roche
Transcriptor RT reaction buffer (5x)	Roche
Triethanolamine hydrochloride	Sigma
Triton X-100	AppliChem
TRIZMA® Base (Tris base)	Sigma
Trypsin-EDTA	Gibco
Tryptone	Fluka
Tween® 20	Merck
Xylol	Fluka
Yeast extract	Sigma

Kit	manufacturer
Light Cycler FastStart DNA Master Hybridization Probes	Roche
Light Cycler Control Kit DNA	Roche
MinElute® Gel Extraction Kit	Qiagen
MinElute® PCR Purification Kit	Qiagen
MinElute® Reaction Cleanup Kit	Qiagen
QIAquick® Gel Extraction Kit	Qiagen
QIAquick® PCR Purification Kit	Qiagen
QIAquick® Nucleotide Removal Kit	Qiagen
QIAGEN® Plasmid Midi, Maxi, Mega and Giga Kits	Qiagen
QIAprep® Miniprep Kit	Qiagen
Qproteome Cell Compartment Kit	Qiagen
Vectastain® Elite ABC Kit	Vector Laboratories
Vector® SG Peroxidase Substrate Kit	Vector Laboratories

5.2.1 Molecular biology

Ampicillin stock solution

100 mg/ml in H_2O bidest. Aliquots were stored at –20°C.

Kanamycin stock solution

30 mg/ml in H_2O bidest. Aliquots were stored at –20°C.

LB medium

10 g Tryptone, 5 g Bacto-Yeast extract, 10 g NaCl, in 900 ml H_2O, pH adjusted to 7.0 with 10 M NaOH. Adjusted to 1 liter volume with H_2O bidest and sterilized by auto-claving. Ampicillin (50 µg/ml) was added after cooling down to approximately 50°C.

LB agar plates

10 g Bacto-Tryptone, 5 g Yeast extract, 10 g NaCl in 900 ml H_2O, pH was adjusted to 7.0 with 10 M NaOH and volume to 1 liter with H_2O bidest. 15 g Bacto-Agar were added to 1 liter medium and sterilized by autoclaving. Ampicillin (100 µg/ml) was added after cooling down to approximately 50°C.

10x DNA gel loading buffer

250 mg bromphenol blue, 33 ml 150 mM Tris base (pH 7.6), 60 ml glycerol, 7 ml H_2O bidest. Stored at 4°C.

Tris-borate buffer (TBE) 10x

108 g Tris, 55 g Boric acid in 900 ml H_2O bidest. 40 ml 0.5 M Na_2EDTA (pH 8.0) was added and volume adjusted to 1 liter with H_2O bidest.

1% (w/v) Agarose gel

1 g agarose was dissolved in 100 ml 1x TBE by microwave heating. 3.0 µl of ethi-dium bromide were added to the cooled (~50°C) solution.

5.2.2 Protein biochemistry

SDS-PAGE stacking gel buffer

0.5 M Tris base, pH 6.8 and 0.4% SDS.

SDS-PAGE resolving gel buffer

1.5 M Tris base, pH 8.8 and 0.4% SDS.

10x SDS-PAGE running buffer

30.3 g Tris base, 144.1 g glycin, 10 g SDS in 1 liter H_2O bidest.

4x SDS-PAGE sample buffer

2.5 ml 1 M Tris base (pH 6.8), 2.0 ml 20% SDS, 4.0 ml glycerol, 1.0 ml ß-mercapto-ethanol, 250 mg bromphenol blue, adjusted to 10 ml volume with H_2O bidest. Aliquots were stored at –20°C.

1x Transfer buffer

3.03 g Tris base, 14.41 g glycin, 200 ml methanol, adjusted to 1 liter volume with H_2O bidest.

10x TBS - Tris buffered saline

302.85 g Tris, 438.3 g NaCl in 4 liter H_2O. pH was adjusted to 7.5 with 1 M HCl and volume was filled to 5 liter with H_2O. Stable at 4°C for three months.

1x TBS-T - Tris buffered saline/0.1% Tween 20

Dissolving of 1.0 ml Tween 20 in 1 liter 1x TBS.

1x PBS-T – phosphate buffered saline/0.1 % Tween 20

Dissolving of 1.0 ml Tween 20 in 1 liter 1x PBS.

10% Blocking solution

Dissolving of 50 g non fat milk powder in 500 ml 1x TBS.

Stripping solution

7.57 g Tris base (pH 7.6), 20 g SDS, 6.98 ml ß-mercaptoethanol, adjusted to 1 liter volume with H_2O bidest.

Antibody solution - immunoblotting

Dissolving 1 g BSA and 1 g NaN_3 in 100 ml TBS-T. Stored at 4°C.

MBP-Lysis buffer

30 mM HEPES (pH 7.6), 400 mM KCl, 5% glycerol, 3 mM $MgCl_2$, ß-mercaptoethanol (350 µl/500 ml buffer).

MBP-Elution buffer

30 mM HEPES (pH 7.6), 100 mM KCl, 5% glycerol, 3 mM $MgCl_2$, ß-mercaptoethanol (350 µl/500 ml buffer), 10 mM maltose.

Affinity precipitation washing buffer

30 mM HEPES (pH 7.6), 100 mM KCl, 5% glycerol, 3 mM $MgCl_2$, ß-mercaptoethanol (350 µl/500 ml buffer).

Immunoprecipitation washing buffer

150 mM NaCl, 50 mM Tris base (pH 8.0), 5 mM EDTA and 10% glycerol.

HEPES-buffered sucrose - Subcellular fractionation

0.32 M sucrose, 4 mM HEPES (pH 7.4), 1 mM EDTA, 1 mM EGTA and freshly added 1x Complete® protease inhibitor cocktail.

0.25 M sucrose buffer

0.25 M sucrose, 20 mM HEPES (pH 7.3), 1 mM EDTA, 1 mM EGTA and freshly added 1x Complete® protease inhibitor cocktail.

1.9 M sucrose buffer

1.9 M sucrose, 20 mM HEPES (pH 7.3), 1 mM EDTA, 1 mM EGTA and freshly added 1x Complete® protease inhibitor cocktail.

5.2.3 Cell biology

10x PBS - Phosphate buffered saline

80 g NaCl, 2 g KCl, 26.8 g Na_2HPO_4-7 H_2O and 2.4 g KH_2PO_4 in 800 ml H_2O. pH was adjusted to 7.4 with HCl and volume filled to 1 liter with H_2O.

Freezing medium

40 ml of the appropriate culture medium, 40 ml fetal bovine serum and 20 ml DMSO were mixed, sterile filtrated using a 0.22 µm filter and stored at 4°C.

RIPA cell lysis buffer

150 mM NaCl, 1% NP-40, 50 mM Tris base (pH 8.0), 0.1% SDS and 0.5% sodium deoxycholate in H_2O bidest. 1x Complete® protease inhibitor cocktail (Roche) was added freshly.

NP-40 cell lysis buffer

150 mM NaCl, 0.1-1.0% NP-40 and 50 mM Tris base (pH 8.0). 1x Complete® protease inhibitor cocktail (Roche) was added freshly.

4% PFA/PBS solution

Dissolving 10 g paraformaldehyde in 250 ml PBS by heating to 50°C in a water bath.

Triton X-100 permeabilization buffer

0.3% Triton X-100 in 1x TBS.

IF – blocking buffer

10% normal goat serum in 1x PBS.

IF – antibody solution

1% bovine serum albumin in 1x PBS.

IHC – blocking buffer

3% normal goat serum in 1x TBS

IHC - primary antibody solution

0.1% Triton X-100 and 2% normal goat serum in 1x TBS.

IHC – secondary antibody solution

1% normal goat serum in 1x TBS.

1x HBSS solution

35 ml 10x HBSS were diluted in 350 ml sterile H_2O bisdest. 3.5 ml of 250 µg/ml Amphoptericin B (final 2.5 µg/ml) and 3.5 ml of Penicillin/Streptomycin (final 1%) were added. The solution was stored at 4°C.

1x protease solution

0.5 ml trypsin/EDTA were diluted in 3.5 ml 1x HBSS solution and stored at 4°C.

Cell culture media, sera and solutions

medium	manufacturer
DMEM rich medium (high glucose)	Biochrom
DMEM/HAM's-F12 rich medium	Biochrom
Neurobasal™ medium	Gibco
fetal bovine serum	PAA
horse serum	Invitrogen
Amphoptericin B (250 µg/ml)	Sigma
B-27 serum-free supplement	Gibco
L-glutamine	Biochrom
PBS	Gibco
penicillin	Gibco
streptomycin	Gibco
Trypsin/EDTA	Invitrogen

5.3   Antibodies

primary antibody	clone	dilution	manufacturer
rabbit polyclonal			
anti-Bex2 (74495) (recognizes aa 1-13 of human Bex2)	-	IB 1:1000 ICC 1:800 IP 1:60 IHC 1:800	Xandra O. Breakefield (Massachusetts General Hospital, not published)
anti-calnexin (recognizes aa 575-593, sequence identical in mouse, rat and human)	-	IB 1:2000 ICC 1:2000	Stressgen
anti-torsinA TAB1 (recognizes aa 299-312 of human torsinA, also detects torsinB)	-		Hewett et al., 2000
PDI (H-160)		IB 1:200	Santa Cruz Biotechnology

primary antibody	clone	dilution	manufacturer
mouse monoclonal			
anti-acetyl Histone H3		IB 1:4000	Upstate
Alexa Fluor® 568 phalloidin (labels F-actin)	-	ICC 1:200	Invitrogen
anti-EEA1	14	ICC 1:100	BD Transduction Laboratories
anti-FLAG® M2	M2	IB 1:2000 ICC 1:3000	Sigma
GAPDH (Glyceraldehyde-3-Phosphate Dehydrogenase)	6G5	IB 1:100	Biotrend Chemikalien GmbH
anti-GM130	35	IB 1:250	BD Transduction Laboratories
anti-Hsp90	AC88	IB 1:1000	Stressgen
anti-kinesin, heavy chain	H2	IB 1:1000 ICC 1:200	Chemicon
anti-MAP2	HM-2	ICC 1:500	Sigma
anti-nucleoporin p62	53	IB 1:1000 IF 1:100	BD Transduction Laboratories
anti-PSD-95	16	IB 1:200	BD Transduction Laboratories
anti-SNAP-25	SP12	IB 1:2000	BD Transduction Laboratories
anti-synaptophysin	SVP-38	IB 1:500 ICC 1:100	Sigma
anti-torsinA D-MG10 (recognizes exon 4 of human torsinA)	-	ICC 1:200 IP 1:75 IHC 1:200	Hewett et al., 2000
anti-torsinA D-M2A8 (recognizes aa 51-332 of human torsinA)	-	IB 1:200 IP 1:75	Hewett et al., 2000
anti-α-tubulin	DM 1A	IB 1:8000	Sigma

secondary antibody	dilution	manufacturer
goat anti-mouse Alexa Fluor® 488	ICC 1:1500	Molecular Probes
goat anti-mouse Alexa Fluor® 568	ICC 1:1000	Molecular Probes
donkey anti-rabbit-HRP	IB 1:8000	Amersham Biosciences
sheep anti-mouse-HRP	IB 1:8000	Amersham Biosciences

5.4   Expression and cloning vectors

Following expression vectors and cloning plasmids were used in this study.

pcDNA3/5'FLAG-wildtype torsinA and pcDNA3/5'FLAG-ΔGAG torsinA

The entire coding sequence for human wildtype and mutant (ΔGAG) torsinA, respectively, have been cloned into the pcDNA3/5'FLAG mammalian expression vector (Invitrogen), containing a FLAG tag in-frame at the 5'-end of the multiple cloning site (56).

pMal-c1-wildtype torsinA and pMal-c1- ΔGAG torsinA

This vector contains a *malE* gene, encoding maltose-binding protein, fused to human wildtype and mutant (ΔGAG) torsinA sequences, respectively, corresponding to amino acids 55-332 (46).

pMal-c2X-hBex2

The pMal-c2X vector (NEB) contains a *malE* gene, encoding maltose-binding protein, fused to the entire human Bex2 sequence. This vector is used to isolate the fusion protein in one-step affinity purification.

pcDNA3/5'FLAG-hBex2

The entire coding sequence for human Bex2 has been cloned into the pcDNA3/5'FLAG mammalian expression vector (Invitrogen), containing a FLAG tag in-frame at the 5'-end of the multiple cloning site. Cloning was analogous to the subcloning of the KLC-coding sequence into pcDNA3/5'FLAG (66).

pcDNA3/5'FLAG-hBex2 deletion constructs

The pcDNA3/5'FLAG mammalian expression vector (Invitrogen) contains truncated sequences for human Bex2, corresponding to hBex2 protein variants comprising amino acids 1-20, 1-50, 1-70, 1-121, 71-121 and 71-125, respectively. The coding sequences of hBex2 deletion variants were amplified by PCR from the pcDNA3/5'FLAG-hBex2 plasmid and were subcloned into restriction sites BamH I and Xho I of pcDNA3/5'FLAG.

5.5   Oligonucleotides

Table 5: List of oligonucleotides used in this study.

Oligonucleotide	Sequence 5'→3'	RS	Description
hBex_ATG-for	CGC**GGATCC**_ATGGAGTCCAAAG AGAAAC_	BamH I	hBex2 cloning primer, starts at ATG, forward
hBex_d71-121-for	CGC**GGATCC**_GGAGAACCACAGG CAAGG_	BamH I	hBex2 cloning primer, starts at nucleotide 211 downstream of ATG, forward
hBex_d1-20-rev	CCG**CTCGAG**TCA_TTCTTGGTTGG CATTTTCC_	Xho I	hBex2 cloning primer, starts at nucleotide 60 downstream of ATG, reverse
hBex_d1-50-rev	CCG**CTCGAG**TCA_ACGATTTCCTC TAGGCAC_	Xho I	hBex2 cloning primer, starts at nucleotide 150 downstream of ATG, reverse
hBex_d1-70-rev	CCG**CTCGAG**TCA_AAGCCTATGC ATCATATCCC_	Xho I	hBex2 cloning primer, starts at nucleotide 210 downstream of ATG, reverse
hBex_d1-121-rev	CCG**CTCGAG**TCA_AAAACTCATCAT GATGGTCAT_	Xho I	hBex2 cloning primer, starts at nucleotide 363downstream of ATG, reverse
hBex_d71-125-rev	CCG**CTCGAG**TCA_GGGCATAAGG CAAAACTC_	Xho I	hBex2 cloning primer, starts at nucleotide 373 downstream of ATG, reverse
hBex_d1-20-Hind III-rev	CCC**AAGCTT**TCA_TTCTTGGTTGG CATTTTCC_	Hind III	hBex2 cloning primer, starts at nucleotide 60 downstream of ATG, reverse
hBex_d1-50-Hind III-rev	CCC**AAGCTT**TCA_ACGATTTCCTC TAGGCAC_	Hind III	hBex2 cloning primer, starts at nucleotide 150 downstream of ATG, reverse
hBex_d1-70-Hind III-rev	CCG**AAGCTT**TCA_AAGCCTATGCA TCATATCCC_	Hind III	hBex2 cloning primer, starts at nucleotide 210 downstream of ATG, reverse
hBex_d1-121-Hind III-rev	CCG**AAGCTT**TCA_AAAACTCATCAT GATGGTCAT_	Hind III	hBex2 cloning primer, starts at nucleotide 363downstream of ATG, reverse
hBex_d71-125-Hind III-rev	CCG**AAGCTT**TCA_GGGCATAAGG CAAAACTC_	Hind III	hBex2 cloning primer, starts at nucleotide 373 downstream of ATG, reverse
Tip2-LC-for	_AACGAGCAGTAAACAGTC_	-	qRT-PCR primer, forward
Tip2-LC-rev	_GTGGTTCTCCAAGCCT_	-	qRT-PCR primer, reverse
Tip2-LC-probe-for	_AGAGGAAATCGTAGGCGGT_-Fluorescein	-	qRT-PCR probe
Tip2-LC-probe-rev	LCRed-640-_CGCGTTAGGCAGCCCA_-Phosphate	-	qRT-PCR probe

RS, restriction site; _italic_ letters in the oligonucleotide sequence correspond to the hBex2 coding sequence.

5.6   Methods in molecular biology

5.6.1   Polymerase chain reaction (PCR)

For analytical purposes the *Taq* DNA polymerase (Qiagen) was used. For cloning reactions the *Pfu* DNA polymerase (Stratagene) was used, as it exhibits proofreading activity.

PCR master mix

reagents	*Taq* DNA polymerase	*Pfu* DNA polymerase
cDNA/vector	5 ng	50 ng
10x PCR buffer	2.5 µl (1x)	2.5 µl (1x)
dNTP mix (10 mM each)	0.75 µl (300 µM)	0.75 µl (300 µM)
Primer forward (10 pmol)	0.75 µl (300 nM)	0.75 µl (300 nM)
Primer reverse (10 pmol)	0.75 µl (300 nM)	0.75 µl (300 nM)
DNA polymerase	0.2 µl (1 Unit)	0.5 µl (1.25 Units)
distilled water	up to 25 µl final volume	up to 25 µl final volume

PCR reaction

segment	cycles	temperature	duration
initial denaturation	1	95°C	45 s
1 denaturation		95°C	45 s
2 annealing	25	Primer $_{Tm}$ – 5°C (50-68°C)	45 s
3 extension		72°C	1 min/kb PCR target
final extension	1	72°C	10 min

5.6.2   Reverse transcriptase PCR (RT-PCR)

This method is used to transcribe single-stranded RNA into double-stranded reverse cDNA for use in subsequent amplification reactions, such as quantitative real time PCR. Transcription of mRNA was performed with Transcriptor Reverse Transcriptase (Roche) expressed in *E. coli*, an enzyme that offers RNA-directed DNA polymerase activity and DNA-dependent DNA polymerase activity, which work together to perform transcription. Furthermore, this enzyme exhibits an unwinding activity and RNase H activity which degrades RNA in RNA:DNA hybrids.

Total RNA from human brain and peripheral tissues (Clontech) was used as RNA template and random hexamer primers p(dN)$_6$ (Roche) as initiation site for cDNA synthesis along RNA. All components were thawed and placed on ice. The reaction was set up in 10 µl volume in RNase- and DNase-free reaction tubes as described below. The resulting single-stranded cDNA was directly used for qRT-PCR analysis (see 5.6.3), without prior purification.

RT-PCR reaction setup

reagents	volume [µl]	final conc.
random primer p(dN)$_6$ 5 A$_{260}$ Units	1.0	0.08 A$_{260}$ Units
total RNA	1.0	1 µg
H$_2$O bidest	4.5	-
The mix was incubated for 5 min at 65°C to denature RNA secondary structures. The tube was then immediately placed on ice and following components were added.		
5x Transcriptor RT reaction buffer	2.0	1x
RNase OUT (40 U/µl)	0.25	10 U
dNTP (10 mM each)	1.0	1 mM each
Transcriptor (20 U/µl)	0.25	5 U
Tubes were mixed and afterwards incubated for 10 min at 25°C, 30 min at 55°C and 5 min at 85°C in a thermal cycler, followed by transfer on ice.		

5.6.3 Quantitative Real time PCR (qRT-PCR)

qRT-PCR is a technique used to monitor the progress of a PCR reaction in real time and to quantitate differences in DNA, cDNA or RNA expression with only small amounts of PCR products. qRT-PCR is based on the detection of the fluorescence produced by a reporter molecule which increases, as the reaction proceeds. This occurs due to the accumulation of the PCR product with each cycle of amplification. Dyes that bind to double-stranded DNA (i.e. SYBR® Green) or sequence-specific probes were used as fluorescent reporter molecules.

Specific detection of real time PCR was performed with hybridization probes, consisting of two different oligonucleotides that hybridize to an internal sequence of the amplified fragment during the annealing phase of PCR cycles. One probe is labeled at the 5'-end with a Light Cycler Red fluorophore, and modified at the 3'-end by phosphorylation to avoid extension. The second probe is labeled at the 3'-end with fluorescein. Only after hybridization are the probes in close proximity, resulting in

fluorescence resonance energy transfer (FRET) between the fluorophores. The emitted fluorescence of the Light Cycler Red fluorophore is measured. Thus the more abundant a particular cDNA (and thus mRNA), the earlier it will be detected during repeated cycles of amplification. Amplifying oligonucleotides and hybridization probes are listed below and depicted in Fig. 29. The fluorescence signal of the amplified ß-Globin housekeeping gene using specific oligonucleotides and labeled hybridization probes was used as an internal standard (Light Cycler control kit DNA).

amplifying oligonucleotides (synthesis scale 20 nmol, purification desalted)

hBex2-LC-forward, 5' – AACGAGCAGTAAACAGTC – 3'
hBex2-LC-reverse, 5' – GTGGTTCTCCAAGCCT – 3'

hybridization probes (synthesis scale 1 nmol, purification HPLC)

hBex2-LC-probe-forward, 5' – AGAGGAAATCGTAGGCGGT – 3'- Fluorescein
hBex2-LC-probe-reverse, 5' – LC-640 – CGCGTTAGGCAGCCCA – 3'- Phosphate

```
   1 cggcacgagg ctccccgctg ccctgcgctc ggcgggctgg catccggccc gggggaaagc
  61 ggaccagccc ttctgcaggt ctgcggggcc aagtgtcccg gcacgaggcg cacctcgtgg
 121 cgagaatcgg gagaaggagg agactacaag gataggccca ggagtaatgg agtccaaaga
 181 gaaacgagca gtaaacagtc tcagcatgga aaatgccaac caagaaaatg aagaaaagga
 241 gcaagttgct aataaggggg agcccttggc cctccctttg gatgctggtg aatactgtgt
 301 gcctagagga aatcgtaggc ggttccgcgt taggcagccc atcctgcagt atagatggga
 361 tatgatgcat aggcttggag aaccacaggc aaggatgaga gaagagaata tggaaaggat
 421 tggggaggag gtgagacagc tgatggaaaa gctgagggaa aagcagttga gtcatagtct
 481 gcgggcagtc agcactgacc cccctcacca tgaccatcat gatgagtttt gccttatgcc
 541 ctgaatcctg atggtttccc taaagttatt acggaaacag acccctgctt tcgaatttac
 601 atgttcatga tgtgcccttg ttgtaaacct ttacctgtca cttgtttacg tgggtctcct
 661 attaccagct tctaattgaa tattgtgttt ttgaaccagt ctgtaagatt tttgttagca
 721 gaagaatttt acctattgca tggaaagatg ctcattatag tgaagttaat aaagcacctt
 781 taaaaagcaa aaaaaaaaaa aaaaaaaaaa aaaaaaaaaa aaaaaaa
```
Fig. 29: The hBex2 cDNA sequence (AF220189).
Sequences for hBex2-LC oligonucleotides (marked in green) and labeled probes (marked in blue) are depicted. The ATG transcription start and TGA stop are highlighted in grey.

qRT-PCR reaction setup

ß-Globin			hBex2		
reagent	volume	final conc.	reagent	volume	final conc.
ß-Globin oligo mix	0.5 µl	-	oligonucleotide mix (50 pmol each)	1.0 µl	5 pmol
ß-Globin hybridization probe mix	1.0 µl	-	probe mix (20 pmol each)	1.0 µl	2 pmol
Light Cycler FastStart reaction mix hybridization probes*	1.0 µl	1x	Light Cycler FastStart reaction mix hybridization probes*	1.0 µl	1x
$MgCl_2$ (25 mM)	0.8 µl	3 mM	$MgCl_2$ (25 mM)	1.2 µl	4 mM
H_2O, PCR grade	6.7 µl	-	H_2O, PCR grade	4.8 µl	-
cDNA	1.0 µl	-	cDNA	1.0 µl	-
total volume	10 µl		total volume	10 µl	

*contains FastStart Taq DNA polymerase, reaction buffer, dNTP mix , 10 mM $MgCl_2$

5.6.4   Agarose gel electrophoresis

Separation of DNA fragments, coiled and super-coiled plasmid DNA was carried out by electrophoresis in 1% (w/v) agarose gels. 1 g of agarose powder in 100 ml TBE buffer was dissolved by boiling up in a microwave. 3-4 µl of a 1% ethidium bromide solution was added to 100 ml agarose solution and poured into an agarose gel chamber. The appropriate comb was inserted immediately. DNA samples were interspersed with 1/10 volume of 10x DNA gel loading buffer before loading onto the gel. A 100 bp or 1 kb DNA ladder was used for comparing sizes. DNA fragments were separated using a voltage of 120V.

5.6.5   Isolation and purification of DNA-fragments

DNA fragments were excised from the agarose gel on a UV monitor and purified using the MinElute® Gel Extraction or QIAquick® Gel Extraction Kit (Quiagen) according to the manufacturer's instruction.

5.6.6   Enzymatic digestion of DNA

1 µg of purified plasmid DNA or PCR product was digested with 2 Units of the appropriate restriction enzyme in the recommended buffer in a total volume of 25 µl. Incubation was carried out at 37°C overnight if the DNA was subsequently used for the ligation reaction. Heat inactivation of the enzyme was accomplished at 65°C for 15

min. Linearized plasmid DNA and digested PCR product were loaded on an agarose gel, separated by gel electrophoresis (see 5.6.4), isolated and purified as described in chapter 5.6.5.

5.6.7 Ligation of DNA

60 to 100 ng of linearized, purified plasmid DNA and digested and purified PCR product (molar ratio 1:3 to 1:10) were incubated with 1 Unit of T4 DNA Ligase in the recommended ligation buffer in a total reaction volume of 15 µl overnight at 16°C. As a positive control, plasmid DNA, digested with a single enzyme, was incubated with T4 DNA ligase under the same conditions.

5.6.8 Transformation of DNA into One Shot® TOP10Electrocomp™ *E. coli*

1 µl of the ligation product and 5 ng of plasmid DNA control were each added to 50 µl of One Shot® TOP10Electrocomp™*E. coli* cells (Invitrogen) on ice and mixed by gently tapping at the reaction tube. Samples were pipetted into pre-cooled 0.2 cm cuvettes and pulsed with 2.5 kV using an electroporator. 1 ml LB medium without antibiotics was immediately added to pulsed *E. coli* and transferred to 15 ml Falcon tubes. After incubation in a shaker for 30 min, at 37°C and 240 rpm, 50-200 µl of bacteria were spread on LB agar plates including the appropriate selective antibiotic and grown overnight at 37°C in an incubator.

5.6.9 Production of bacterial glycerol stocks

After plasmid DNA transformation and growing of *E. coli* cells on selective LB agar plates (see 5.6.8), a single positive clone was picked from the plate using a sterile pipette tip and inoculated in 3 ml LB medium containing the appropriate selective antibiotic. Following incubation overnight at 37°C in a shaker, 1 ml of bacteria suspension was mixed with 250 µl glycerol (99 %) and stored at –80°C.

5.6.10 Production of electrocompetent cells

Fresh colonies from the desired strain (One Shot® TOP10, BL21) were produced by streaking out bacteria from competent cell stocks onto an ampicillin containing LB agar plate and growing them overnight at 37°C. One single colony was used to

inoculate 50 ml of fresh ampicillin containing LB medium and grown overnight at 37°C and 220 rpm. The next day, the culture was diluted 1:100 in two flasks with 1 liter LB medium and incubated at 37°C with 220 rpm until an OD_{600} of 0.5 was reached. Thereafter, all steps were done on ice and only cold equipment and solutions were used. Cells were centrifuged for 25 min, 4200 rpm (F34-6-38 rotor, Eppendorf) at 4°C. The supernatant was discarded and the pellet washed in 10% glycerol (diluted in ultrapure water and autoclaved). Each cell pellet was then resuspended in 10 ml 10% glycerol, transferred to two 500 ml bottles, filled up to 400 ml with 10% glycerol and centrifuged for 20 min at 4000 rpm (F34-6-38 rotor, Eppendorf), 4°C. The supernatant was again discarded, the two remaining pellets resuspended in 10 ml 10% glycerol and combined into one bottle. After centrifugation as above, the pellet was resuspended in 10 ml 10 % glycerol and transferred to a 50 ml conical tube. Volume was adjusted to 50 ml and the cell suspension was centrifuged again as above. The resulting cell pellet was resuspended in 1-1.5 ml 10 % glycerol and 50 µl aliquots were prepared. Aliquots were shock-frozen in liquid nitrogen and stored at –80°C.

5.6.11 Preparation and purification of plasmid DNA

Preparation

A single colony from a freshly streaked selective plate was picked to inoculate 2-5 ml LB medium containing the appropriate selective antibiotic. Incubation was carried out for ~8 hours at 37°C with vigorous shaking (~250 rpm). This starter culture was then diluted 1/500 in selective LB medium and grown at 37°C for 12-16 hours, vigorous shaking. Bacterial cells were harvested by centrifugation at 6000 g for 15 min at 4°C.

Purification

DNA purification was conducted using the Qiagen® Plasmid Midi, Maxi, Mega and Giga Kits according to the manufacturer's instructions. The air-dried DNA pellets were redissolved in 10 mM Tris-HCl (pH 8.5) and DNA concentration was determined by UV spectrophotometry.

5.7 Methods in protein biochemistry

5.7.1 Preparation of protein extracts

Protein extracts from cells

After removing medium from 10 cm dishes, cells were once washed with cold PBS. Cells were subsequently detached from the culture dish with a cell scraper, transferred to a 1.5 ml reaction tube on ice and spun down at 900 g for 5 min at 4°C. Cell pellets were resuspended in 700 µl NP-40 cell lysis buffer, incubated for 30 min on ice and centrifuged at 14000 rpm for 30 min at 4°C. The protein containing supernatant was removed and stored at –80°C.

Protein extracts from brain tissues

Whole brain tissue was dissected from rats, immediately washed in ice-cold PBS and cut into smaller pieces. Tissue pieces were shock-frozen in liquid nitrogen, subsequently pulverized using mortar and pestle on dry ice and transferred to 1.5 ml reaction tubes for storage at –80°C. Human brain tissue was kindly provided by Prof. Dr. A. Bornemann (Institute for Brain Research, Tübingen). 1 ml RIPA cell lysis buffer was added to 250 mg of pulverized brain tissue and sonicated approximately 3 min with 50% pulse and 70% intensity at 4°C. Thereafter, lysates were centrifuged at 20,000 g for 30 min at 4°C. Protein containing supernatant was removed and stored at –80°C.

5.7.2 Protein quantification by Bradford and Bicinchoninic Acid Assay (BCA)

Protein quantification by Bradford

After protein extraction from cells or tissues, the total amount of protein was determined using the Protein Assay Kit (Biorad). Therefore, the five-fold concentrated reagent was diluted ¼ in bidest H_2O prior to use. The lyophilized bovine gamma globulin protein standard was reconstituted to a concentration of approximately 1.4 mg/ml by adding bidest H_2O, and aliquots were stored at –20°C. A standard curve was generated by preparing several dilutions of protein standard from 4 to 20 µg (4-20 µg/ml) in 1 ml diluted reagent. 5 µl of protein sample was diluted in 1 ml diluted reagent and mixed by pipetting up and down. The OD_{595} of protein standard and samples was measured versus reagent blank, and OD_{595} values were plotted versus

concentrations of standards. Unknown protein sample concentrations were calculated from the standard curve.

Bicinchoninic Acid Assay (BCA)

10 µl of diluted protein extract was incubated with 200 µl of a 50:1 mixture consisting of BCA reagents A and B, respectively. A standard curve was generated by preparing several dilutions of BSA protein standard ranging from 50 µg/ml to 1.5 mg/ml.

5.7.3   SDS-polyacrylamid gel electrophoresis (PAGE)

SDS-PAGE separates proteins under denaturing conditions, depending on their molecular weights. For this purpose, mini gels, composed of 10% resolving gel and 4.5% stacking gel with a thickness of 1.5 mm, were prepared. The composition of resolving and stacking gel is given in table 6. Protein extracts were mixed 1:4 with 4x SDS-PAGE sample buffer and incubated for 5 min at 95°C, followed by a short spin down. Approximately 50 µg protein per well was loaded onto the gel. As a molecular weight standard 10 µl of a protein marker was loaded onto the gel. Separation occurred in 1x SDS-PAGE running buffer at a voltage of 140-160 V. Subsequently, proteins were either visualized with Gel code blue stain R-250 (Pierce, see 5.7.6) or transferred to nitrocellulose or PVDF membranes by immunoblotting (see 5.7.4).

Table 6: Preparation of the SDS-PAGE gel

resolving gel	10 %
SDS-PAGE resolving gel buffer (1.5 M Tris base (pH 8.8), 0.4% SDS)	2.50 ml
Acrylamide 40% (19:1)	2.50 ml
H$_2$O bidest	4.95 ml
10% APS	62.50 µl
TEMED	6.25 µl
SDS-PAGE resolving gel buffer (1.5 M Tris base (pH 8.8), 0.4% SDS)	2.50 ml

stacking gel	4.5%
SDS-PAGE stacking gel buffer (0.5 M Tris base (pH 6.8), 0.4% SDS)	0.624 ml
Acrylamide 40% (19:1)	0.282 ml
H$_2$O bidest	1.594 ml
10% APS	10.0 µl
TEMED	4.0 µl

5.7.4 Immunoblotting

After separation by SDS-PAGE proteins were transferred from polyacrylamid gels to nitrocellulose or PVDF membranes by electroblotting using either wet or semi-dry blotting procedures. Wet blotting was performed for approximately 2 hours with 100 V at RT or overnight with 25 V at 4°C. Semi-dry blotting was carried out for 1 ½ hours with 75 mA per membrane (7.5 x 8.0 cm) at 4°C. The following assembly was used:

wet blotting
· cathode · sponge · 1x gel blotting paper (0.2 mm) · polyacrylamide gel · membrane · 1x gel blotting paper (0.2 mm) · sponge · anode

semi-dry blotting
· cathode · 3x gel blotting paper (1.5 mm) · membrane · polyacrylamide gel · 3x gel blotting paper (1.5 mm) · anode

5.7.5 Stripping of PVDF and nitrocellulose membranes

PVDF and nitrocellulose membranes were incubated in stripping solution for 30 min at 56°C, subsequently washed three times in PBS-T for 10 min and finally incubated in 10% blocking solution.

5.7.6 Coomassie staining of polyacrylamid gels

For protein staining on polyacrylamide gels the GelCode® Blue Stain Reagent (Pierce) was used, which utilizes the colloidal properties of Coomassie® G-250. This reagent stains only protein and allows bands to be viewed directly on the gel during the staining process. After SDS-PAGE electrophoresis the gel was placed in a clean tray and rinsed three times 5 min with 100-200 ml of ultrapure water. GelCode® Blue Stain Reagent was mixed immediately before use, and 20 ml of the solution were added to a mini gel. Staining intensity reached a maximum within approximately 1 hour. Subsequently, the stain reagent was replaced with ultrapure water to de-stain the gel. Water was changed several times and incubation was continued overnight.

5.7.7 Ponceau S staining of PVDF- and nitrocellulose membranes

This staining technique allows the detection of 250 ng protein after separation by electrophoresis in polyacrylamide gels and transfer to nitrocellulose or PVDF membranes. The Ponceau S Staining Solution (Sigma) contains 0.1% Ponceau S (w/v) and 5.0% acetic acid (w/v). Membranes were incubated in a sufficient amount of the solution for 5-10 min until staining reached maximum intensity. Removal of stain was accomplished by washing the membrane thoroughly in PBS-T.

5.7.8 Expression and purification of MBP fusion proteins

The pMAL™ Protein Fusion and Purification System provides a method for expressing and purifying a protein, produced from a cloned gene. The gene is inserted into a pMAL vector downstream from the *malE* gene of *E. coli*, which encodes maltose-binding protein (MBP). This results in the expression of an MBP-fusion protein. This technique uses the strong Ptac promoter and the translation initiation signals of MBP to achieve high-level expression of the fusion protein. The fusion protein is then purified by one-step affinity purification specific for MBP. The vector carries the *lacI^q* gene, which codes for the Lac repressor and keeps expression from Ptac low in the absence of IPTG.

Electroporation of E. coli BL21-CodonPlus® Competent Cells
A 50 µl aliquot of *E. coli* BL21-CodonPlus® Competent cells (Stratagene) was thawed on ice. 5 ng of the appropriate pMal-c2X plasmid was added to cells and gently mixed. Cells were transferred to a 0.2 cm cuvette and pulsed with 2.5 kV in an electroporator (Biorad). Subsequently, 250 µl of S.O.C. medium (Invitrogen) was added and cells were transferred to a 15 ml tube. After incubating transformed cells for 30 min at 37°C, 220 rpm, 50 µl of the cell suspension was uniformly spread on LB agar plates containing 100 µg/ml ampicillin and grown overnight at 37°C. Positive clones were screened by colony PCR.

Induction with IPTG
One single positive colony was used to inoculate 50 ml of ampicillin containing (50 µg/ml) LB medium overnight at 37°C, 220 rpm. The next day, the starter culture was poured into 1 liter of fresh LB medium without antibiotics and grown at 37°C with 220 rpm until growth was in log phase and reached an OD$_{600}$ of 0.6. At this point, the

culture was induced to express the recombinant protein by adding IPTG at a concentration of 0.5-1.0 mM for 2-4 hours at 37°C with 220 rpm. Subsequent centrifugation was carried out for 20 min at 5000 g and 4°C to precipitate bacteria. Cells were then resuspended and lysed in 25 ml MBP-lysis buffer and frozen at –20°C overnight and thereafter at –80°C for long-term storage.

Sonication and Purification

Bacterial cell extract was thawed on ice water. Subsequently, sonication was conducted for 3 min with 50% pulse at an intensity of 70%. Subsequent centrifugation at 9000 g for 30 min at 4°C resulted in precipitation of cell membranes and release of proteins into the supernatant. This crude bacterial protein extract was diluted 1/5 with affinity precipitation washing buffer prior to purification. For experiments in which the crude bacterial protein extract was used non-purified (i.e. affinity precipitation assays), the concentration of the MBP fusion proteins was estimated by Coomassie staining using a BSA protein standard.

For purification ~15 ml of amylose resin (NEB) was poured into an Econo-Pac column (Biorad) and washed with 8 column volumes of affinity precipitation washing buffer. The crude bacterial protein extract was applied to the column and allowed to enter the resin by gravity flow. After binding of MBP fusion protein to the amylose resin, the column was washed with 12 column volumes of affinity precipitation washing buffer. MBP fusion protein was released from the column by incubating with MBP-elution buffer and collected in 1 ml fractions. The protein concentration was determined using the Bradford Assay and purified MBP fusion protein was stored at -80°C.

5.7.9   Affinity precipitation assays (pull down)

This assay is an *in vitro* method used to determine physical interactions between proteins. It requires the availability of a tagged protein (the bait), which is used to capture a protein binding partner (protein Y). Here the bait is a MBP-tagged fusion protein, which is captured on an immobilized affinity ligand, the amylose. The immobilized bait can then be incubated with cell lysates derived from tissues or cultured cells that are expressing the binding partner. After elution of proteins from beads, proteins are seperated by SDS-PAGE and stained with a specific antibody. A scheme of this method is depicted in figure 30. Approximately 600 pmol of the relevant

recombinant MBP protein (crude bacterial extracts containing either MBP-hBex2, MBP-hBex2 deletions, MBP-torsinA or MBP-ΔE torsinA) was bound to 100 µl amylose resin. The proteins were allowed to bind by rotation for 1 hour at 4°C. Beads were washed 3 times with affinity precipitation washing buffer to remove unbound proteins by inverting the tube several times. The same procedure was carried out with a MBP protein extract not fused to any bait protein as a negative control. In parallel, cell lysates were prepared as described above (see 5.7.1). 40 µl of lysate was kept as a positive control for total protein extract. 300 µl of cell lysate was then added to the amylose beads/MBP fusion protein complex and rotated overnight at 4°C. The next day, beads were centrifuged at 8000 g for 1 min at 4°C. The supernatant was discarded and beads were washed 3 times with affinity precipitation washing buffer to remove unbound proteins by inverting the tube several times. Each wash was followed by a centrifugation step at 8000 g for 1 min at 4°C. Finally, beads were resuspended in 60 µl 1x SDS-PAGE sample buffer (4x SDS-PAGE sample buffer diluted with affinity precipitation washing buffer) and incubated at 95°C for 5 min to detach proteins from amylose beads. The supernatant was either loaded on a SDS-PAGE gel for further examination via immunoblotting or frozen at -80°C.
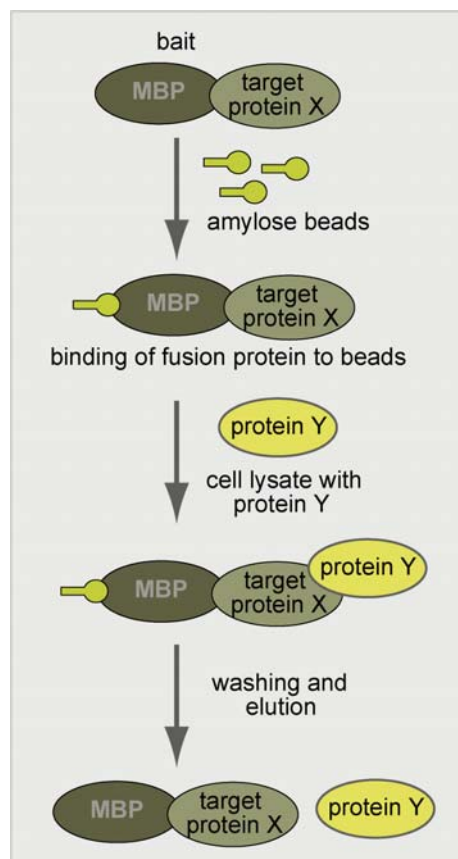
Fig. 30: Scheme of the affinity precipitation assay.

5.7.10 Co-Immunoprecipitation assay

The immunoprecipitation assay is a method, used to precipitate and enrich an antigen out of an extract or solution using a specific antibody, which is non-covalently bound to beads. Co-Immunoprecipitation can identify protein complexes from cell extracts. These complexes are isolated by immunoprecipitating the antibody-binding protein with protein A/G beads. Subsequently washing steps reduce unspecific protein binding. Finally, the antibody-bound protein and complex-associated proteins can be eluted and precipitates are subsequently analyzed using SDS-PAGE and immunoblotting.

In this approach hBex2 protein was immunoprecipitated using the anti-Bex2 (74495) polyclonal antibody. Normal rabbit serum was used as a negative control. TorsinA was immunoprecipitated with a mixture of the torsinA specific antibodies D-MG10 and D-M2A8. Mouse IgG was used as a negative control:

anti-Bex2 (74495)	5 µl
normal rabbit serum	5 µl
anti-torsinA (D-MG10/D-M2A8)	4 µl each
purified mouse IgGs	10 µl (20 µg)

Protein extracts were prepared as described in chapter 5.7.1, and the following steps were done on ice or at 4°C. To avoid unspecific binding, the protein extract (~ 1mg) was pre-cleared by incubation with 60 µl of protein A/G agarose beads for 1 hour or overnight rotating. The next day, beads were spun down for 1 min at 8000 g, the pre-cleared lysate was removed, and 300 µl of pre-cleared lysate was added to the appropriate antibody. Incubation was carried out overnight on a rotor. The next day, the antibody-lysate mixture was added to beads and incubated for 2 hours on a rotor. Subsequently, beads were spun down for 1 min at 8000 g, and the resulting supernatant was discarded except for 60 µl, which were saved as a control. Beads were washed three times with immunoprecipitation washing buffer, spun down for 1 min at 8000 g, and the resulting supernatant was discarded. Protein was eluted by adding 1x SDS-PAGE sample buffer and incubation at 95°C for 5 min. The resulting supernatant was directly loaded onto SDS-PAGE, followed by immunoblotting.

5.7.11 Subcellular fractionation assay

The following method was adapted from a published protocol (179) with slight modifications. Lysed cells are separated into fractions containing distinct subcellular compartments by a series of centrifugation steps at increasing speeds (Fig. 31). Following each centrifugation, the organelles that sedimented to the bottom are recovered in the pellet. The supernatant is then re-centrifuged at higher speeds to sediment the next-largest organelle fraction. All procedures were carried out at 4°C, and resulting pellets were rinsed with ice-cold HEPES-buffered sucrose (HB) after each centrifugation to avoid crossover contamination.

A single adult rat brain was dissected and immediately transferred into HB buffer. Approximately 10 volumes of HB (~10-15 ml) were added and tissue was mechanically homogenized using a glass-teflon homogenizer. The homogenate (H) was then centrifuged at 1000 g for 10 min to obtain the pelleted nuclear fraction (P1). The supernatant (S1) was removed and centrifuged at 10,000 g for 15 min to yield the crude synaptosomal pellet (P2) and supernatant S2 (kept on ice). Pellet P2 was resuspended in 10 volumes of HB (~5 ml) and centrifuged again at 10,000 g for 15 min, resulting in a washed crude synaptosomal pellet (P2'). The supernatant was discarded. Subsequently, the washed P2 pellet was lysed by hypo-osmotic shock in 9 volumes of ice-cold bidest water (including Complete® protease inhibitor cocktail) and 3 strokes of a glass-teflon homogenizer. The lysate was rapidly adjusted to 4 mM HEPES using 1 M HEPES (pH 7.4) and continuously mixed for 30 min to ensure complete lysis. Subsequently, centrifugation at 25,000 g for 20 min resulted in fractionation of synaptosomal membranes (pellet LP1) and crude synaptic vesicles (supernatant LS1). Pellet LP1 was resuspended in 1-2 ml HB, and LS1 was centrifuged at 165,000 g for 90 min to obtain the synaptic vesicle-enriched fraction (pellet LP2, resuspended in 1-2 ml HB) and supernatant LS2. Finally, supernatant S2 was centrifuged at 165,000 g for 90 min to yield the cytosolic fraction S3 and light membranes/microsomes in the pellet P3. Pellet P3 was resuspended in 1-2 ml HB.
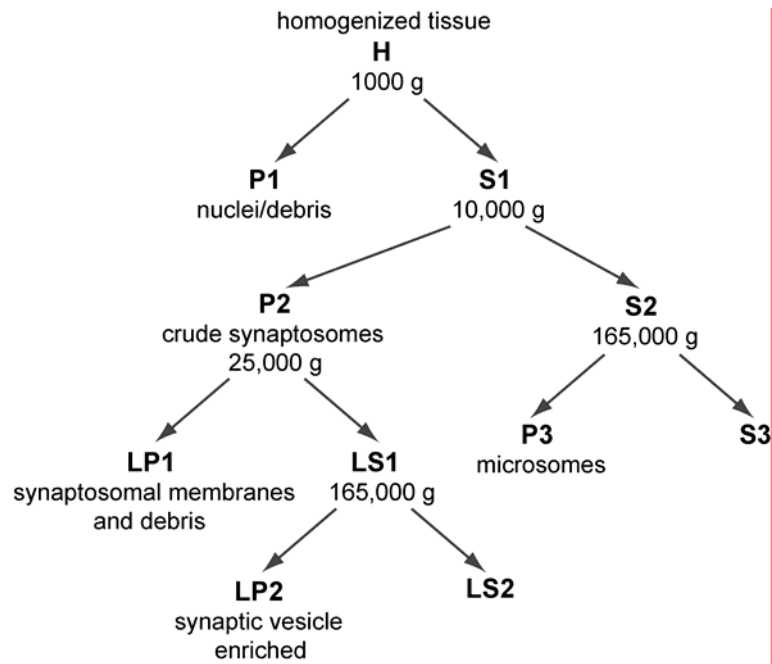
Fig. 31: Scheme of the subcellular fractionation assay.

5.7.12 Subcellular fractionation using the Qproteome cell compartment kit

The Qproteome cell compartment kit (Qiagen) is designed for fast and easy subcellular fractionation of intact eukaryotic cells. Proteins of different compartments are selectively isolated by sequential addition of different extraction buffers to a cell pellet. Buffer CE1 selectively disrupts the plasma membrane without solubilizing it, resulting in the isolation of cytosolic proteins. Buffer CE2 solubilizes the plasma membrane and organelle membranes, except for the nuclear membrane, resulting in the isolation of membrane proteins and proteins from the lumen of organelles. Buffer CE3 solubilizes nuclei and thus extracts all soluble and most membrane-bound nuclear proteins. Buffer CE4 is finally used to solubilize all residual, mainly cyto-skeletal proteins in the pellet. In our approach, either endogenous cells (CAD, Neuro-2a) or cells overexpressing hBex2 and TorsinA protein, at a density of 5 x 10^6 cells, were used. The subcellular fractionation procedure was done according to the manufacturer's instructions. Resulting protein lysates were resolved by SDS-PAGE, followed by immunoblotting.

5.7.13 Sucrose gradient centrifugation

Sucrose gradient centrifugation is a technique, used to separate cell organelles from crude cellular extracts. The sucrose density gradient was created by gently

overlaying lower concentrations of sucrose onto higher concentrations. For this reason, freshly made sucrose buffers containing either 0.25 M (8.6%) or 1.9 M (65%) sucrose were poured into an 11 ml continuous gradient using a gradient mixer and kept at 4°C. Three flasks (75 cm^2) of confluent CAD cells were harvested and transferred into 0.25 M sucrose buffer. Cells were centrifuged at 900 g for 5 min at 4°C, and pellets were resuspended in 1-2 ml 0.25 M sucrose buffer. Cell lysis was performed by passing cells through a 1 ml syringe with a 23 gauge needle for 20-30 passages. The lysate was then centrifuged for 5 min at 900 g and 4°C to pellet cell membranes, unlysed cells and nuclei. The resulting supernatant was loaded on top of the sucrose gradient. Gradients were centrifuged at 30,000 rpm in a TH-641 swinging-bucket rotor (Sorvall) for 18 hours at 4°C. Subsequently, 0.5 ml fractions were collected from the top of the gradient, and protein precipitation was performed by the methanol-chloroform-precipitation method ((180), see 5.7.14). Air-dried pellets were resuspended in 100 µl RIPA and immediately used for SDS-PAGE or stored at –20°C.

5.7.14 Protein precipitation by the methanol-chloroform method

The quantification of diluted proteins or proteins solutions that contain salts, detergents, phospholipids or ß-mercaptoethanol is difficult because of the interference of these substances with the analysis method. The method reported by Wessel and Flugge (1984) (180) allows precipitation of soluble and hydrophobic membrane proteins, that is not sensitive to interfere with the substances described above. The method was used as described by Wessel and Flugge (1984) with only slight modifications. In brief, 0.4 ml methanol were added to 0.1 ml of protein sample, vortexed and centrifuged for 10 seconds at 9000 g. Then, 0.1 ml chloroform was added, and samples were vortexed and centrifuged again (10 seconds, 9000 g). For phase separation 0.3 ml water was added and samples were vortexed vigorously and centrifuged for 5 min at 9000 g. The upper phase was carefully removed and discarded. A further 0.3 ml methonal was added to the remaining chloroform phase and interphase. Samples were mixed and centrifuged again for 5 min at 9000 g to pellet the protein. The supernatant was removed, the pellet air-dried and afterwards resuspended in 100 µl RIPA.

5.7.15 Yeast two-hybrid screen

The yeast two-hybrid screen was carried out by Kamm and colleagues (2004) using a LexA-based system (66, 181). Library screening was performed by transforming a conditionally expressed human adult whole brain cDNA library (MoBiTec), constructed in the vector pJG4-5, into the yeast strain EGY48, containing the l*acZ* reporter plasmid pSH18-34 and the pEG202-torAwt-(251–332) bait construct. Positive interacting clones were selected for growth on Ura_/His_/Trp_/Leu_/gal plates and tested for ß-galactosidase activity on Ura_/His_/Trp_/X-gal/glu and Ura_/His_/Trp_/X-gal/gal plates. 15 clones were found to have a consistent galactose-dependent phenotype. To confirm the specificity of the interactions, cDNA clones in pJG4-5 were rescued and transformed into EGY48 cells containing either pEG202-torAwt-(251–332), pEG202-torA_GAG-(251–332), or one of the following bait plasmids as negative controls: 1) pEG202, 2) pEG202- cdc2, 3) pEG202-bicoid, 4) pEG202-fus3, or 5) pEG202-TubSH3 (182). The pEG202-cdc2, pEG202-bicoid, and pEG202-fus3 interactor control plasmids (183) were kindly provided by Dr. R. Brent (The Molecular Sciences Institute, Berkeley, CA). Liquid ß-galactosidase assays were performed following a standard protocol (184). The same untransformed yeast strain used for subsequent transformation with bait and library constructs, EGY48, containing the *lacZ* reporter plasmid pSH18–34, was used as a negative control. One unit of ß-galactosidase is defined as´the amount that hydrolyzes 1 µmol of *O*-nitrophenyl-ß-D-galactopyranoside (Sigma) to *O*-nitrophenol and D-galactose per min per cell (185).

5.8   Methods in cell biology

5.8.1   Culturing of cell lines

Human embryonic kidney fibroblasts (HEK 293T/17), human brain neuroblastoma (SK-N-BE), rat pheochromocytoma (PC-12), human bone marrow neuroblastoma (SH-SY5Y), mouse brain neuroblastoma (Neuro-2a), mouse neural catechol-aminergic differentiated cells (CAD, Cath.a cell line-derived) (186), rat primary cortical neurons (RCN) and mouse primary cortical neurons (MCN) were incubated with 5% CO_2 at 37°C in humid atmosphere in an incubator (table 7). The appropriate media and origins are listed in table 7.

Table 7: List of cell lines used in this study

cell line	organism	medium	origin
HEK 293T/17	human	DMEM + 10% FBS	Dr. D. Baltimore, MIT *
SK-N-BE	human	DMEM + 10% FBS	American Type Culture Collection (ATCC)
PC-12	rat	DMEM + 5% FBS, 10% HS	American Type Culture Collection (ATCC)
SH-SY5Y	human	DMEM/HAM's-F12 + 10% FBS	American Type Culture Collection (ATCC)
Neuro-2A	mouse	DMEM/HAM's-F12 + 10% FBS	American Type Culture Collection (ATCC)
CAD	mouse	DMEM/HAM's-F12 + 10% FBS	Dr. J. Wang, Tufts University **
RCN	rat primary	Neurobasal™ + 1x B-27, 50 U/ml penicillin, 50 µg/ml streptomycin, 2 mM L-glutamine	self -produced

*Pear et al. (1993) (187); **Qi et al., (1997) (186)

Passaging of cells

Medium of confluent grown cells was removed, and cells were then rinsed once with PBS. 1 ml trypsin/EDTA solution was added to a 75 cm^2 flask and incubated for 3-5 min to detach cells from the surface. Subsequently, 10 ml serum containing medium was added to stop the reaction. Cell clumps were disrupted by pipetting the suspension up and down, followed by a 1:5 – 1:10 splitting into serum-containing medium in 75 cm^2 flasks.

Determination of cell number

Cell counting was carried out in a Neubauer counting chamber. The area of one large quadrate in this chamber is 1 mm^2, with a depth of 0.1 mm. From the number of cells in this quadrate, which consists of 16 smaller quadrates, the cell density can be deduced using the following formula: cells/milliliter = cells/large quadrate x 10,000. A minimum of 2 large quadrates was counted.

Freezing and thawing of cells

Cells were grown in a 75 cm^2 flask until a confluency of 80-90 % was reached, medium was removed and cells were washed once with 1x PBS. Cells were de-tached by trypsination for 3-5 min with 1 ml trypsin/EDTA solution, and cells were subsequently resuspended in 10 ml serum-containing medium. Following centrifu-gation for 5 min at 900 g and 4°C, the supernatant was discarded, the cell pellet resuspended in 1-2 ml freezing medium and transferred to a sterile tube. To ensure

slow freezing, tubes were placed in a pre-cooled isopropanol filled chamber and stored at -80°C for one week. Afterwards, cells were transferred to and stored at -140°C. After one week, cell viability was assessed. For this purpose cells were thawed at 37°C and immediately transferred into serum containing medium in a 75 cm^2 flask. Cells were then grown for several days, and cell number was counted as described above.

5.8.2 Transient transfection by lipofection using Lipofectamine™ 2000 or Fugene 6

Cells were grown, separated and counted as described in 5.8.1. Table 8 shows the amount of cells/ml, used for transfection in different culture vessels to reach the appropriate confluency, depending on the method of transfection, as well as the amount of DNA and transfection reagents used.

Table 8: Reaction setup for transfection of mammalian cells.

Transfection with Lipofectamine™ 2000, 80-90 % cell confluence				
culture vessel	cells/ml	volume of plating	DNA [µg] diluted	Lipofectamine ™ 2000 [µl] diluted
6-well (10 cm^2)	1 x 10^6	1 ml	4.0 µg in 50 µl Opti-MEM	5 µl in 50 µl Opti-MEM
60 mm (20 cm^2)	1.5 x 10^6	2 ml	5-10 µg in 100 µl Opti-MEM	10 µl in 100 µl Opti-MEM
10 cm (60 cm^2)	3 x 10^6	4 ml	15 µg in 300 µl Opti-MEM	20 µl in 300 µl Opti-MEM

Transfection with Fugene 6, 50-60 % cell confluence				
culture vessel	cells/ml	volume of plating	DNA [µg]	Fugene 6	total volume of complex in serum-free medium
6-well (10 cm^2)	0.7 x 10^6	2 ml	1 – 2 µg	3 – 9 µl	100 µl
60 mm (20 cm^2)	1 x 10^6	4 – 6 ml	2 – 4.5 µg	6 – 20 µl	200 µl
10 cm (60 cm^2)	2 x 10^6		6 – 11 µg	17 – 51 µl	600 µl

Transfection was carried out according to the manufacurer's instruction: Roche, Fugene 6 transfection reagent or Invitrogen, Lipofectamine™ 2000, with slight modifications. The DNA and transfection reagent were mixed and incubated for 30-50 min at RT and then added to the cells without removing medium from the culture vessel. Subsequently, cells were incubated for 24-48 hours at 37°C to allow gene expression

from the transfected plasmid DNA. To obtain the overexpressed protein(s), cells were harvested, lysed, and protein was extracted as described in chapter 5.7.1. For culture vessels smaller than 10 cm an appropriate smaller amount of lysis buffer was used.

5.8.3   Poly-D-lysine coating of cell culture vessels and coverslips

12 mm round glass coverslips were placed into wells of a 24 well plate, incubated with 500 µl poly-D-lysine (PDL, stock solution 100 ng/ml) for 10 min and subsequently washed with 1x PBS. Coated coverslips were then exposed to UV light for 30 min and afterwards stored at 4°C.

5.8.4   Collagen coating of culture vessels

Collagen type I from rat tail was used at a concentration of 100 µg/ml. 7.5 ml of this solution were added to a 75 cm^2 flask to yield 10 µg/cm^2. Incubation was carried out for 30 min at RT. Subsequently, the solution was aspirated, the flask once washed with 1x PBS and dried overnight at 4°C.

5.8.5   Differentiation of PC-12 cells

12 mm round glass coverslips were first coated with PDL (see 5.8.3) and thereafter with collagen (see 5.8.4) and stored at 4°C. PC-12 cells were plated at a density of 1x 10^6 cells/ml on coated coverslips and incubated overnight to allow for cell adhesion. The next day, PC-12 cells were differentiated by treatment with mouse nerve growth factor (mNGF 2.5S, grade I) at 100 ng/ml for 3-4 days in D-MEM supplemented with 1.5 % FBS.

5.8.6   Primary cortical rat neuronal cultures

Primary cortical rat neuronal cultures were prepared according to Lin et al. (2000) (188), with the following modifications. First, 12 mm round glass coverslips were coated with PDL as described in chapter 5.8.3. One ml Neurobasal™ medium supplemented with 1x B-27, 50 U/ml penicillin, 50 µg/ml streptomycin and 2 mM L-glutamine was added to coated coverslips and placed in the 37°C incubator. Then, an embryonic day 18 pregnant Sprague-Dawley rat (Charles River) was sacrificed by CO_2 inhalation, and embryos were removed and placed into 10 cm culture vessels

containing 1x HBSS solution. Fetuses were decapitated, and heads were transferred into a new 10 cm culture vessel with 1x HBSS to remove residual blood. Brains were dissected, meninges removed and cortices excised using a dissecting microscope. Subsequent steps were conducted on ice and under a laminar hood. Cortices were first cut into small pieces and then transferred to a 50 ml falcon tube. After two washes in 10 ml 1x HBSS solution, the supernatant was discarded except for 1 ml. 4 ml of 1x protease solution was added, followed by incubation for 10 min at 37°C to dissociate cells. Dissociation was carried out by pipetting cells gently ten times up and down with a 10 ml pipette. Tissue was then allowed to precipitate for 5 min before the supernatant (~ 5 ml) was transferred to a new 50 ml tube containing 5 ml Neurobasal™ medium. Another 5 ml 1x HBSS solution was added to precipitated tissue and resuspended again with a 10 ml pipette. After 5 min of precipitation, the supernatant was again transferred to the new 50 ml tube. This step was repeated another four times up to a total volume of 35 ml supernatant, which then contains single cells. Subsequently, cells were strained by pouring the supernatant slowly through a cell strainer (40 µl, nylon) into a 50 ml tube. The cell number was determined as described in chapter 5.8.1. Finally, cells were plated onto coated coverslips at a cell density of 1x 10^5 – 5x 10^5 cells/ml in Neurobasal™ medium. After 1 hour incubation in a 37°C incubator the medium was removed, replaced by 1 ml new Neurobasal™ medium and placed back into the 37°C incubator. For immunocyto-chemical studies cells were fixed after 3, 6, 7 and 10 days of differentiation (see 5.8.7).

5.8.7   Immunocytochemistry

Cells were grown on 12 mm round glass coverslips in the appropriate medium at a density of 1x 10^6 cells/ml for cell lines and 1x10^5 – 4x10^5 cells/ml for primary cortical neurons, respectively. Medium was removed, and cells were washed once with 1x PBS, followed by incubation in 4% PFA/PBS for 20-30 min at RT. Then cells were thoroughly washed three times in 1x PBS and subsequently lysed with 0.1 % Nonidet P40 (Igepal) for 30 min at RT, followed by three washing steps in 1x PBS. Thereafter, cells were incubated with IF blocking buffer for 1 hour at RT to saturate unoccupied protein binding sites and prevent non-specific binding of antibody reagents. Subse-quently, coverslips were placed on Parafilm® M, 50 µl of the diluted primary antibody (dilution in IF-antibody solution) was added, and cells were incubated for 1 hour at

RT. After washing coverslips three times in 1x PBS the secondary antibody was added and incubated on cells for 45 min at RT. Coverslips were washed three times in 1x PBS, mounted on Super-Frost® chamber slides in fluorescence mounting medium and finally sealed with nail polish.

5.8.8   Immunohistochemistry – free floating

PFA - fixed rat and mice brains frozen at –80°C (5.9) were sliced on dry ice into 25-30 µm sections using a microtome. Sections were transferred into a TBS-containing 12 well cell culture plate (three sections/well) and washed three times in TBS. Unless otherwise indicated, the following incubations were conducted at room temperature (RT) on a shaker. 1 % H_2O_2 in TBS was added, followed by incubation for 10 min to quench endogenous peroxidases. Sections were washed three times in TBS and then incubated with 0.3% Triton X-100 in TBS for 10 min for permeabilization of cell membranes. After washing sections three times in TBS, 3% normal goat serum in TBS was added and incubated for 30 min to block unoccupied protein binding sites and prevent non-specific binding of antibody reagents. The diluted primary antibody was added (diluted in IHC-antibody solution) and incubated overnight at 4°C. After three more washing steps in TBS the diluted biotinylated secondary antibody was added (diluted in IHC-secondary antibody solution) and incubated for 90 min at 4°C. Sections were washed three times in TBS before the Vectastain® Elite ABC (**A**vidin and **B**iotinylated horseradish peroxidase macromolecular **C**omplex) reagent was added and incubated for 90 min at 4°C. After washing sections three times in TBS the Vector® SG peroxidase substrate was added, followed by incubation at RT until visible staining developed. Tissue sections were then washed for 5 min in TBS, rinsed briefly in water and subsequently dehydrated: 70% ethanol for 5 min, 95% ethanol for 5 min, 100% ethanol for 5 min, and xylol for 5 min. Finally sections were mounted in Entellan® rapid mounting medium onto chamber slides.

5.9   Fixation of rat brain tissue by transcardial perfusion

Adult rats were anethezised with CO_2. The abdominal wall was opened along the linea alba. Subsequently, the diaphragm was dissected from the rib cage, opening the thorax aperture. Transcardial perfusion was initiated by placing a canula in the left cardial ventricle, simultaneously opening the right atrium to ensure draining of

blood and perfusion solution. Using a pump generating a constant pressure of 150 mmHg, the entire blood circulation system of the animal was rinsed thoroughly with 150-200 ml of 0.1 M ice-cold PBS (pH 7.2). Subsequently, 150-200 ml of 4% PFA in PBS (pH 7.2) were perfused to ensure complete fixation of brain tissue, followed by careful removal of cranial bones and dissection of the entire brain.

6   REFERENCES

1. Fahn, S. (1988) Concept and classification of dystonia. *Adv Neurol,* **50,** 1-8.
2. Oppenheim, H. (1911) Über eine eigenartige Krampfkrankheit des kindlichen und jugendlichen Alters (dysbasia lordotica progressiva, dystonie musculorum deformans. *Neuro Centrabl*, 1090-1107.
3. Herz, E. (1944) Dystonia. *Arch Neurol Psych,* **51,** 305-355.
4. Marsden, C.D., Harrison, M.J. and Bundey, S. (1976) Natural history of idiopathic torsion dystonia. *Adv Neurol,* **14,** 177-87.
5. Klein, C., Breakefield, X.O. and Ozelius, L.J. (1999) Genetics of primary dystonia. *Semin Neurol,* **19,** 271-80.
6. Muller, U., Steinberger, D. and Nemeth, A.H. (1998) Clinical and molecular genetics of primary dystonias. *Neurogenetics,* **1,** 165-77.
7. Valente, E.M., Bentivoglio, A.R., Cassetta, E., Dixon, P.H., Davis, M.B., Ferraris, A., Ialongo, T., Frontali, M., Wood, N.W. and Albanese, A. (2001) DYT13, a novel primary torsion dystonia locus, maps to chromosome 1p36.13- -36.32 in an Italian family with cranial-cervical or upper limb onset. *Ann Neurol,* **49,** 362-6.
8. Bressman, S.B. (2004) Dystonia genotypes, phenotypes, and classification. *Adv Neurol,* **94,** 101-7.
9. Nemeth, A.H. (2002) The genetics of primary dystonias and related disorders. *Brain,* **125,** 695-721.
10. Berardelli, A., Rothwell, J.C., Hallett, M., Thompson, P.D., Manfredi, M. and Marsden, C.D. (1998) The pathophysiology of primary dystonia. *Brain,* **121 (Pt 7),** 1195-212.
11. DeLong, M.R. (1990) Primate models of movement disorders of basal ganglia origin. *Trends Neurosci,* **13,** 281-5.
12. Alexander, G.E. and Crutcher, M.D. (1990) Functional architecture of basal ganglia circuits: neural substrates of parallel processing. *Trends Neurosci,* **13,** 266-71.
13. Albin, R.L., Young, A.B. and Penney, J.B. (1989) The functional anatomy of basal ganglia disorders. *Trends Neurosci,* **12,** 366-75.
14. Marsden, C.D. and Obeso, J.A. (1994) The functions of the basal ganglia and the paradox of stereotaxic surgery in Parkinson's disease. *Brain,* **117 (Pt 4),** 877-97.
15. Bressman, S.B., Sabatti, C., Raymond, D., de Leon, D., Klein, C., Kramer, P.L., Brin, M.F., Fahn, S., Breakefield, X., Ozelius, L.J. *et al.* (2000) The DYT1 phenotype and guidelines for diagnostic testing. *Neurology,* **54,** 1746-52.
16. Bressman, S.B., de Leon, D., Kramer, P.L., Ozelius, L.J., Brin, M.F., Greene, P.E., Fahn, S., Breakefield, X.O. and Risch, N.J. (1994) Dystonia in Ashkenazi Jews: clinical characterization of a founder mutation. *Ann Neurol,* **36,** 771-7.
17. Balas, M., Peretz, C., Badarny, S., Scott, R.B. and Giladi, N. (2006) Neuropsychological profile of DYT1 dystonia. *Mov Disord,* **21,** 2073-7.
18. Risch, N., de Leon, D., Ozelius, L., Kramer, P., Almasy, L., Singer, B., Fahn, S., Breakefield, X. and Bressman, S. (1995) Genetic analysis of idiopathic torsion dystonia in Ashkenazi Jews and their recent descent from a small founder population. *Nat Genet,* **9,** 152-9.

19. Zeman, W. and Dyken, P. (1967) Dystonia musculorum deformans. Clinical, genetic and pathoanatomical studies. *Psychiatr Neurol Neurochir,* **70,** 77-121.

20. Ozelius, L., Kramer, P.L., Moskowitz, C.B., Kwiatkowski, D.J., Brin, M.F., Bressman, S.B., Schuback, D.E., Falk, C.T., Risch, N., de Leon, D. *et al.* (1989) Human gene for torsion dystonia located on chromosome 9q32-q34. *Neuron,* **2,** 1427-34.

21. Ozelius, L.J., Hewett, J.W., Page, C.E., Bressman, S.B., Kramer, P.L., Shalish, C., de Leon, D., Brin, M.F., Raymond, D., Corey, D.P. *et al.* (1997) The early-onset torsion dystonia gene (DYT1) encodes an ATP-binding protein. *Nat Genet,* **17,** 40-8.

22. Ozelius, L.J., Kramer, P.L., de Leon, D., Risch, N., Bressman, S.B., Schuback, D.E., Brin, M.F., Kwiatkowski, D.J., Burke, R.E., Gusella, J.F. *et al.* (1992) Strong allelic association between the torsion dystonia gene (DYT1) andloci on chromosome 9q34 in Ashkenazi Jews. *Am J Hum Genet,* **50,** 619-28.

23. Kramer, P.L., Heiman, G.A., Gasser, T., Ozelius, L.J., de Leon, D., Brin, M.F., Burke, R.E., Hewett, J., Hunt, A.L., Moskowitz, C. *et al.* (1994) The DYT1 gene on 9q34 is responsible for most cases of early limb-onset idiopathic torsion dystonia in non-Jews. *Am J Hum Genet,* **55,** 468-75.

24. Leung, J.C., Klein, C., Friedman, J., Vieregge, P., Jacobs, H., Doheny, D., Kamm, C., DeLeon, D., Pramstaller, P.P., Penney, J.B. *et al.* (2001) Novel mutation in the TOR1A (DYT1) gene in atypical early onset dystonia and polymorphisms in dystonia and early onset parkinsonism. *Neurogenetics,* **3,** 133-43.

25. Doheny, D., Danisi, F., Smith, C., Morrison, C., Velickovic, M., De Leon, D., Bressman, S.B., Leung, J., Ozelius, L., Klein, C. *et al.* (2002) Clinical findings of a myoclonus-dystonia family with two distinct mutations. *Neurology,* **59,** 1244-6.

26. Brassat, D., Camuzat, A., Vidailhet, M., Feki, I., Jedynak, P., Klap, P., Agid, Y., Durr, A. and Brice, A. (2000) Frequency of the DYT1 mutation in primary torsion dystonia without family history. *Arch Neurol,* **57,** 333-5.

27. Tuffery-Giraud, S., Cavalier, L., Roubertie, A., Guittard, C., Carles, S., Calvas, P., Echenne, B., Coubes, P. and Claustres, M. (2001) No evidence of allelic heterogeneity in the DYT1 gene of European patients with early onset torsion dystonia. *J Med Genet,* **38,** E35.

28. Kamm, C., Castelon-Konkiewitz, E., Naumann, M., Heinen, F., Brack, M., Nebe, A., Ceballos-Baumann, A. and Gasser, T. (1999) GAG deletion in the DYT1 gene in early limb-onset idiopathic torsion dystonia in Germany. *Mov Disord,* **14,** 681-3.

29. Major, T., Svetel, M., Romac, S. and Kostic, V.S. (2001) DYT1 mutation in primary torsion dystonia in a Serbian population. *J Neurol,* **248,** 940-3.

30. Valente, E.M., Warner, T.T., Jarman, P.R., Mathen, D., Fletcher, N.A., Marsden, C.D., Bhatia, K.P. and Wood, N.W. (1998) The role of DYT1 in primary torsion dystonia in Europe. *Brain,* **121 (Pt 12),** 2335-9.

31. Bressman, S.B., de Leon, D., Brin, M.F., Risch, N., Burke, R.E., Greene, P.E., Shale, H. and Fahn, S. (1989) Idiopathic dystonia among Ashkenazi Jews: evidence for autosomal dominant inheritance. *Ann Neurol,* **26,** 612-20.

32. Opal, P., Tintner, R., Jankovic, J., Leung, J., Breakefield, X.O., Friedman, J. and Ozelius, L. (2002) Intrafamilial phenotypic variability of the DYT1 dystonia: from asymptomatic TOR1A gene carrier status to dystonic storm. *Mov Disord,* **17,** 339-45.

33. Gambarin, M., Valente, E.M., Liberini, P., Barrano, G., Bonizzato, A., Padovani, A., Moretto, G., Fiorio, M., Dallapiccola, B., Smania, N. *et al.* (2006) Atypical phenotypes and clinical variability in a large Italian family with DYT1-primary torsion dystonia. *Mov Disord,* **21,** 1782-4.

34. Edwards, M., Wood, N. and Bhatia, K. (2003) Unusual phenotypes in DYT1 dystonia: a report of five cases and a review of the literature. *Mov Disord,* **18,** 706-11.

35. Playford, E.D., Fletcher, N.A., Sawle, G.V., Marsden, C.D. and Brooks, D.J. (1993) Striatal [18F]dopa uptake in familial idiopathic dystonia. *Brain,* **116 (Pt 5),** 1191-9.

36. Eidelberg, D. (1998) Abnormal brain networks in DYT1 dystonia. *Adv Neurol,* **78,** 127-33.

37. Eidelberg, D., Moeller, J.R., Antonini, A., Kazumata, K., Nakamura, T., Dhawan, V., Spetsieris, P., deLeon, D., Bressman, S.B. and Fahn, S. (1998) Functional brain networks in DYT1 dystonia. *Ann Neurol,* **44,** 303-12.

38. Augood, S.J., Martin, D.M., Ozelius, L.J., Breakefield, X.O., Penney, J.B., Jr. and Standaert, D.G. (1999) Distribution of the mRNAs encoding torsinA and torsinB in the normal adult human brain. *Ann Neurol,* **46,** 761-9.

39. Augood, S.J., Hollingsworth, Z., Albers, D.S., Yang, L., Leung, J.C., Muller, B., Klein, C., Breakefield, X.O. and Standaert, D.G. (2002) Dopamine transmission in DYT1 dystonia: a biochemical and autoradiographical study. *Neurology,* **59,** 445-8.

40. Ichinose, H., Ohye, T., Takahashi, E., Seki, N., Hori, T., Segawa, M., Nomura, Y., Endo, K., Tanaka, H., Tsuji, S. *et al.* (1994) Hereditary progressive dystonia with marked diurnal fluctuation caused by mutations in the GTP cyclohydrolase I gene. *Nat Genet,* **8,** 236-42.

41. Bhatia, K.P. and Marsden, C.D. (1994) The behavioural and motor consequences of focal lesions of the basal ganglia in man. *Brain,* **117 (Pt 4),** 859-76.

42. Munchau, A., Mathen, D., Cox, T., Quinn, N.P., Marsden, C.D. and Bhatia, K.P. (2000) Unilateral lesions of the globus pallidus: report of four patients presenting with focal or segmental dystonia. *J Neurol Neurosurg Psychiatry,* **69,** 494-8.

43. Rostasy, K., Augood, S.J., Hewett, J.W., Leung, J.C., Sasaki, H., Ozelius, L.J., Ramesh, V., Standaert, D.G., Breakefield, X.O. and Hedreen, J.C. (2003) TorsinA protein and neuropathology in early onset generalized dystonia with GAG deletion. *Neurobiol Dis,* **12,** 11-24.

44. McNaught, K.S., Kapustin, A., Jackson, T., Jengelley, T.A., Jnobaptiste, R., Shashidharan, P., Perl, D.P., Pasik, P. and Olanow, C.W. (2004) Brainstem pathology in DYT1 primary torsion dystonia. *Ann Neurol,* **56,** 540-7.

45. Liu, Z., Zolkiewska, A. and Zolkiewski, M. (2003) Characterization of human torsinA and its dystonia-associated mutant form. *Biochem J,* **374,** 117-22.

46. Hewett, J., Ziefer, P., Bergeron, D., Naismith, T., Boston, H., Slater, D., Wilbur, J., Schuback, D., Kamm, C., Smith, N. *et al.* (2003) TorsinA in PC12 cells: localization in the endoplasmic reticulum and response to stress. *J Neurosci Res,* **72,** 158-68.

47. Breakefield, X.O., Kamm, C. and Hanson, P.I. (2001) TorsinA: movement at many levels. *Neuron,* **31,** 9-12.

48. Neuwald, A.F., Aravind, L., Spouge, J.L. and Koonin, E.V. (1999) AAA+: A class of chaperone-like ATPases associated with the assembly, operation, and disassembly of protein complexes. *Genome Res,* **9,** 27-43.

49.   Lupas, A.N. and Martin, J. (2002) AAA proteins. *Curr Opin Struct Biol,* **12,** 746-53.

50.   Gaudet, R. and Wiley, D.C. (2001) Structure of the ABC ATPase domain of human TAP1, the transporter associated with antigen processing. *Embo J,* **20,** 4964-72.

51.   Gorbalenya, A.E. and Koonin, E.V. (1989) Viral proteins containing the purine NTP-binding sequence pattern. *Nucleic Acids Res,* **17,** 8413-40.

52.   Saraste, M., Sibbald, P.R. and Wittinghofer, A. (1990) The P-loop--a common motif in ATP- and GTP-binding proteins. *Trends Biochem Sci,* **15,** 430-4.

53.   Guenther, B., Onrust, R., Sali, A., O'Donnell, M. and Kuriyan, J. (1997) Crystal structure of the delta' subunit of the clamp-loader complex of E. coli DNA polymerase III. *Cell,* **91,** 335-45.

54.   Putnam, C.D., Clancy, S.B., Tsuruta, H., Gonzalez, S., Wetmur, J.G. and Tainer, J.A. (2001) Structure and mechanism of the RuvB Holliday junction branch migration motor. *J Mol Biol,* **311,** 297-310.

55.   Ogura, T. and Wilkinson, A.J. (2001) AAA+ superfamily ATPases: common structure--diverse function. *Genes Cells,* **6,** 575-97.

56.   Hewett, J., Gonzalez-Agosti, C., Slater, D., Ziefer, P., Li, S., Bergeron, D., Jacoby, D.J., Ozelius, L.J., Ramesh, V. and Breakefield, X.O. (2000) Mutant torsinA, responsible for early-onset torsion dystonia, forms membrane inclusions in cultured neural cells. *Hum Mol Genet,* **9,** 1403-13.

57.   Kustedjo, K., Bracey, M.H. and Cravatt, B.F. (2000) Torsin A and its torsion dystonia-associated mutant forms are lumenal glycoproteins that exhibit distinct subcellular localizations. *J Biol Chem,* **275,** 27933-9.

58.   Shashidharan, P., Kramer, B.C., Walker, R.H., Olanow, C.W. and Brin, M.F. (2000) Immunohistochemical localization and distribution of torsinA in normal human and rat brain. *Brain Res,* **853,** 197-206.

59.   Ozelius, L.J., Page, C.E., Klein, C., Hewett, J.W., Mineta, M., Leung, J., Shalish, C., Bressman, S.B., de Leon, D., Brin, M.F. *et al.* (1999) The TOR1A (DYT1) gene family and its role in early onset torsion dystonia. *Genomics,* **62,** 377-84.

60.   Augood, S.J., Penney, J.B., Jr., Friberg, I.K., Breakefield, X.O., Young, A.B., Ozelius, L.J. and Standaert, D.G. (1998) Expression of the early-onset torsion dystonia gene (DYT1) in human brain. *Ann Neurol,* **43,** 669-73.

61.   Augood, S.J., Keller-McGandy, C.E., Siriani, A., Hewett, J., Ramesh, V., Sapp, E., DiFiglia, M., Breakefield, X.O. and Standaert, D.G. (2003) Distribution and ultrastructural localization of torsinA immunoreactivity in the human brain. *Brain Res,* **986,** 12-21.

62.   Siegert, S., Bahn, E., Kramer, M.L., Schulz-Schaeffer, W.J., Hewett, J.W., Breakefield, X.O., Hedreen, J.C. and Rostasy, K.M. (2005) TorsinA expression is detectable in human infants as young as 4 weeks old. *Brain Res Dev Brain Res,* **157,** 19-26.

63.   Walker, R.H., Brin, M.F., Sandu, D., Good, P.F. and Shashidharan, P. (2002) TorsinA immunoreactivity in brains of patients with DYT1 and non-DYT1 dystonia. *Neurology,* **58,** 120-4.

64.   Bragg, D.C., Kaufman, C.A., Kock, N. and Breakefield, X.O. (2004) Inhibition of N-linked glycosylation prevents inclusion formation by the dystonia-related mutant form of torsinA. *Mol Cell Neurosci,* **27,** 417-26.

65.   Grundmann, K., Reischmann, B., Vanhoutte, G., Huebner, J., Teismann, P., Hauser, T. K., Bonin, M., Wilbertz, J., Horn, S., Nguyen, H. P., Kuhn, M., Chanarat, S., Wolburg, H., Van der Linden, A., Riess, O. (2007)

Overexpression of human wildtype and human ΔGAG torsinA in a transgenic mouse model causes phenotypic abnormalities. *Neurobiol Dis,* **doi:10.1016/j.nbd.2007.04.015**.

66. Kamm, C., Boston, H., Hewett, J., Wilbur, J., Corey, D.P., Hanson, P.I., Ramesh, V. and Breakefield, X.O. (2004) The Early Onset Dystonia Protein TorsinA Interacts with Kinesin Light Chain 1. *J Biol Chem,* **279,** 19882-92.

67. Confalonieri, F. and Duguet, M. (1995) A 200-amino acid ATPase module in search of a basic function. *Bioessays,* **17,** 639-50.

68. Schirmer, E.C., Glover, J.R., Singer, M.A. and Lindquist, S. (1996) HSP100/Clp proteins: a common mechanism explains diverse functions. *Trends Biochem Sci,* **21,** 289-96.

69. Kuner, R., Teismann, P., Trutzel, A., Naim, J., Richter, A., Schmidt, N., von Ahsen, O., Bach, A., Ferger, B. and Schneider, A. (2003) TorsinA protects against oxidative stress in COS-1 and PC12 cells. *Neurosci Lett,* **350,** 153-6.

70. Goodchild, R.E. and Dauer, W.T. (2004) Mislocalization to the nuclear envelope: an effect of the dystonia-causing torsinA mutation. *Proc Natl Acad Sci U S A,* **101,** 847-52.

71. Naismith, T.V., Heuser, J.E., Breakefield, X.O. and Hanson, P.I. (2004) TorsinA in the nuclear envelope. *Proc Natl Acad Sci U S A,* **101,** 7612-7.

72. Gonzalez-Alegre, P. and Paulson, H.L. (2004) Aberrant cellular behavior of mutant torsinA implicates nuclear envelope dysfunction in DYT1 dystonia. *J Neurosci,* **24,** 2593-601.

73. Koo, J.H., Gill, S., Pannell, L.K., Menco, B.P., Margolis, J.W. and Margolis, F.L. (2004) The interaction of Bex and OMP reveals a dimer of OMP with a short half-life. *J Neurochem,* **90,** 102-16.

74. Torres, G.E., Sweeney, A.L., Beaulieu, J.M., Shashidharan, P. and Caron, M.G. (2004) Effect of torsinA on membrane proteins reveals a loss of function and a dominant-negative phenotype of the dystonia-associated DeltaE-torsinA mutant. *Proc Natl Acad Sci U S A,* **101,** 15650-5.

75. Helfand, B.T., Chang, L. and Goldman, R.D. (2003) The dynamic and motile properties of intermediate filaments. *Annu Rev Cell Dev Biol,* **19,** 445-67.

76. Hewett, J.W., Zeng, J., Niland, B.P., Bragg, D.C. and Breakefield, X.O. (2006) Dystonia-causing mutant torsinA inhibits cell adhesion and neurite extension through interference with cytoskeletal dynamics. *Neurobiol Dis,* **22,** 98-111.

77. Callan, A.C., Bunning, S., Jones, O.T., High, S. and Swanton, E. (2007) Biosynthesis of the dystonia-associated AAA+ ATPase torsinA at the endoplasmic reticulum. *Biochem J,* **401,** 607-12.

78. Hirokawa, N. (1998) Kinesin and dynein superfamily proteins and the mechanism of organelle transport. *Science,* **279,** 519-26.

79. Goldstein, L.S. and Philp, A.V. (1999) The road less traveled: emerging principles of kinesin motor utilization. *Annu Rev Cell Dev Biol,* **15,** 141-83.

80. Lupas, A., Flanagan, J.M., Tamura, T. and Baumeister, W. (1997) Self-compartmentalizing proteases. *Trends Biochem Sci,* **22,** 399-404.

81. Vale, R.D. (2000) AAA proteins. Lords of the ring. *J Cell Biol,* **150,** F13-20.

82. McLean, P.J., Kawamata, H., Shariff, S., Hewett, J., Sharma, N., Ueda, K., Breakefield, X.O. and Hyman, B.T. (2002) TorsinA and heat shock proteins act as molecular chaperones: suppression of alpha-synuclein aggregation. *J Neurochem,* **83,** 846-54.

83. Caldwell, G.A., Cao, S., Sexton, E.G., Gelwix, C.C., Bevel, J.P. and Caldwell, K.A. (2003) Suppression of polyglutamine-induced protein aggregation in Caenorhabditis elegans by torsin proteins. *Hum Mol Genet,* **12,** 307-19.

84.   Suntharalingam, M. and Wente, S.R. (2003) Peering through the pore: nuclear pore complex structure, assembly, and function. *Dev Cell,* **4,** 775-89.

85.   Bragg, D.C., Slater, D.J. and Breakefield, X.O. (2004) TorsinA and early-onset torsion dystonia. *Adv Neurol,* **94,** 87-93.

86.   Burke, B. and Stewart, C.L. (2002) Life at the edge: the nuclear envelope and human disease. *Nat Rev Mol Cell Biol,* **3,** 575-85.

87.   Gruenbaum, Y., Goldman, R.D., Meyuhas, R., Mills, E., Margalit, A., Fridkin, A., Dayani, Y., Prokocimer, M. and Enosh, A. (2003) The nuclear lamina and its functions in the nucleus. *Int Rev Cytol,* **226,** 1-62.

88.   Goldman, R.D., Gruenbaum, Y., Moir, R.D., Shumaker, D.K. and Spann, T.P. (2002) Nuclear lamins: building blocks of nuclear architecture. *Genes Dev,* **16,** 533-47.

89.   Holaska, J.M., Wilson, K.L. and Mansharamani, M. (2002) The nuclear envelope, lamins and nuclear assembly. *Curr Opin Cell Biol,* **14,** 357-64.

90.   Schirmer, E.C., Florens, L., Guan, T., Yates, J.R., 3rd and Gerace, L. (2003) Nuclear membrane proteins with potential disease links found by subtractive proteomics. *Science,* **301,** 1380-2.

91.   Goodchild, R.E. and Dauer, W.T. (2005) The AAA+ protein torsinA interacts with a conserved domain present in LAP1 and a novel ER protein. *J Cell Biol,* **168,** 855-62.

92.   Sherman, M.Y. and Goldberg, A.L. (2001) Cellular defenses against unfolded proteins: a cell biologist thinks about neurodegenerative diseases. *Neuron,* **29,** 15-32.

93.   Shashidharan, P., Good, P.F., Hsu, A., Perl, D.P., Brin, M.F. and Olanow, C.W. (2000) TorsinA accumulation in Lewy bodies in sporadic Parkinson's disease. *Brain Res,* **877,** 379-81.

94.   Cao, S., Gelwix, C.C., Caldwell, K.A. and Caldwell, G.A. (2005) Torsin-mediated protection from cellular stress in the dopaminergic neurons of Caenorhabditis elegans. *J Neurosci,* **25,** 3801-12.

95.   Augood, S.J., Hollingsworth, Z.R., Standaert, D.G., Emson, P.C. and Penney, J.B., Jr. (2000) Localization of dopaminergic markers in the human subthalamic nucleus. *J Comp Neurol,* **421,** 247-55.

96.   Augood, S.J., Hollingsworth, Z., Albers, D.S., Yang, L., Leung, J., Breakefield, X.O. and Standaert, D.G. (2004) Dopamine transmission in DYT1 dystonia. *Adv Neurol,* **94,** 53-60.

97.   Basham, S.E. and Rose, L.S. (1999) Mutations in ooc-5 and ooc-3 disrupt oocyte formation and the reestablishment of asymmetric PAR protein localization in two-cell Caenorhabditis elegans embryos. *Dev Biol,* **215,** 253-63.

98.   Basham, S.E. and Rose, L.S. (2001) The Caenorhabditis elegans polarity gene ooc-5 encodes a Torsin-related protein of the AAA ATPase superfamily. *Development,* **128,** 4645-56.

99.   Wang, N. and Stamenovic, D. (2002) Mechanics of vimentin intermediate filaments. *J Muscle Res Cell Motil,* **23,** 535-40.

100.   Paramio, J.M. and Jorcano, J.L. (2002) Beyond structure: do intermediate filaments modulate cell signalling? *Bioessays,* **24,** 836-44.

101.   Chang, L. and Goldman, R.D. (2004) Intermediate filaments mediate cytoskeletal crosstalk. *Nat Rev Mol Cell Biol,* **5,** 601-13.

102.   Boyne, L.J., Fischer, I. and Shea, T.B. (1996) Role of vimentin in early stages of neuritogenesis in cultured hippocampal neurons. *Int J Dev Neurosci,* **14,** 739-48.

103. Dubey, M., Hoda, S., Chan, W.K., Pimenta, A., Ortiz, D.D. and Shea, T.B. (2004) Reexpression of vimentin in differentiated neuroblastoma cells enhances elongation of axonal neurites. *J Neurosci Res,* **78,** 245-9.

104. Shashidharan, P., Sandu, D., Potla, U., Armata, I.A., Walker, R.H., McNaught, K.S., Weisz, D., Sreenath, T., Brin, M.F. and Olanow, C.W. (2005) Transgenic mouse model of early-onset DYT1 dystonia. *Hum Mol Genet,* **14,** 125-33.

105. Sharma, N., Baxter, M.G., Petravicz, J., Bragg, D.C., Schienda, A., Standaert, D.G. and Breakefield, X.O. (2005) Impaired motor learning in mice expressing torsinA with the DYT1 dystonia mutation. *J Neurosci,* **25,** 5351-5.

106. Dang, M.T., Yokoi, F., McNaught, K.S., Jengelley, T.A., Jackson, T., Li, J. and Li, Y. (2005) Generation and characterization of Dyt1 DeltaGAG knock-in mouse as a model for early-onset dystonia. *Exp Neurol,* **196,** 452-63.

107. Goodchild, R.E., Kim, C.E. and Dauer, W.T. (2005) Loss of the dystonia-associated protein torsinA selectively disrupts the neuronal nuclear envelope. *Neuron,* **48,** 923-32.

108. Pisani, A., Martella, G., Tscherter, A., Bonsi, P., Sharma, N., Bernardi, G. and Standaert, D.G. (2006) Altered responses to dopaminergic D2 receptor activation and N-type calcium currents in striatal cholinergic interneurons in a mouse model of DYT1 dystonia. *Neurobiol Dis,* **24,** 318-25.

109. Walker, R.H. and Shashidharan, P. (2003) Developments in the molecular biology of DYT1 dystonia. *Mov Disord,* **18,** 1102-7.

110. Dang, M.T., Yokoi, F., Pence, M.A. and Li, Y. (2006) Motor deficits and hyperactivity in Dyt1 knockdown mice. *Neurosci Res,* **56,** 470-4.

111. Hewett, J.W., Kamm, C., Boston, H., Beauchamp, R., Naismith, T., Ozelius, L., Hanson, P.I., Breakefield, X.O. and Ramesh, V. (2004) TorsinB--perinuclear location and association with torsinA. *J Neurochem,* **89,** 1186-94.

112. Bragg, D.C., Camp, S.M., Kaufman, C.A., Wilbur, J.D., Boston, H., Schuback, D.E., Hanson, P.I., Sena-Esteves, M. and Breakefield, X.O. (2004) Perinuclear biogenesis of mutant torsin-A inclusions in cultured cells infected with tetracycline-regulated herpes simplex virus type 1 amplicon vectors. *Neuroscience,* **125,** 651-61.

113. Bahn, E., Siegert, S., Pfander, T., Kramer, M.L., Schulz-Schaeffer, W.J., Hewett, J.W., Breakefield, X.O., Hedreen, J.C. and Rostasy, K.M. (2006) TorsinB expression in the developing human brain. *Brain Res,* **1116,** 112-9.

114. Konakova, M., Huynh, D.P., Yong, W. and Pulst, S.M. (2001) Cellular distribution of torsin A and torsin B in normal human brain. *Arch Neurol,* **58,** 921-7.

115. Schliwa, M. and Woehlke, G. (2003) Molecular motors. *Nature,* **422,** 759-65.

116. Vale, R.D. and Milligan, R.A. (2000) The way things move: looking under the hood of molecular motor proteins. *Science,* **288,** 88-95.

117. Kamal, A. and Goldstein, L.S. (2002) Principles of cargo attachment to cytoplasmic motor proteins. *Curr Opin Cell Biol,* **14,** 63-8.

118. Verhey, K.J. and Rapoport, T.A. (2001) Kinesin carries the signal. *Trends Biochem Sci,* **26,** 545-50.

119. Roy, S., Zhang, B., Lee, V.M. and Trojanowski, J.Q. (2005) Axonal transport defects: a common theme in neurodegenerative diseases. *Acta Neuropathol (Berl),* **109,** 5-13.

120. Julien, J.P. (1999) Neurofilament functions in health and disease. *Curr Opin Neurobiol,* **9,** 554-60.

121. Johnston, J.A., Ward, C.L. and Kopito, R.R. (1998) Aggresomes: a cellular response to misfolded proteins. *J Cell Biol,* **143,** 1883-98.

122. Cairns, N.J., Lee, V.M. and Trojanowski, J.Q. (2004) The cytoskeleton in neurodegenerative diseases. *J Pathol,* **204,** 438-49.

123. Hyman, B.T. and Tanzi, R.E. (1992) Amyloid, dementia and Alzheimer's disease. *Curr Opin Neurol Neurosurg,* **5,** 88-93.

124. Walker, R.H., Good, P.F. and Shashidharan, P. (2003) TorsinA immunoreactivity in inclusion bodies in trinucleotide repeat diseases. *Mov Disord,* **18,** 1041-4.

125. McNaught, K.S., Shashidharan, P., Perl, D.P., Jenner, P. and Olanow, C.W. (2002) Aggresome-related biogenesis of Lewy bodies. *Eur J Neurosci,* **16,** 2136-48.

126. Sharma, N., Hewett, J., Ozelius, L.J., Ramesh, V., McLean, P.J., Breakefield, X.O. and Hyman, B.T. (2001) A close association of torsinA and alpha-synuclein in Lewy bodies: a fluorescence resonance energy transfer study. *Am J Pathol,* **159,** 339-44.

127. Senior, A. and Gerace, L. (1988) Integral membrane proteins specific to the inner nuclear membrane and associated with the nuclear lamina. *J Cell Biol,* **107,** 2029-36.

128. Foisner, R. and Gerace, L. (1993) Integral membrane proteins of the nuclear envelope interact with lamins and chromosomes, and binding is modulated by mitotic phosphorylation. *Cell,* **73,** 1267-79.

129. Rapp, G., Freudenstein, J., Klaudiny, J., Mucha, J., Wempe, F., Zimmer, M. and Scheit, K.H. (1990) Characterization of three abundant mRNAs from human ovarian granulosa cells. *DNA Cell Biol,* **9,** 479-85.

130. Faria, T.N., LaRosa, G.J., Wilen, E., Liao, J. and Gudas, L.J. (1998) Characterization of genes which exhibit reduced expression during the retinoic acid-induced differentiation of F9 teratocarcinoma cells: involvement of cyclin D3 in RA-mediated growth arrest. *Mol Cell Endocrinol,* **143,** 155-66.

131. Brown, A.L. and Kay, G.F. (1999) Bex1, a gene with increased expression in parthenogenetic embryos, is a member of a novel gene family on the mouse X chromosome. *Hum Mol Genet,* **8,** 611-9.

132. Mukai, J., Hachiya, T., Shoji-Hoshino, S., Kimura, M.T., Nadano, D., Suvanto, P., Hanaoka, T., Li, Y., Irie, S., Greene, L.A. *et al.* (2000) NADE, a p75NTR-associated cell death executor, is involved in signal transduction mediated by the common neurotrophin receptor p75NTR. *J Biol Chem,* **275,** 17566-70.

133. Alvarez, E., Zhou, W., Witta, S.E. and Freed, C.R. (2005) Characterization of the Bex gene family in humans, mice, and rats. *Gene,* **357,** 18-28.

134. Mukai, J., Suvant, P. and Sato, T.A. (2003) Nerve growth factor-dependent regulation of NADE-induced apoptosis. *Vitam Horm,* **66,** 385-402.

135. Zhang, F.L. and Casey, P.J. (1996) Protein prenylation: molecular mechanisms and functional consequences. *Annu Rev Biochem,* **65,** 241-69.

136. Behrens, M., Margolis, J.W. and Margolis, F.L. (2003) Identification of members of the Bex gene family as olfactory marker protein (OMP) binding partners. *J Neurochem,* **86,** 1289-96.

137. Koo, J.H., Saraswati, M. and Margolis, F.L. (2005) Immunolocalization of Bex protein in the mouse brain and olfactory system. *J Comp Neurol,* **487,** 1-14.

138. Hodel, A. (1998) Snap-25. *Int J Biochem Cell Biol,* **30,** 1069-73.

139. Wiedenmann, B. and Franke, W.W. (1985) Identification and localization of synaptophysin, an integral membrane glycoprotein of Mr 38,000 characteristic of presynaptic vesicles. *Cell,* **41,** 1017-28.

140. Melchior, F. (2000) SUMO--nonclassical ubiquitin. *Annu Rev Cell Dev Biol,* **16,** 591-626.

141. Muller, S., Hoege, C., Pyrowolakis, G. and Jentsch, S. (2001) SUMO, ubiquitin's mysterious cousin. *Nat Rev Mol Cell Biol,* **2,** 202-10.

142. Kim, K.I., Baek, S.H. and Chung, C.H. (2002) Versatile protein tag, SUMO: its enzymology and biological function. *J Cell Physiol,* **191,** 257-68.

143. Bernier-Villamor, V., Sampson, D.A., Matunis, M.J. and Lima, C.D. (2002) Structural basis for E2-mediated SUMO conjugation revealed by a complex between ubiquitin-conjugating enzyme Ubc9 and RanGAP1. *Cell,* **108,** 345-56.

144. Basso, A.D., Kirschmeier, P. and Bishop, W.R. (2006) Lipid posttranslational modifications. Farnesyl transferase inhibitors. *J Lipid Res,* **47,** 15-31.

145. Sinensky, M. (2000) Functional aspects of polyisoprenoid protein substituents: roles in protein-protein interaction and trafficking. *Biochim Biophys Acta,* **1529,** 203-9.

146. Gerace, L. and Blobel, G. (1980) The nuclear envelope lamina is reversibly depolymerized during mitosis. *Cell,* **19,** 277-87.

147. Sinensky, M., Fantle, K., Trujillo, M., McLain, T., Kupfer, A. and Dalton, M. (1994) The processing pathway of prelamin A. *J Cell Sci,* **107 (Pt 1),** 61-7.

148. Lutz, R.J., Trujillo, M.A., Denham, K.S., Wenger, L. and Sinensky, M. (1992) Nucleoplasmic localization of prelamin A: implications for prenylation-dependent lamin A assembly into the nuclear lamina. *Proc Natl Acad Sci U S A,* **89,** 3000-4.

149. Weber, K., Plessmann, U. and Traub, P. (1989) Maturation of nuclear lamin A involves a specific carboxy-terminal trimming, which removes the polyisoprenylation site from the precursor; implications for the structure of the nuclear lamina. *FEBS Lett,* **257,** 411-4.

150. Hennekes, H. and Nigg, E.A. (1994) The role of isoprenylation in membrane attachment of nuclear lamins. A single point mutation prevents proteolytic cleavage of the lamin A precursor and confers membrane binding properties. *J Cell Sci,* **107 (Pt 4),** 1019-29.

151. Silvius, J.R. and l'Heureux, F. (1994) Fluorimetric evaluation of the affinities of isoprenylated peptides for lipid bilayers. *Biochemistry,* **33,** 3014-22.

152. Villa, A., Sharp, A.H., Racchetti, G., Podini, P., Bole, D.G., Dunn, W.A., Pozzan, T., Snyder, S.H. and Meldolesi, J. (1992) The endoplasmic reticulum of Purkinje neuron body and dendrites: molecular identity and specializations for Ca2+ transport. *Neuroscience,* **49,** 467-77.

153. Horton, A.C. and Ehlers, M.D. (2003) Dual modes of endoplasmic reticulum-to-Golgi transport in dendrites revealed by live-cell imaging. *J Neurosci,* **23,** 6188-99.

154. Konakova, M. and Pulst, S.M. (2001) Immunocytochemical characterization of torsin proteins in mouse brain. *Brain Res,* **922,** 1-8.

155. Xiao, J., Gong, S., Zhao, Y. and LeDoux, M.S. (2004) Developmental expression of rat torsinA transcript and protein. *Brain Res Dev Brain Res,* **152,** 47-60.

156. Fukuda, M., Asano, S., Nakamura, T., Adachi, M., Yoshida, M., Yanagida, M. and Nishida, E. (1997) CRM1 is responsible for intracellular transport mediated by the nuclear export signal*,* **390,** 308-311.

157. Talcott, B. and Moore, M.S. (1999) Getting across the nuclear pore complex. *Trends Cell Biol,* **9,** 312-8.

158. Foltz, G., Ryu, G.Y., Yoon, J.G., Nelson, T., Fahey, J., Frakes, A., Lee, H., Field, L., Zander, K., Sibenaller, Z. *et al.* (2006) Genome-wide analysis of epigenetic silencing identifies BEX1 and BEX2 as candidate tumor suppressor genes in malignant glioma. *Cancer Res,* **66,** 6665-74.

159. McGuire, E.A., Hockett, R.D., Pollock, K.M., Bartholdi, M.F., O'Brien, S.J. and Korsmeyer, S.J. (1989) The t(11;14)(p15;q11) in a T-cell acute lymphoblastic leukemia cell line activates multiple transcripts, including Ttg-1, a gene encoding a potential zinc finger protein. *Mol Cell Biol,* **9,** 2124-32.

160. Boehm, T., Foroni, L., Kaneko, Y., Perutz, M.F. and Rabbitts, T.H. (1991) The rhombotin family of cysteine-rich LIM-domain oncogenes: distinct members are involved in T-cell translocations to human chromosomes 11p15 and 11p13. *Proc Natl Acad Sci U S A,* **88,** 4367-71.

161. Han, C., Liu, H., Liu, J., Yin, K., Xie, Y., Shen, X., Wang, Y., Yuan, J., Qiang, B., Liu, Y.J. *et al.* (2005) Human Bex2 interacts with LMO2 and regulates the transcriptional activity of a novel DNA-binding complex. *Nucleic Acids Res,* **33,** 6555-65.

162. Anchan, R.M., Drake, D.P., Haines, C.F., Gerwe, E.A. and LaMantia, A.S. (1997) Disruption of local retinoid-mediated gene expression accompanies abnormal development in the mammalian olfactory pathway. *J Comp Neurol,* **379,** 171-84.

163. Misiti, S., Koibuchi, N., Bei, M., Farsetti, A. and Chin, W.W. (1999) Expression of steroid receptor coactivator-1 mRNA in the developing mouse embryo: a possible role in olfactory epithelium development. *Endocrinology,* **140,** 1957-60.

164. Zhang, Q.Y. (1999) Retinoic acid biosynthetic activity and retinoid receptors in the olfactory mucosa of adult mice. *Biochem Biophys Res Commun,* **256,** 346-51.

165. Vilar, M., Murillo-Carretero, M., Mira, H., Magnusson, K., Besset, V. and Ibanez, C.F. (2006) Bex1, a novel interactor of the p75 neurotrophin receptor, links neurotrophin signaling to the cell cycle. *Embo J,* **25,** 1219-30.

166. Carter, B.D. (2006) A Bex-cycle built for two. *EMBO Rep,* **7,** 382-4.

167. Roux, P.P. and Barker, P.A. (2002) Neurotrophin signaling through the p75 neurotrophin receptor. *Prog Neurobiol,* **67,** 203-33.

168. O'Farrell, C., Lockhart, P.J., Lincoln, S., De Lucia, M., Singleton, A.B., Dickson, D.W. and Cookson, M.R. (2004) Biochemical characterization of torsinB. *Brain Res Mol Brain Res,* **127,** 1-9.

169. Kustedjo, K., Deechongkit, S., Kelly, J.W. and Cravatt, B.F. (2003) Recombinant expression, purification, and comparative characterization of torsinA and its torsion dystonia-associated variant Delta E-torsinA. *Biochemistry,* **42,** 15333-41.

170. Callan, A.C., Bunning, S., Jones, O.T., High, S. and Swanton, E. (2006) Biosynthesis of the dystonia-associated AAA + ATPase torsinA at the endoplasmic reticulum. *Biochem J.*

171. Hewett, J.W., Tannous, B., Niland, B.P., Nery, F.C., Zeng, J., Li, Y. and Breakefield, X.O. (2007) Mutant torsinA interferes with protein processing through the secretory pathway in DYT1 dystonia cells. *Proc Natl Acad Sci U S A,* **104,** 7271-6.

172. Rich, R.L. and Myszka, D.G. (2000) Survey of the 1999 surface plasmon resonance biosensor literature. *J Mol Recognit,* **13,** 388-407.

173. Malmqvist, M. (1999) BIACORE: an affinity biosensor system for characterization of biomolecular interactions. *Biochem Soc Trans,* **27,** 335-40.

174. Johnsson, B., Lofas, S. and Lindquist, G. (1991) Immobilization of proteins to a carboxymethyldextran-modified gold surface for biospecific interaction analysis in surface plasmon resonance sensors. *Anal Biochem,* **198,** 268-77.

175. Kerppola, T.K. (2006) Visualization of molecular interactions by fluorescence complementation. *Nat Rev Mol Cell Biol,* **7,** 449-56.

176. Tsukita, S. and Ishikawa, H. (1980) The movement of membranous organelles in axons. Electron microscopic identification of anterogradely and retrogradely transported organelles. *J Cell Biol,* **84,** 513-30.

177. Ellisman, M.H. and Lindsey, J.D. (1983) The axoplasmic reticulum within myelinated axons is not transported rapidly. *J Neurocytol,* **12,** 393-411.

178. Bannai, H., Inoue, T., Nakayama, T., Hattori, M. and Mikoshiba, K. (2004) Kinesin dependent, rapid, bi-directional transport of ER sub-compartment in dendrites of hippocampal neurons. *J Cell Sci,* **117,** 163-75.

179. Huttner, W.B., Schiebler, W., Greengard, P. and De Camilli, P. (1983) Synapsin I (protein I), a nerve terminal-specific phosphoprotein. III. Its association with synaptic vesicles studied in a highly purified synaptic vesicle preparation. *J Cell Biol,* **96,** 1374-88.

180. Wessel, D. and Flugge, U.I. (1984) A method for the quantitative recovery of protein in dilute solution in the presence of detergents and lipids. *Anal Biochem,* **138,** 141-3.

181. Brent, R. and Finley, R.L., Jr. (1997) Understanding gene and allele function with two-hybrid methods. *Annu Rev Genet,* **31,** 663-704.

182. Murthy, V., Han, S., Beauchamp, R.L., Smith, N., Haddad, L.A., Ito, N. and Ramesh, V. (2004) Pam and its ortholog highwire interact with and may negatively regulate the TSC1.TSC2 complex. *J Biol Chem,* **279,** 1351-8.

183. Gyuris, J., Golemis, E., Chertkov, H. and Brent, R. (1993) Cdi1, a human G1 and S phase protein phosphatase that associates with Cdk2. *Cell,* **75,** 791-803.

184. Reynolds, A., Lundblad, V., Dorris, D., and Keaveney, M. (1994) In (Ausubel, F.M., Brent, R., Kingston, R.E., Moore, D.D., Seidman, J.G., Smith, J.A., and Struhl, K., ed) (ed.), *Current Protocols in Molecular Biology*. John Wiley & Sons, Inc., New York, pp. 13.16.12-13.17.15.

185. Miller, J. (1992) *A short course in bacterial genetics*. Cold Spring Harbor Laboratory Press, Cold Spring Harbor, NY.

186. Qi, Y., Wang, J.K., McMillian, M. and Chikaraishi, D.M. (1997) Characterization of a CNS cell line, CAD, in which morphological differentiation is initiated by serum deprivation. *J Neurosci,* **17,** 1217-25.

187. Pear, W.S., Nolan, G.P., Scott, M.L. and Baltimore, D. (1993) Production of high-titer helper-free retroviruses by transient transfection. *Proc Natl Acad Sci U S A,* **90,** 8392-6.

188. Lin, J.W., Ju, W., Foster, K., Lee, S.H., Ahmadian, G., Wyszynski, M., Wang, Y.T. and Sheng, M. (2000) Distinct molecular mechanisms and divergent endocytotic pathways of AMPA receptor internalization. *Nat Neurosci,* **3,** 1282-90.

Abbreviations

°C	degree Celcius
6-OHDA	6-hydroxydopamine
7	facial nu
Δ	deletion
µg	microgram
µl	microliter
µM	micromolar
aa	amino acid
AAA$^+$	<u>A</u>TPases <u>a</u>ssociated with a variety of cellular <u>a</u>ctivities
AD	autosomal dominant
ALS	amyotrophic lateral sclerosis
APir	amygdalopiriform transition area
AR	autosomal recessive
BCA	Bicinchoninic Acid Assay
bp	base pair
BSA	bovine serum albumine
C. elegans	*Caenorhabditis elegans*
CA1-CA3	hippocampal formation
cDNA	complementary deoxyribonucleic acid
CMV	cytomegalovirus
CNS	central nervous system
Co	cortex
CPu	caudate putamen
D. melanogaster	*Drosophila melanogaster*
DA	dopamine
DAT	dopamine transporter
DC	dorsal cochlear nucleus
DG	dentate gyrus
DMEM	Dulbecco's Minimal Essential Medium
DMP	dimethyl pimelimidate·2HCl
DMSO	dimethylsulfoxide
DNA	deoxyribonucleic acid
dNTP	desoxynucleotide-5'-triphosphate
DOPAC	3, 4-dihydroxyphenylacetic acid
DRD	dopa-responsive dystonia

DTT	1,4-dithiothreitol
DYT	dystonia type
E. coli	*Escherichia coli*
EDTA	ethylenediaminetetraacetic acid
EEA1	early endosome antigen 1
EGTA	ethyleneglycoltetraacetic acid
EOTD	early-onset torsion dystonia
ER	endoplasmic reticulum
FRET	fluorescence resonance energy transfer
g	gravitation constant or gramm
GIV	gigantocellular reticular nucleus, ventral part
GPe	external globus pallidus
GPi	internal globus pallidus
H_2O_2	hydrogen peroxide
HBSS	Hank's balanced salt solution
HCl	hydrochloric acid
HEPES	4-(2-hydroxyethyl)-1-piperazineethanesulfonic acid
Hip	hippocampus
HRP	*horseradish*-peroxidase
HC	antibody heavy chain
HSP	heat-shock protein (chaperone)
IB	immunoblotting
ICC	immunocytochemistry
IFD	idiopathic focal dystonia
Ig	immunoglobulin
IHC	immunohistochemistry
IntA	interposed cerebellar nu
IP	immunoprecipitation
IPTG	isopropyl-ß-D-thiogalactopyranoside
IR	immunoreactivity
ITD	idiopathic torsion dystonia
KH_2PO_4	potassium dihydrogen phosphate
kb	kilobase
kD	kilodalton
KCl	potassium chloride
KHC	kinesin heavy chain
KLC	kinesin light chain

LAP1	lamina associated protein
Lat	lateral cerebellar nu
LB	Luria-Bertani
LC	antibody light chain
L-DOPA	Levodopa (L-3,4-dihydroxyphenylalanine)
LULL1	lumenal domain like LAP1
M	molar
MAP-2	microtubule associated protein 2
MBP	maltose binding protein
MED	medial cerebellar nucleus
$MgCl_2$	magnesium chloride
MGP	medial globus pallidus
min	minute
ml	milliliter
Mm	millimeter
mM	millimolar
Mo5	motor trigeminal nucleus
mRNA	messenger ribonucleic acid
Na_2HPO_4-7 H_2O	sodium phosphate dibasic heptahydrate
NaCl	sodium chloride
NaN_3	sodium azide
NaOH	sodium hydroxide
NE	nuclear envelope
ng	nanogram
NGF	nerve growth factor
NLS	nuclear localization signal
nmol	nanomole
nM	nanomolar
nu	nucleus
NPC	nuclear pore complexes
OMP	olfactory marker protein
ORF	open reading frame
PAGE	polyacrylamide gelelectrophoresis
PBS	phosphate buffered saline
PCR	polymerase chain reaction
PDI	protein disulfide isomerase
PDL	poly-D-lysine

PFA	paraformaldehyde
pg	picogram
PNKD	paroxysomal non-kinesigenic dyskenisia
PPy	parapyramidal nu
Pir	piriform cortex
RCN	primary rat cortical neurons
RDP	rapid-onset dystonia-parkinsonism
RIP2	receptor interacting protein 2
RNA	ribonucleic acid
RNAi	ribonucleic acid interference
rpm	rounds per minute
RT	room temperature
qRT-PCR	quantitative real-time PCR
RT-PCR	reverse transcriptase PCR
SDS	sodium dodecyl sulphate
SN	substantia nigra
SNCD	substantia nigra, compact part, dorsal tier
SNR	substantia nigra reticular part
Sp5O	spinal 5 nu, oral part
SP	signal peptide
SPC	signal peptidase complex
STN	subthalamic nucleus
SuG	superficial gray layer of superior colliculus
SUMO	small ubiquitin-related modifier
TD	torsion dystonia
TBE	Tris-borate buffer
TBS	Tris buffered saline
TEMED	N,N,N',N'-tetramethylethylendiamine
Tu	olfactory tubercle
U	units
VPM	ventral posteromedial thalamic nu
XP	X-linked dystonia parkinsonism
XR	X-linked recessive

Danksagungen

Herrn **Prof. Dr. Gasser** möchte ich für die Möglichkeit danken, die vorliegende Arbeit in seiner Arbeitsgruppe für Neurodegenerative Erkrankungen durchführen zu können und für die Bereitstellung des Arbeitsplatzes.

Herrn **Prof. Dr. Rieß** danke ich für die Bereitschaft, die vorliegende Dissertation an der Fakultät für Biologie der Eberhard-Karls-Universität Tübingen zu vertreten.

Herrn **Dr. Christoph Kamm** danke ich für die Überlassung des interessanten Themas und seine Betreuung.

Besonderer Dank gilt Herrn **Prof. Dr. Philipp Kahle** für seine Bereitschaft, das Zweitgutachten für diese Dissertation zu erstellen, vor allem aber für die interessanten, wissenschaftlichen Diskussionen und seine Unterstützung, die maßgeblich zum Gelingen dieser Dissertation beigetragen haben.

Bei Frau **Stephanie Kullmann** möchte ich mich besonders für die ausgezeichnete, technische Unterstützung, erfolgreiche Zusammenarbeit, sowie für die interessanten und aufmunternden Gespräche bedanken.

Bei den Mitgliedern der Arbeitsgruppe für Neurodegenerative Erkrankungen und der Arbeitsgruppe für Funktionelle Neurogenetik bedanke ich mich für eine gute Zusammenarbeit und ein angenehmes Arbeitsklima.

Ganz besonders bedanke ich mich bei **Christian Klein**, von dem ich viel Unterstützung während der Dissertation erhalten habe, der immer zu wissenschaftlichen Diskussionen bereit war und mir ganz viel Kraft und Zuversicht gegeben hat.

Bedanken möchte ich mich auch bei meiner Familie: Mama **Marion**, meinen Geschwistern **Fine** und **Philipp**, sowie **Gerhard**, die ganz fest an mich glauben und für mich da sind, wann immer ich ihre Hilfe benötige.

Curriculum vitae

Persönliche Daten

Name	Susann Horn
Wohnort	Tübingen, 72074
Straße	Am Bronnen 15
Telefon	+49 07071 856499
e-mail	susann.horn@uni-tuebingen.de
Geburtstag	06.01.1979

Schulausbildung

1985 – 1991	POS (Polytechnische Oberschule)-Sahnschule in Crimmitschau
1992 – 1997	Julius-Motteler-Gymnasium in Crimmitschau
1997	Allgemeine Hochschulreife

Hochschulausbildung

1997 – 2002	Studium der Biologie (Diplom) an der Universität Bayreuth
09.2001 – 07.2002	Diplomarbeit am Lehrstuhl für Genetik der Universität Bayreuth unter Leitung von Prof. Dr. Christian Lehner mit dem Thema: „Regulation der meiotischen Chromosomenverteilung durch proteolytische Spaltung von Mei-910."
31.07.2002	Abschluss als Diplom-Biologin
03.2003 – 07.2007	Dissertation am Hertie-Institut für klinische Hirnforschung in der Arbeitsgruppe für Neurodegenerative Erkrankungen unter Leitung von Prof. Dr. Thomas Gasser mit dem Thema „Functional characterization of Bex2 and torsinA, a protein involved in early-onset torsion dystonia."